NAVAL
POSTGRADUATE
SCHOOL

MONTEREY, CALIFORNIA

THESIS

GENERATION OF MID-WAVE INFRARED SIGNATURE USING MICRORADIATING DEVICES FOR VEHICLE MOUNTED IDENTIFICATION FRIEND OR FOE APPLICATIONS

by

Eric Rose

June 2009

Thesis Advisor:	Nancy M. Haegel
Second Reader:	Richard M. Harkins

Approved for public release; distribution is unlimited

THIS PAGE INTENTIONALLY LEFT BLANK

REPORT DOCUMENTATION PAGE		Form Approved OMB No. 0704-0188

Public reporting burden for this collection of information is estimated to average 1 hour per response, including the time for reviewing instruction, searching existing data sources, gathering and maintaining the data needed, and completing and reviewing the collection of information. Send comments regarding this burden estimate or any other aspect of this collection of information, including suggestions for reducing this burden, to Washington headquarters Services, Directorate for Information Operations and Reports, 1215 Jefferson Davis Highway, Suite 1204, Arlington, VA 22202-4302, and to the Office of Management and Budget, Paperwork Reduction Project (0704-0188) Washington DC 20503.

1. AGENCY USE ONLY *(Leave blank)*	2. REPORT DATE	3. REPORT TYPE AND DATES COVERED
	June 2009	Master's Thesis

4. TITLE AND SUBTITLE Generation of Mid-Wave Infrared Signature Using Microradiating Devices for Vehicle Mounted Identification Friend or Foe Applications	5. FUNDING NUMBERS
6. AUTHOR(S) Eric Rose	
7. PERFORMING ORGANIZATION NAME(S) AND ADDRESS(ES) Naval Postgraduate School Monterey, CA 93943-5000	8. PERFORMING ORGANIZATION REPORT NUMBER
9. SPONSORING /MONITORING AGENCY NAME(S) AND ADDRESS(ES) N/A	10. SPONSORING/MONITORING AGENCY REPORT NUMBER

11. SUPPLEMENTARY NOTES The views expressed in this thesis are those of the author and do not reflect the official policy or position of the Department of Defense or the U.S. Government.

12a. DISTRIBUTION / AVAILABILITY STATEMENT	12b. DISTRIBUTION CODE
Approved for public release; distribution is unlimited	

13. ABSTRACT (maximum 200 words)

Friendly fire continues to be a major source of casualties on the modern battlefield. The Vehicle Mounted Identification Friend or Foe (VMIFF) is a device designed to provide instantaneous feedback to the shooter identifying itself as friendly when interrogated by a friendly target laser designator or laser range finder. Current prototypes provide an omni-directional near infrared signature visible through night vision devices but not thermal imagers, and therefore are only effective during night operations. Thermal imagers require a 3–5 μm mid-wave infrared (MWIR) signature. The integration of a MWIR signature into VMIFF will add a daytime capability.

A new generation of compact MWIR sources is emerging to meet demands from a range of spectroscopy and communications applications. An evaluation was conducted on three commercially available thermal microradiators to determine suitability as MWIR signature generators for VMIFF applications. Frequency response and angular irradiance measurements were made in both the 3–5 μm and 8–12 μm regions using single-pixel thermal detectors and thermal imaging cameras. Based on data collected, a next-generation VMIFF design incorporating a thermal signature is proposed.

14. SUBJECT TERMS	15. NUMBER OF PAGES
Anti-fratricide, Thermal Emitter, Vehicle Mounted Identification Friend or Foe, night vision device (NVD), Thermal Imaging	116
	16. PRICE CODE

17. SECURITY CLASSIFICATION OF REPORT	18. SECURITY CLASSIFICATION OF THIS PAGE	19. SECURITY CLASSIFICATION OF ABSTRACT	20. LIMITATION OF ABSTRACT
Unclassified	Unclassified	Unclassified	UU

NSN 7540-01-280-5500

Standard Form 298 (Rev. 8-98)
Prescribed by ANSI Std. Z39.18

THIS PAGE INTENTIONALLY LEFT BLANK

Approved for public release; distribution is unlimited

GENERATION OF MID-WAVE INFRARED SIGNATURE USING MICRORADIATING DEVICES FOR VEHICLE MOUNTED IDENTIFICATION FRIEND OR FOE APPLICATIONS

Eric Q. Rose
Captain, United States Marine Corps
B.S., The Pennsylvania State University, 1999

Submitted in partial fulfillment of the
requirements for the degree of

MASTER OF SCIENCE IN PHYSICS

from the

NAVAL POSTGRADUATE SCHOOL
June 2009

Author: Eric Q. Rose

Approved by: Nancy Haegel
Thesis Advisor

Richard Harkins
Second Reader

James H. Luscombe
Chairman, Department of Physics

THIS PAGE INTENTIONALLY LEFT BLANK

ABSTRACT

Friendly fire continues to be a major source of casualties on the modern battlefield. The Vehicle Mounted Identification Friend or Foe (VMIFF) is a device designed to provide instantaneous feedback to the shooter identifying itself as friendly when interrogated by a friendly target laser designator or laser range finder. Current prototypes provide an omni-directional near infrared signature visible through night vision devices but not thermal imagers, and therefore are only effective during night operations. Thermal imagers require a 3–5 μm mid-wave infrared (MWIR) signature. The integration of a MWIR signature into VMIFF will add a daytime capability.

A new generation of compact MWIR sources is emerging to meet demands from a range of spectroscopy and communications applications. An evaluation was conducted on three commercially available thermal microradiators to determine suitability as MWIR signature generators for VMIFF applications. Frequency response and angular irradiance measurements were made in both the 3–5 μm and 8–12 μm regions using single-pixel thermal detectors and thermal imaging cameras. Based on data collected, a next-generation VMIFF design incorporating a thermal signature is proposed.

THIS PAGE INTENTIONALLY LEFT BLANK

TABLE OF CONTENTS

I. BACKGROUND 1
A. FRIENDLY FIRE 1
B. COMBAT IDENTIFICATION 3
1. Thermal Identification Panels and Combat Identification Panels 3
2. Infrared Beacons 7
C. A NEW APPROACH TO COMBAT IDENTIFICATION 9

II. MIDWAVE INFRARED RADIATORS 13
A. PHYSICAL APPROACHES 13
1. Blackbody Radiators 13
2. Infrared Light Emitting Diodes 15
3. Quantum Cascade Lasers 18
B. COMMERCIALLY AVAILABLE DEVICES 19
1. Blackbody Radiators 20
a. Cal Sensors SVF360-8M3 20
b. ICX Photonics NL84ACC 20
c. HawkEye Technologies IR-50 21
2. Infrared Light Emitting Diodes 22
3. Quantum Cascade Lasers 22

III. SINGLE MICRORADIATOR EMITTER MEASUREMENTS 23
A. TEST METHODOLOGY 23
1. Device Setup and Drive Circuit 23
2. Bench Setup 28
B. 3–5 MICRON EMISSION CHARACTERIZATION 30
1. Maximum Irradiance at Constant Power 32
2. Device Rise and Fall Time 33
3. Frequency Response 36
a. Maximum Irradiance versus Frequency 37
b. Minimum Irradiance versus Frequency 38
c. Delta Irradiance versus Frequency 40
4. Off-Axis Irradiance 41
C. 8–12 MICRON EMISSION CHARACTERIZATION 42
1. Maximum Irradiance at Constant Power 43
2. Device Rise and Fall Time 44
3. Frequency Response 46
a. Maximum Irradiance versus Frequency 46
b. Minimum Irradiance versus Frequency 49
c. Delta Irradiance versus Frequency 50
D. SUMMARY OF SINGLE DEVICE MEASUREMENTS 52

IV. TWELVE-EMITTER ARRAY MEASUREMENTS 53

A. LABORATORY MEASUREMENTS 53
B. CAMP PENDLETON FIELD TEST 54
V. CONCLUSION 59
A. EXPERIMENTAL RESULTS 59
B. VMIFF GENERATION III DESIGN RECOMMENDATION 60
APPENDIX A DEVICE SPECIFICATION SHEETS 63
APPENDIX B 3–5 MICRON FREQUENCY RESPONSE 75
A. CAL SENSORS SVF360-8M3, SINGLE-DEVICE, ON AXIS FREQUENCY RESPONSE 75
B. ICX PHOTONICS NL84ACC, SINGLE-DEVICE, ON AXIS FREQUENCY RESPONSE 77
C. HAWKEYE TECHNOLOGIES IR-50, SINGLE-DEVICE, ON AXIS FREQUENCY RESPONSE 79
APPENDIX C 8–12 MICRON FREQUENCY RESPONSE 81
A. CAL SENSORS SVF360-8M3, SINGLE-DEVICE, ON AXIS FREQUENCY RESPONSE 81
B. ICX PHOTONICS NL84ACC, SINGLE-DEVICE, ON AXIS FREQUENCY RESPONSE 83
C. HAWKEYE TECHNOLOGIES IR-50, SINGLE-DEVICE, ON AXIS FREQUENCY RESPONSE 85
APPENDIX D OFF-AXIS SINGLE DEVICE IRRADIANCE 87
APPENDIX E PANEL ON-AXIS IRRADIANCE VS DISTANCE 91
LIST OF REFERENCES 95
INITIAL DISTRIBUTION LIST 97

LIST OF FIGURES

Figure 1. Thermal Identification Panels [From The Canadian Infantry Association, Retrieved from www.ducimus.com]. 4
Figure 2. Combat Identification Panels [From Krause] 4
Figure 3. Improperly Employed TIP, Haditha, IZ [From Marine Corpse Systems Command, Force Protection Office]..... 5
Figure 4. Threat Imaging Capabilities [From Cline] 7
Figure 5. Vehicle-Mounted Infrared Beacon [From Krause] 8
Figure 6. Pheonix IR Beacon [From Night Vision Systems, Retrieved from www.nightvisionsystems.com]..... 8
Figure 7. VMIFF Generation II [From Williams] 10
Figure 8. Radiated Power per Unit Area Versus Wavelength for Two Radiators at 300K and 500K 14
Figure 9. Electron Hole Pair Generation and Recombination 16
Figure 10. Representation of QCL Semiconductor Layers [From Quimby]..... 18
Figure 11. Photon Generation in QCL [From Quimby]..... 19
Figure 12. Cal Sensors Panel With Devices..... 23
Figure 13. Square-wave Generating Circuit 24
Figure 14. Panel Switching Circuit..... 25
Figure 15. Single Element 8–12 µm (left) and 3–5 µm (right) Detectors..... 26
Figure 16. MCT Detector Spectral Response [From Detector Specification Sheet] 27
Figure 17. 8–13.5 µm Band-Pass Filter Transmittance [From Filter Specification Sheet]..... 27
Figure 18. LabVIEW Interface Circuit 29
Figure 19. Experimental Bench Set-up..... 30
Figure 20. Detector Output Versus Time for Single Cal Sensors Device, On-Axis..... 31
Figure 21. Detector Output Versus Time for Single Cal Sensors Device, On-Axis..... 31
Figure 22. DC Response of IR-50, Cal Sensors, and ICX Devices 32
Figure 23. Normalized Transient Rise Response of IR-50, Cal Sensors, and ICX Devices..... 33
Figure 24. Rise Time Response Comparison of IR-50, Cal Sensors, and ICX Devices..... 34
Figure 25. Normalized Transient Fall Response of IR-50, Cal Sensors, and ICX Devices..... 35
Figure 26. Fall Time Response Comparison of IR-50, Cal Sensors, and ICX Devices..... 36
Figure 27. Maximum Irradiance Versus Frequency of IR-50, Cal Sensors, and ICX Devices..... 37
Figure 28. Normalized Maximum Irradiance Versus Frequency of IR-50, Cal Sensors, and ICX Devices..... 38

Figure 29. Minimum Irradiance Versus Frequency of IR-50, Cal Sensors, and ICX Devices 39
Figure 30. Normalized Minimum Irradiance Versus Frequency of IR-50, Cal Sensors, and ICX Devices 39
Figure 31. Delta Irradiance Versus Frequency of IR-50, Cal Sensors, and ICX Devices 40
Figure 32. Normalized Delta Irradiance Versus Frequency of IR-50, Cal Sensors, and ICX Devices 41
Figure 33. Sensor Voltage Versus Half Angle for IR-50, Cal Sensors, and ICX Devices 42
Figure 34. DC Response of IR-50, Cal Sensors, and ICX Devices 43
Figure 35. Normalized Transient Rise Response of IR-50, Cal Sensors, and ICX Devices 44
Figure 36. Rise Time Response Comparison of IR-50, Cal Sensors, and ICX Devices 45
Figure 37. Normalized Transient Fall Response of IR-50, Cal Sensors, and ICX Devices 46
Figure 38. Fall Time Response Comparison of IR-50, Cal Sensors, and ICX Devices 47
Figure 39. Maximum Irradiance Versus Frequency of IR-50, Cal Sensors, and ICX Devices 48
Figure 40. Normalized Maximum Irradiance Versus Frequency of IR-50, Cal Sensors, and ICX Devices 48
Figure 41. Minimum Irradiance Versus Frequency of IR-50, Cal Sensors, and ICX Devices 49
Figure 42. Normalized Minimum Irradiance Versus Frequency of IR-50, Cal Sensors, and ICX Devices 50
Figure 43. Delta Irradiance Versus Frequency of IR-50, Cal Sensors, and ICX Devices 51
Figure 44. Normalized Delta Irradiance Versus Frequency of IR-50, Cal Sensors, and ICX Devices 51
Figure 45. Twelve-Device Array, 3–5 Micron On-Axis Irradiance Versus Distance 53
Figure 46. Twelve-Device Array, 8–12 Micron On-Axis Irradiance Versus Distance 54
Figure 47. PAS-13B Thermal Weapon Sight [From Raytheon, Retrieved from www.raytheon.com] 55

LIST OF TABLES

Table 1. Fratricide Rates in this Century's Conflicts [From Steinweg]. 2
Table 2. Band Gap Energy of Common Semiconductors [From Streetman and Sanjay] 17
Table 3. Specification Sheet Information for Cal Sensors, ICX, and IR-50 Devices [From Device Specification Sheets] 21
Table 4. Summary of Single Device Experimental Data 52
Table 5. Camp Pendleton Field Test Results- Day 56
Table 6. Camp Pendleton Field Test Results- Night 57
Table 7. Summary of Experimental Data 59

THIS PAGE INTENTIONALLY LEFT BLANK

LIST OF ACCRONYMS AND ABBREVIATIONS

CID	Combat Identification
CIP	Combat Identification Panel
IR	Infrared
JCIMS	Joint Combat Identification and Marking System
LED	Light Emitting Diode
NVD	Night Vision Devices
MWIR	Mid-wave Infrared
QCL	Quantum Cascade Laser
TIP	Thermal Identification Panel
VMIFF	Vehicle Mounted Identification Friend or Foe

THIS PAGE INTENTIONALLY LEFT BLANK

ACKNOWLEDGMENTS

This work was supported by the Rapid Reaction Technology Office of the Office of the Secretary of Defense.

I would like to thank Rick Sams at the Marine Corps Experimentation Center, Pacific for coordinating the Camp Pendleton field experiment, and the Marines of 4th Light Armored Reconnaissance Battalion for viewing my devices through their tactical imagers. The data collected really tied this thesis work together.

I would also like to thank Professor Crooker for his help with LabView and my circuit designs and Professor Harkins for his help with my circuit and motor design. The revised test set-up based on your recommendations led to the capture of data at the heart of this research.

I would like to extend a special thanks to Sam Barone and George Jaksha for their professional, timely assistance throughout this work. Their help really kept the process running smoothly.

It is not possible to express the amount of appreciation and respect I have for Professor Haegel. Her knowledge and ability to focus in on relevant issues was the real catalyst behind my research. I have never worked with such a capable problem solver and natural leader. Thank you for the opportunity to work for you and learn from you.

Last, but most certainly not least, I would like to thank my family for their unfailing support over the past two years. Kim, your love sustained me through this, the most challenging and rewarding tour of my career. Thank you from the bottom of my heart. I love you.

THIS PAGE INTENTIONALLY LEFT BLANK

I. BACKGROUND

A. FRIENDLY FIRE

War is a violent clash of interests between, or among, organized groups, characterized by the use of military force, with the objective of imposing one's will on the enemy [1]. A key requirement to impose one's will on the enemy is the effective application of military force against appropriate targets to achieve tactical objectives. Several aspects of warfare complicate the effective use of military force on the battlefield including friction, uncertainty, fluidity, disorder, and complexity [1]. In early warfare, military units sought to minimize these effects by organizing into large tightly controlled formations and confronting each other on an open battlefield. Horns, drums and flags served as effective means of command and control. As tactics evolved and technology improved, military units have become smaller and more dispersed, but significantly more lethal. Today, multiple radio nets are required to link maneuver units and headquarters to each other.

In the midst of these difficulties, service men and women must make timely targeting decisions on imperfect information, or risk being shot first. Targeting is defined as the process of selecting and prioritizing targets and matching the appropriate response to them, considering operations requirements and capabilities [2]. One key to targeting, is the ability to sense potential targets and engage them with accurate fire, preferably at the maximum range tactically possible. The maximum effective ranges of the most lethal weapon systems, however, have long out-ranged the unaided human eye. To assist them in the targeting and engagement process, service members deploy with various sensors and imaging devices. Service members must act on the information gathered from these sensors and imagers when making engagement decisions. Far too often, these decisions result in friendly fire.

Joint Publication 1-02 defines friendly fire as a casualty circumstance applicable to persons killed in action, or wounded in action, mistakenly or accidentally, by friendly forces actively engaged with the enemy, who are directing fire at a hostile force, or what is thought to be a hostile force [2]. Friendly fire has been a problem since the advent of warfare. Table 1 shows American friendly fire casualty figures for the last century. The figures are calculated using this formula;

$$\frac{\text{American Casualties caused by Friendly Fire}}{\text{Total American Casualties}}$$

Conflict	Source Data	Fratricide Rate
World War I	Besecker Diary (Europe)	10% Wounded in Action
World War II	Bouganville Study	12% Wounded in Action 16% Killed in action
Korea	25th Infantry Division	7% Casualties
Vietnam	WEDMT[1] (autopsy) WEDMT (autopsy) WEDMT	14% Killed in Action (rifle) 11% Killed in Action (Fragments) 11% Casualties
Just Cause	US Department of Defense	5–12% Wounded in Action 13% Killed in Action
Desert Storm	U.S. Department of Defense	15% Wounded in Action 24% Killed in Action

Table 1. Fratricide Rates in this Century's Conflicts [From Steinweg].

U.S. military units deploy with the most sophisticated command, control, computers, communications and Intelligence (C4I) equipment of any modern military. Its officers and enlisted are well trained in the tactical employment of these systems and military planning. Yet, casualty figures from Operation Iraqi

Freedom show that 17 % of Americans killed in action or wounded in action were a result of friendly fire. Why? A partial answer to this question lies in how we distinguish between friend and foe on the battlefield, commonly known as combat identification.

B. COMBAT IDENTIFICATION

Combat identification (CID) is the process of attaining an accurate characterization of detected objects in the operational environment sufficient to support an engagement decision [2]. CID is an integral part of the target engagement process in order to ensure fire is directed at the enemy and not friendly or neutral entities. The shooter leverages every piece of combat information and intelligence available to aid in the process. To aid in CID and target engagement, the more lethal weapon platforms in the U.S. military are typically outfitted with sophisticated target acquisition systems and imagers. Some of these systems include laser range finders, laser target designators, night vision devices (NVD) and thermal imagers. One CID goal is to leverage these systems' capabilities such that friendly forces can identify other friendly forces quickly and confidently, with minimal impact on standard operating procedures (SOP). If achieved, such a solution gives the shooter valuable data during the targeting process that can potentially prevent a friendly fire incident. The U.S. military currently uses a system of devices called Joint Combat Identification and Marking System (JCIMS). Combat Identification Panels, Thermal Identification Panels, and infrared beacons are the vehicle mounted JCIMS devices.

1. Thermal Identification Panels and Combat Identification Panels

TIP are two-sided devices with day-use international orange on one side, and thermal reflective tape on the other (Figure 1). Hereafter, reference made to TIP implies it is in "thermal mode" with the thermally reflective tape facing out. Combat Identification Panels (CIP) are ground-to-ground CID devices that mount

on the side of tactical vehicles. CIP may be louvered or flat plates (Figure 2). Thermal Identification Panels (TIP) are air-to-ground CID devices that strap to the top, or other horizontal surfaces, of tactical vehicles. Both CIP and TIP are designed to reflect away a portion of the heat radiated by the vehicle creating a relatively cool area on a relatively hot background.

Figure 1. Thermal Identification Panels [From The Canadian Infantry Association, Retrieved from www.ducimus.com].

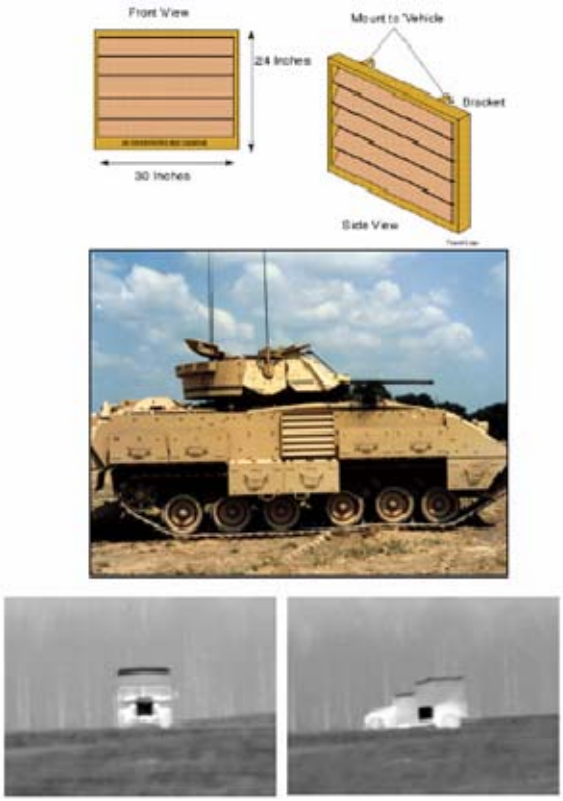

Figure 2. Combat Identification Panels [From Krause]

There are several critical requirements for optimum effectiveness of CIP and TIP. First, service members must be trained to properly deploy CIP and TIP on their combat vehicles. Coalition Combat Identification Advanced Technology Demonstration, BOLD QUEST 08, post exercise surveys show some 40% of Mounted ground troops felt that their CIPs training was inadequate [4]. Survey data also revealed significant confusion regarding TIP standard operating procedures (SOP) [4]. Confusion regarding proper employment of CIP/TIP is observed not only during training exercises, but among forward deployed troops. Figure 3 shows an improperly employed thermal identification panel on a supply truck in Haditha, IZ. In addition to properly mounting CIP and TIP, the panels must be kept clean for maximum effectiveness. Panel visibility range through imagers is reduced by up to 50% when the panels are dirty [4].

Figure 3. Improperly Employed TIP, Haditha, IZ [From Marine Corpse Systems Command, Force Protection Office]

Next, service members must train to search for, and recognize, the signature of CIP and/or TIP equipped vehicles through thermal imagers as part of the targeting process. At Bold Quest 08, only one third of the surveyed pilots stated that they searched for TIPs using Forward Looking InfraRed (FLIR), thermal imagers, daylight electro-optics (EO), or the naked eye as a routine part of the ground target identification process [4]. Survey data shows the TIP maximum observable range is pilot dependent ranging from under 4 km to more

than 5 km [4]. Beyond 5 km, where most air-to-ground engagements are initiated, TIPs cannot be used to reliably identify friendly vehicles, greatly reducing the panels military utility. This appears to be the primary reason most pilots do not search for TIP as a routine part of the ground target identification process.

In addition to the human factors outlined above, CIP and TIP have several inherent vulnerabilities. Again, CIP and TIP are “always on” devices, intended to create a recognizable signature when viewed through a thermal imager. The goal of force protection and operational security, on the other hand, is to minimize friendly battlefield signatures in order to avoid observation by the enemy, in direct contrast to the conditions required for CIP to be visible. The fundamental problem with passive device solutions, like CIP and TIP, is that if friendly forces can obtain a positive ID on a friendly vehicle, so can a properly equipped enemy. Several threat countries employ thermal imagers and night vision devices [3]. From left to right, Figure 4 shows: Chinese Z-9WA night attack helicopter with day/night observing and tracking unit, Iranian-manufactured thermal weapon sight employed on the Zulfiqar Iranian main battle tank, and a Hezbollah Insurgent equipped with “Takavar” night vision monocular sight. Given the proliferation of NVD and thermal imagers, it a safe assumption that the enemy will have a capability. Post exercise surveys from JCIMS opposing forces (OPFOR)OPFOR Exploitation Assessment URGENT QUEST 05 show that 50% of OPFOR used CIP to identify blue forces (BLUFOR) during night missions while a staggering 90% of OPFOR used CIP to identify BLUFOR During Day missions [5].

Figure 4. Threat Imaging Capabilities [From Cline]

Another fundamental problem with CIP and TIP is the maximum observable range. Several field experiments show TIP maximum observable range as about 4–5 km and CIP maximum observable range of about 2 km when viewed through a thermal imager under ideal conditions. Under adverse weather conditions like rain, fog, or dust the maximum observable range is significantly reduced [4]. The maximum effective range of many ground-to-ground weapon systems that utilize thermal imagers for CID, is significantly greater than the maximum observable range of CIP. The problem is even worse in the air-to-ground mission area. Targeting and target engagement can take place at ranges of well over 10 nautical miles (nm). Significantly higher observable range is required for the panels to have any military utility in the air-to-ground mission area. Finally, CIP and TIP require a significant amount of surface area when properly outfitted on a tactical vehicle. Since tactical vehicles come in different shapes and sizes, there is no standard mounting kit for the panels. As a result, every vehicle's signature looks different through thermal imagers, further complicating the shooter's ability to rapidly ID friendly forces.

2. Infrared Beacons

The vehicle-mounted IR beacon is a device that emits a flashing near-infrared (NIR) signature visible (Figure 5). The IR beacon's emission is visible through NVD but invisible to the naked eye and through thermal imagers,

therefore only visible during night operations. When turned on, the beacon emits a flashing 880 nm IR pulse with a period of 1.3 seconds and pulse width of 20 milliseconds. The IR-14 Pheonix Jr. is a smaller IR beacon powered by a single 9-volt battery issued to individual troops (Figure 6). The IR-14 has the same emission pattern as the vehicle-mounted IR beacon.

Figure 5. Vehicle-Mounted Infrared Beacon [From Krause]

Figure 6. Pheonix IR Beacon [From Night Vision Systems, Retrieved from www.nightvisionsystems.com]

During BOLD QUEST 07, Pheonix beacons were issued to about half of the dismounted troops, while nearly all vehicles were equipped with an IR beacon. Survey data show several participants were concerned with a lack of SOP for IR beacon usage [5]. Seventy-five percent of pilots did not view IR beacons as part of their target engagement process and reported maximum observable ranges from significantly less than 2000 m to greater than 5000 m [5]. Twenty-four percent of the OPFOR claimed to have viewed IR beacons using

NVGs at some point in the exercise [5]. During the JCIMS OPFOR Exploitation Assessment 05 OPFOR commented that BLUFOR IR lights routinely revealed vehicle positions with a staggering 85 % of the OPFOR indicating that the presence of IR lights enabled them to engage BLUFOR [6]. One anecdotal comment from an OPFOR troop, “follow the blinking lights,” summarized the point well [6].

In summary, CIP, TIP and IR beacons require proper training in both employment and signature recognition to maximize effectiveness. Even with proper training, common battlefield conditions such as rain, fog, and dust can significantly degrade CIP/TIP effectiveness. Even under optimal conditions, these devices are not observable at ranges required for CID in many air-to-ground target engagement scenarios. Due to the “always on” nature of the devices, a properly equipped enemy can observe any of these JCIMS devices in order to identify us. We must do better to protect our service men and women.

C. A NEW APPROACH TO COMBAT IDENTIFICATION

Given the high impact of friendly fire incidents and the demonstrated limitations of current CID systems, a new approach is clearly needed. The Vehicle Mounted Identification Friend or Foe (VMIFF) Generation II (Gen II) is a device designed at the Naval Postgraduate School (NPS) (Figure 7) [7]. VMIFF is a triggered device that remains covert unless illuminated by a friendly laser target designator or laser range finder. VMIFF Gen II consists of two major subsystems, a photo receiver and a NIR light emitting diode (LED) array.

The VMIFF receiver consists of four photodiodes, one on each face of the device, and associated circuitry. In order to initiate a response from VMIFF, the receiver requires a recognized input signal. VMIFF will not respond to steady state lasers. At COBRA GOLD 07, VMIFF was successfully interrogated at a distance of 12 nm.

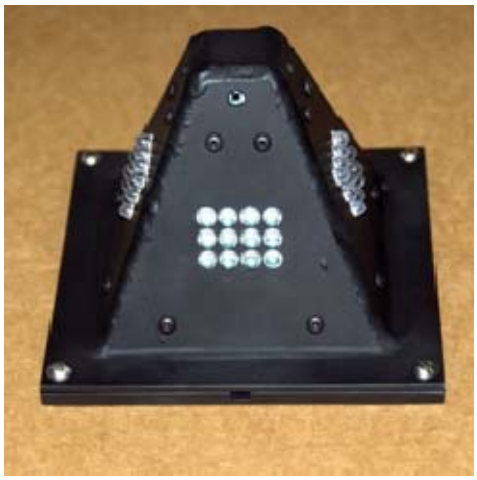

Figure 7. VMIFF Generation II [From Williams]

The current emitter consists of four banks of 12 NIR LEDs each. When the proper signal is received, all four banks blink, creating an omni-directional signal at approximately 3 Hz for 2 seconds with a 50% duty cycle. Once the emission is complete, VMIFF goes back to being completely covert, waiting for the next friendly laser illumination. At COBRA GOLD 07, VMIFF was successfully observed at about 16 nautical miles.

VMIFF offers several advantages over the current CID devices discussed above. First, VMIFF is covert unless interrogated by a friendly laser, providing an instantaneous response to the shooter when illuminated by a target laser designator or range finder. As a result, the enemy cannot exploit VMIFF as easily as the legacy marking systems. Second, VMIFF is triggered by the lasers already part of target engagement procedures, thus requiring minimal change to existing SOPs. Because the same VMIFF can be mounted on any piece of rolling stock, its signature is standardized, making identification of friendly vehicles much easier.

VMIFF Gen II's major limitation is that it is only visible at night using NVD. The device is not visible through thermal imagers used by many shooters during the target engagement process. In order to be visible through thermal imagers

for both day and night operation, a thermal emitter must be added. The purpose of this thesis is to evaluate commercially available and cost-effective possibilities for creating such a signature.

The goal of this thesis work is to procure commercially available sources of MWIR radiation, and evaluate them for suitability in VMIFF applications. At the conclusion of this research, a design for VMIFF Gen III with integrated MWIR response is proposed. At the outset, the following assumptions were made:

1) The laser sensor and NIR LED bank from VMIFF Gen II could be used on VMIFF Gen III.

2) A solid state design with no motors or moving parts is desired.

3) The devices must be pulsed at approximately 1 to 3 hertz (hz) for distinguishability and recognizability.

THIS PAGE INTENTIONALLY LEFT BLANK

II. MIDWAVE INFRARED RADIATORS

Most military aircraft are equipped with tactical infrared imagers that are sensitive to photons in the wavelength range from 3–5 micrometers (microns). While infrared imagers sensitive to 8–12 micron photons exist, they are not typically deployed on the tactical platforms of interest. While additional measurements were made using a single element 8–12 micron detector and microbolometer camera, this thesis focuses on the generation of a 3–5 micron MWIR signature. Discussion of the types of infrared cameras deployed on different platforms is beyond the scope of this thesis.

There are several approaches to generating a mid-wave IR emission for visibility in thermal imagers. Three are discussed below: blackbody radiators, quantum cascade lasers, and IR light emitting diodes.

A. PHYSICAL APPROACHES

1. Blackbody Radiators

The most straightforward way to create a mid-wave IR emission is to heat a material to high temperature. An ideal blackbody perfectly absorbs all incident electromagnetic radiation. If the body is in thermal equilibrium with its surroundings, it must emit the same amount of energy in the form of electromagnetic radiation. The electromagnetic radiation emitted by an ideal blackbody is dictated by Planck's radiation law:

$$I(\lambda,T)=\frac{2\pi c^2 h}{\lambda^5}\frac{1}{e^{\left(\frac{hc}{\lambda kT}\right)}-1}$$

where $I(\lambda,T)$ is the intensity as a function of wavelength and temperature in watts per unit area per wavelength, λ is the wavelength in meters, $c=3\text{x}10^{8}\ \text{m/s}$ is the speed of light, $h=6.6261\text{x}10^{-34}\ \text{J}\bullet\text{s}$ is Planck's constant, $k=1.3807\text{x}10^{-23}\ \text{J/K}$ is Boltzmann's constant, and T is the temperature in Kelvin.

An object in thermal equilibrium with its surroundings will absorb and emit equal amounts of electromagnetic radiation. An object that is warmer than its surroundings will emit more radiation than it absorbs in order to move toward thermal equilibrium. Figure 8 shows the spectral emission of an ideal blackbody radiator at 300 and 500 Kelvin (K).

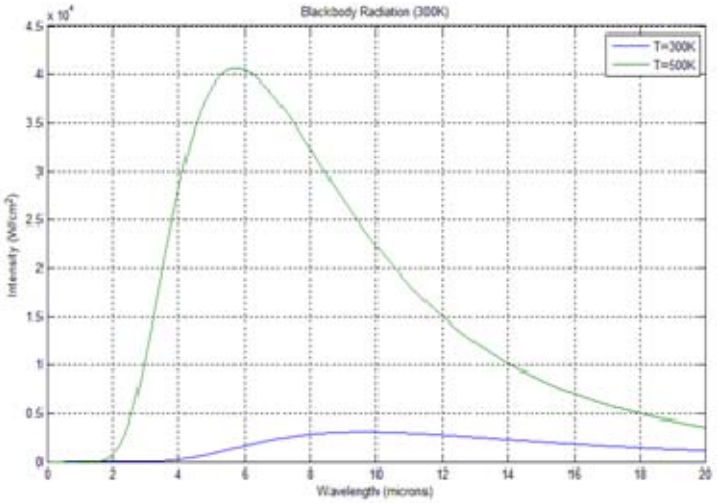

Figure 8. Radiated Power per Unit Area Versus Wavelength for Two Radiators at 300K and 500K

As the temperature of the blackbody increases, the peak emission wavelength becomes shorter. The peak emission wavelength can be determined by setting $\frac{dI}{d\lambda} = 0$ and solving to obtain Wien's displacement law:

$$\lambda_{\max} T = 2.808\text{x}10^{-3}\, mK$$

For a given blackbody, the emission at a given wavelength always increases with increasing temperature. Comparing the blackbody radiation curves in Figure 8, it is clear that as temperature increases, emission increases the most near the peak, and then less significantly at higher wavelengths. The important point here is that emission at a given wavelength does not scale linearly with temperature. To understand the spectral emission at a given

wavelength for two different temperatures, it is necessary to plot the blackbody radiation curve. Eventually, if temperature is increased enough, the body will emit visible light, i.e., the sun, tungsten filament light bulbs, etc.

To obtain the total power radiated per unit area, I must be integrated over all wavelengths to obtain the Stefan-Boltzmann law:

$$R(T) = \varepsilon\sigma T^4$$

where ε is the unitless emissivity of the body and $\sigma = 5.6704\text{x}10^{-8}\ \text{W}/\left(\text{m}^2\text{K}^4\right)$ is the Stefan-Boltzman constant. The emissivity is an experimentally determined ratio of a real material's emission divided by the emission of an ideal blackbody and is always less than one.

For the VMIFF application, we are interested in maximizing the emission of photons having a wavelength between 3 and 5 microns. Clearly, increasing temperature will increase the MWIR photon count, but to avoid observation with the naked eye, the device cannot emit any visible light. To be recognizable and produce a distinguishable signature in the thermal imager's view screen, the devices must be modulated to create a blinking signature. This means the transient response of the blackbody source, affected primarily by device mass and thermal conductivities, will be of interest. Finally, the efficiency of a blackbody source will always be limited by the fact that a significant amount of the power radiated will lie outside the desired 3–5 micron wavelength range.

2. Infrared Light Emitting Diodes

Semiconductors are materials with the proper number of electrons to exactly fill an outer electron shell. When bonded as a solid, the allowed energy states form bands, with a filled valence band and an empty conduction band as the ground state. The energy required for an electron to move from the valence band to the conduction band is called the band gap energy. Semiconductors behave like insulators at absolute zero, $T = 0\ \text{Kelvin}$, because all charge carriers must be in their lowest energy state and are therefore bound to a specific atom in

the lattice. As temperature increases, there is a finite probability that some of the charge carriers will gain enough energy to overcome the band gap and disassociate with its atom creating an electron-hole pair.

Incident electromagnetic radiation can also generate electron hole pairs if the energy of a single photon is greater than the band gap energy. In order to increase the number of a specific type of charge carrier, impurities are added to the semiconductor lattice. This process is called doping and the energy required to liberate a dopant charge carrier is significantly less that the energy require to liberate a charge carrier from a semiconductor atom. In either case, the charge of the sample has not changed, however the excited charge carrier is now free to move about the lattice and conduct electricity. When an electron and hole are sufficiently close to one another, recombination will occur and the energy that was absorbed in the generation of the pair is released in the form of heat in the lattice or a photon. To create desired electromagnetic radiation, light emitting diodes (LED) leverage the electron hole pair recombination, resulting in photon emission as a result of minority carrier injection in a diode structure.

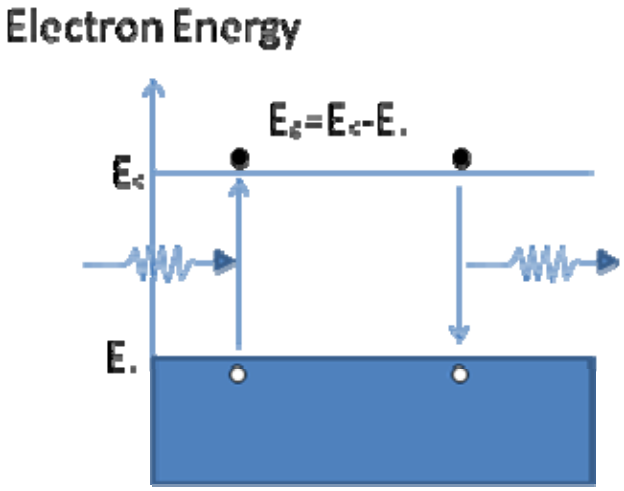

Figure 9. Electron Hole Pair Generation and Recombination

Diodes are constructed by joining two pieces of oppositely doped semiconductor material, called p-type for positively doped and n-type for negatively doped. When the diode is forward biased, charge carriers are injected into the region close to the interface where there is a very high probability of recombination. In the case of LEDs, the dominate recombination mechanism will result in the creation of a photon. The energy of the emitted photon is approximately equal to the band gap of the semiconductor:

$$E_g = h\nu = \frac{hc}{\lambda} = \frac{1.24}{\lambda[microns]}[eV] \text{ or } \lambda = \frac{hc}{E_g} = \frac{1.24}{E_g[eV]}[microns]$$

In order to generate 3–5 micron wavelength photons, $E_g = 0.413\ eV$ to $0.248\ eV$ is required. Table 2 shows the band gap energies for some common semiconductor materials [8].

Material	Symbol	Band gap (eV) @ 300K
Silicon	Si	1.11
Germanium	Ge	0.67
Silicon carbide	SiC	2.86
Aluminum antimonide	AlSb	1.6
Gallium(III) phosphide	GaP	2.26
Gallium(III) arsenide	GaAs	1.43
Gallium(III) nitride	GaN	3.4
Gallium antimonide	GaSb	0.7
Indium(III) nitride	InN	0.7
Indium(III) phosphide	InP	1.35
Indium(III) arsenide	InAs	0.36
Cadmium telluride	CdTe	1.49
Lead(II) sulfide	PbS	0.37
Lead(II) selenide	PbSe	0.27
Lead(II) telluride	PbTe	0.29

Table 2. Band Gap Energy of Common Semiconductors [From Streetman and Sanjay]

Semiconductors that have a band gap energy low enough to generate MWIR photons are generally very soft materials and unable to handle the current required to produce a usable amount of electromagnetic radiation. LED light is nearly monochromatic as opposed to blackbody radiation, which produces photon of many wavelengths. As a result, more of the emitted radiation will be usable than in a blackbody radiator.

3. Quantum Cascade Lasers

Quantum cascade lasers (QCL) are another device that can create 3–5 micron wavelength photons. Electron tunneling from one quantum well through a barrier to another quantum well is the photon generation mechanism in a QCL. The device consists of many alternating layers of semiconductor materials to create an alternating series of potential well/ barrier/ potential well/ barrier, etc. (Figure 10). The material and thickness of each layer is selected based on band gap engineering in order that the device will generate photons of a specific wavelength. Any free electrons in the device will quickly drop into the quantum wells in order to lower their energy. The potential barrier is thin enough that the probability of an electron tunneling from one potential well to another is high. At this point, no photons have been created.

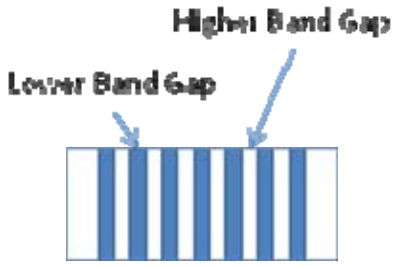

Figure 10. Representation of QCL Semiconductor Layers [From Quimby]

When a bias voltage is applied, a potential difference is created along the growth axis but the device will maintain the quantum well properties (Figure 11). Electrons injected into the left side of the device fall into the first potential well. The electron will occupy the ground state of the first potential well until it tunnels

through the barrier to the second well, which happens quickly because the barrier is designed to have a high probability of tunneling. Once it arrives in the second well, it quickly decays to the ground state of the second well. This small amount of energy lost by the electron creates the photon.

Quantum cascade lasers can be designed to generate light with wavelengths from 3 to 160 microns [9]. Because the wavelength of the emitted photons depends primarily on the width of the quantum wells, they can be fabricated using more robust semiconductor materials than IR LEDs. As a result, QCL can generate significantly more output power, as large as tens of watts, versus LED solutions. QCL light is very nearly monochromatic due to the stimulated nature of the radiation.

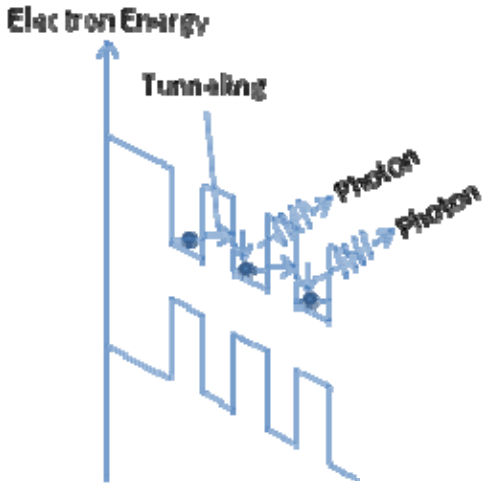

Figure 11. Photon Generation in QCL [From Quimby]

B. COMMERCIALLY AVAILABLE DEVICES

A comprehensive market survey was performed to identify commercially available MWIR sources using the approaches discussed in the beginning of this chapter. The criteria for selection included cost, maximum irradiance, and modulation speed. This section contains general information regarding the cost, physical design, and operating parameters of the different devices.

1. Blackbody Radiators

Three blackbody radiators were selected for testing, the Cal Sensors SVF360-8M3, ICX Photonics NL84ACC, and Hawkeye Technologies IR-50. The devices used in this research all had Calcium Fluoride (CaF_2) windows. The basic operation of all three devices is the same: when a voltage is applied across the filament, a current is induced, the active element heats up and emits as a blackbody. For circuit design purposes, the radiators behave like a simple resistive elements. All devices claim to have low thermal mass enabling pulsed operation and high emissivity.

a. Cal Sensors SVF360-8M3

The SVF360-8M3 is a 2-lead device in a standard TO-8 package that costs $86.00 per device, or less for large quantity orders. The device leads extend through the bottom of the can to a thin flat Nichrome foil filament with 16.8 mm² of active area. The plane of the foil is perpendicular to the window. The device has a parabolic reflector on both sides of the foil to direct the energy out of the device along the optical axis of the window. The foil has an emissivity of $\varepsilon = .88$ and operating temperature of 1000 K. Exceeding this temperature will destroy the foil. The device requires a heat-sink when operated at maximum recommended power. The SVF360-8M3 operates at a peak DC input power of 2.6 W which corresponds to an operating temperature of 1000 K.

b. ICX Photonics NL84ACC

The NL84ACC is a 8-lead device in a standard TO-8 package that costs $71.25 per device, or less for large quantity orders. The device leads extend through the bottom of the can to a four Nichrome filaments with total surface area of 29 mm². The filaments are mounted parallel to the window. The filaments are ion-beam treated to raise the emissivity to $\varepsilon = 0.9$ in the 3–5 micron wavelength region. The operating temperature of the device is about 1050 K.

The SVF360-8M3 operates at a peak DC input power of 6 W, 1.5 W per filament. Exceeding this power will destroy the filaments. The device requires a heat-sink when operated at maximum recommended power.

c. HawkEye Technologies IR-50

The IR-50 is a 3-lead device in a standard TO-5 package that costs $62.00 per device, or less for large quantity orders. Two of the device leads extend through the bottom of the can to a square, thin film resistor made of diamond-like carbon. The active area of the resistive film is 2.9 mm². The third lead is used to ground the can. The planar surface of the emitter is parallel to the window. The foil has an emissivity of $\varepsilon = .80$ and an operating temperature of 1020 K. Exceeding this temperature will destroy the carbon film. The device requires a heat-sink when operated at maximum recommended power. The IR-50 operates at a peak DC input power of 0.96 watts, which corresponds to an operating temperature of 1020 K.

Table 3 shows input power, filament surface area, filament material, and filament operating temperature for the Cal Sensors, ICX, and IR-50 devices. The data was compiled for the device data sheets.

	Input Power	Collimator	Filament Surface Area	Filament Material	Operating Temperature
Cal Sensors SVF360-8M3	2 W	Yes	16.8 mm²	Nichrome	1000 K
ICX Photonics NL84ACC	6 W	No	29 mm²	Nichrome	1030 K
HawkEye Technologies IR-50	0.95 W	No	2.89 mm²	Porous Carbon	1020 K

Table 3. Specification Sheet Information for Cal Sensors, ICX, and IR-50 Devices [From Device Specification Sheets]

2. Infrared Light Emitting Diodes

Ioffe Light Emitting Diodes in St. Petersburg, Russia has developed optically immersed LEDs that emit 3–4 micron wavelength photons. The devices are in a threaded metal package with a positive and negative wire on the back of the package. Optical immersion refers to the round silicon window designed to better couple the light generated by the LED to the atmosphere. The maximum recommended current for operation at 1–3 Hz is 200 mA. The device requires a heat-sink when operated at maximum recommended power. Indium-gallium arsenide (InGaAs) and Indium arsenide-antimonide (InAsSb) hetrostructures are the semiconductor materials used in the LEDs. The MWIR LEDs cost $72.00 per device.

3. Quantum Cascade Lasers

Daylight Solutions, Inc. offers several QCLs that emit in the MWIR. The power of available lasers range from milli-watts to tens of watts. The cost of these lasers range from $20,000 to $500,000, respectively. Though QCLs are a very promising technology for VMIFF applications, they are restrictively expensive at this time, on the order of tens of thousands of dollars for output power on the order of milliwatts. The biggest advantage to the use of a QCL over blackbody radiators and MWIR LEDs in VMIFF applications, is the generation of a specific wavelength determined by the geometry of the device. This, coupled with the directionality of the laser output, would result in observation at long range. This key advantage means that the QCL cannot only be designed to a wavelength within the 3–5 micron atmospheric window, but to the wavelength that best excites the thermal imaging array. This means that more of the output power is coupled to the imager increasing visibility and delectability. In addition, there is no radiation outside the MWIR that might be detected by other battlefield sensors, reducing the enemies ability to detect VMIFF. Due to the restrictive cost, a QCL was not purchased for this thesis work.

III. SINGLE MICRORADIATOR EMITTER MEASUREMENTS

A. TEST METHODOLOGY

This chapter discusses single device measurements taken using single element detectors. The devices were tested for maximum DC power irradiance, rise time, fall time, frequency response and off axis irradiance when driven at the maximum power recommended by the manufacturer. The goal of this portion of the research was to establish a quantitative comparison of the fundamental operating characteristics of each device. The performance data collected are critical to selecting the device that offers the most attractive balance of maximum observable range, cost, power consumption and transient characteristics for the VMIFF MWIR emitter design.

1. Device Setup and Drive Circuit

All the devices tested require a heat sink to operate at maximum power. Four by five inch aluminum heat sinks were fabricated for each device. Each heat sink can house up to 12 devices in a three-device by four-device array (Figure 12). For the single device measurements taken in this chapter, one device was mounted in the heat sink. Metallic paste was used to improve thermal conductivity between the device and the heat sink.

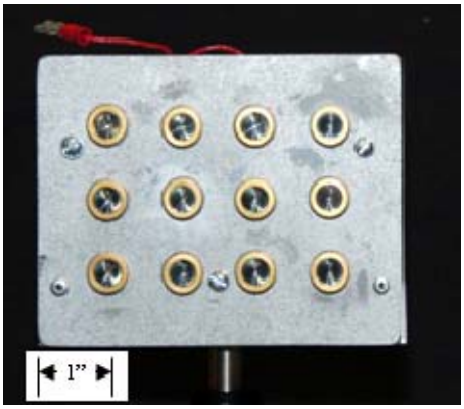

Figure 12. Cal Sensors Panel With Devices

Most tactical vehicles use a 24-volt electrical system, consisting of multiple 12-volt lead acid batteries in series and parallel. All the circuits were built to operate on 12 or 24 volts DC using a lead acid battery bank. In addition to demonstrating compatibility with vehicle electrical systems, this power decision made it easy to take the emitters to the field because no laboratory power supplies were required for operation.

Based on the initial assumptions discussed at the end of Chapter I, a square-wave generating circuit was built to modulate the emitters. The circuit was designed around a standard LM556 dual-timer chip (Figure 13). The output of the circuit is a 0 to 12 V square-wave fully adjustable from 1 Hz to 15 Hz with adjustable duty cycle. All experiments were done using 50% duty cycle. 15 Hz was selected as the upper frequency limit because most imagers operate at 30 frames per second. Potentiometer 1 (Pot 1) adjusts the frequency while Pot 2 adjusts the duty cycle.

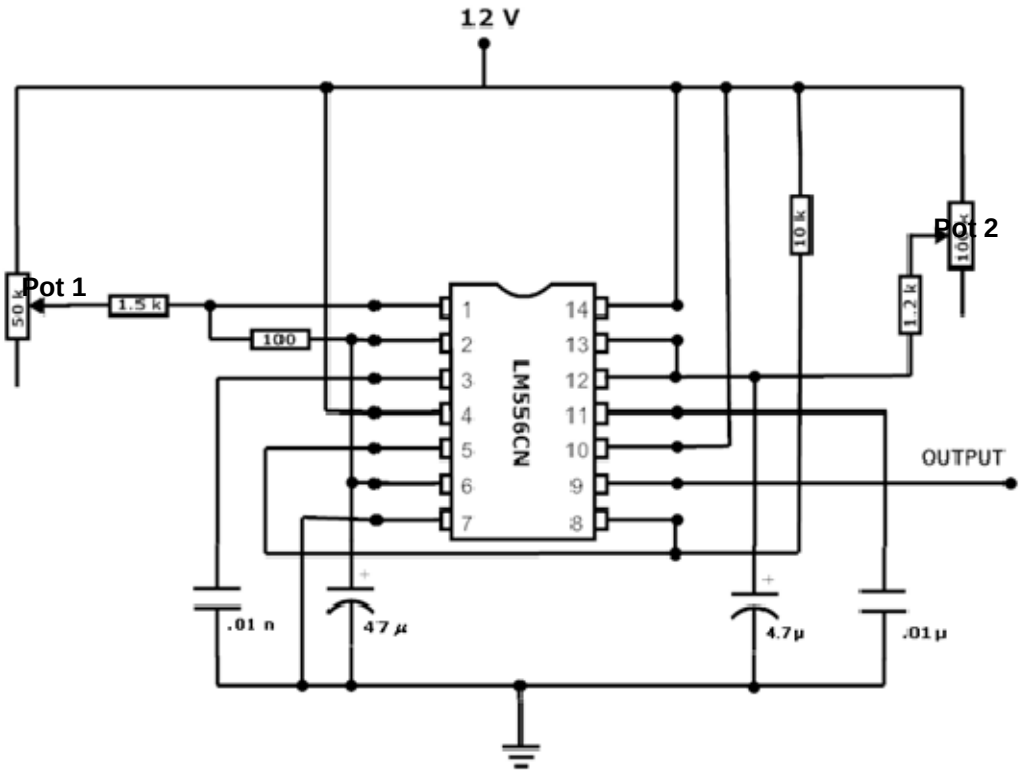

Figure 13. Square-wave Generating Circuit

The output of the square-wave generating circuit was applied to the gate of an IRF530 power MOSFET that switched the emitters on and off. For circuit design purposes, the emitters were modeled as simple resistors. When the gate of the MOSFET is positive, a current path is established between the drain and source and the radiator emits. When the gate of the MOSFET is zero volts, no current flows from the drain to the source and the emitter is off (Figure 14). An additional resistance was added to the device resistance. The amount of resistance added was chosen such that the emitter power was at about the maximum recommended by the manufacturer. In order to improve overall power efficiency, future circuit designs should eliminate the additional resistance and include a dc to dc converter circuit. Pot 3 is a simple thumb wheel pot used to enable or disable the square-wave at the gate. It was used as the emitter "on/off" switch.

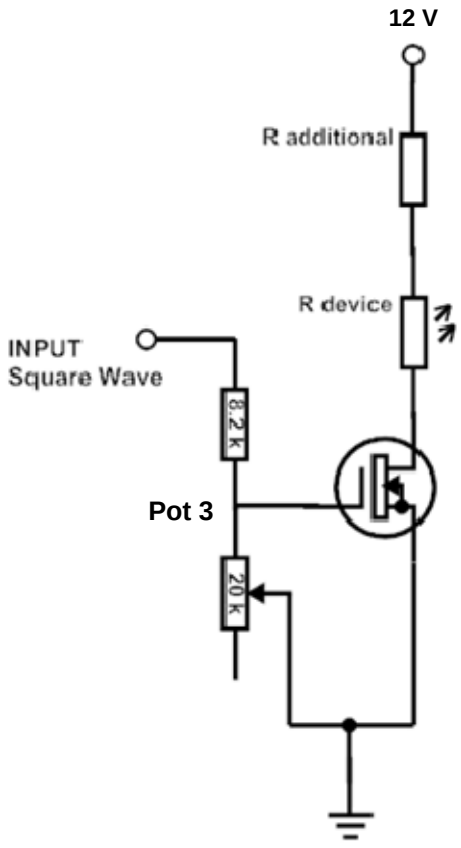

Figure 14. Panel Switching Circuit

Two detectors were used to characterize the devices. A liquid nitrogen cooled, single-element Cincinnati Electronics Indium Antimonide (InSb) detector was used for characterization in the 3–5 micron wavelength regime (Figure 15, Right). A liquid nitrogen cooled, single-element Infrared Associates Mercury-Cadmium Telluride (MCT) detector was used for characterization in the 8–12 micron wavelength regime (Figure 15, Left). The spectral response curve for the InSb detector is not available. Figure 16 shows the MCT detector spectral response curve. A band-pass filter was used to block wavelengths shorter than 8 microns and longer than 13.5 microns. Figure 17 shows the response curve of the filter. No additional optics were used to focus the IR radiation.

Figure 15. Single Element 8–12 µm (left) and 3–5 µm (right) Detectors

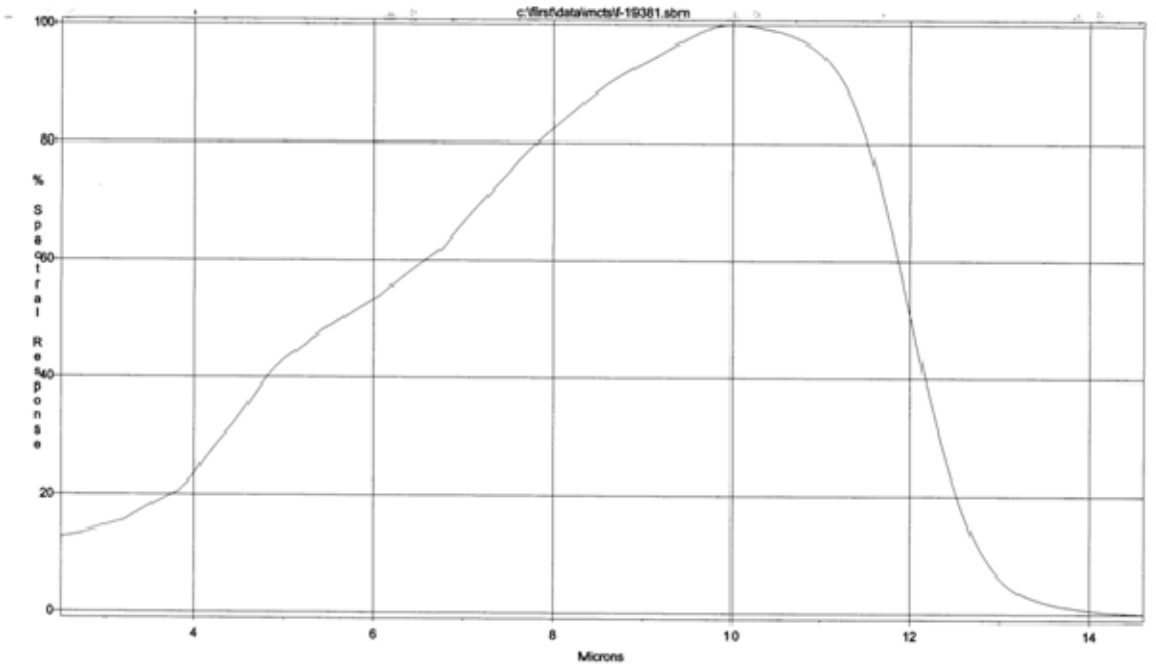

Figure 16. MCT Detector Spectral Response [From Detector Specification Sheet]

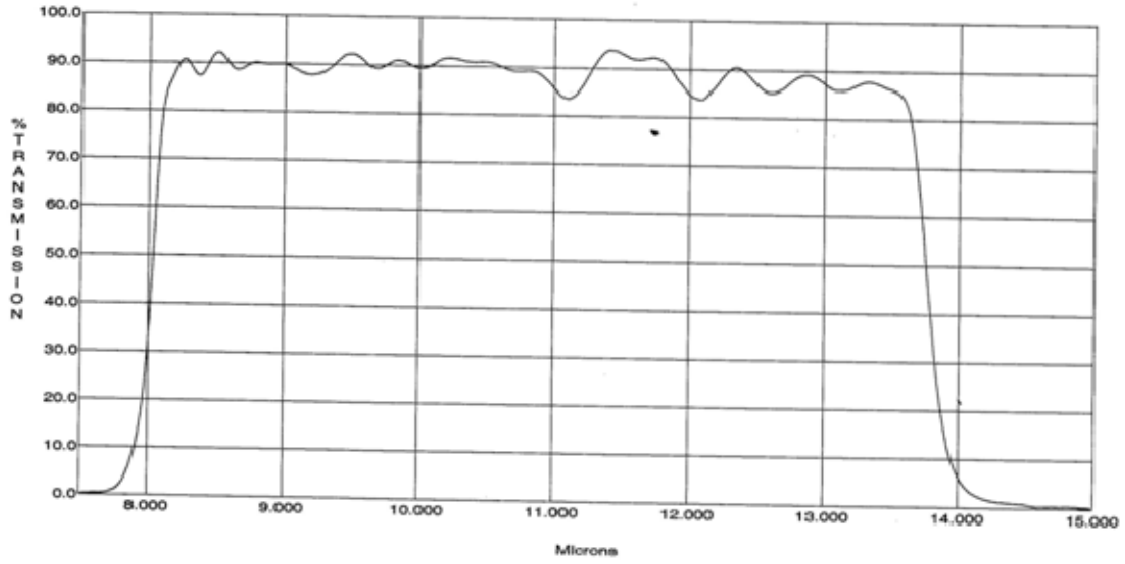

Figure 17. 8–13.5 µm Band-Pass Filter Transmittance [From Filter Specification Sheet]

Initial measurements where made using the two circuits described above. The detector output voltage was read, displayed, and saved using an oscilloscope. The collected data were saved on a 3.5 inch floppy disk and transferred to a computer for analysis. There are several problems with this set-up. First, data capture and transfer to computer were very time consuming and cumbersome. Second, controlling turn on and turn off with pot 3 made it nearly impossible to capture emitter behavior during turn on and turn off. The transient data are very important for VMIFF design purposes because the emitter bank should turn on fast when interrogated for rapid recognition. The emission should also turn off fast to reduce the likelihood of enemy observation. More sophisticated computer-controlled initiation and data capture were required. In order to gather the required data, a LabVIEW program was written to control the circuit and data capture.

2. Bench Setup

In the second-generation set-up, LabVIEW initiated a two-second long, 9 mA current pulse from a Keithley 220 Programmable Current Source. Note, the Keithley is programmed to turn the current off after two seconds. LabVIEW provided the initiation pulse to the Keithley only. The current was placed on the non-inverting input of a LM311 comparator with a 1 kΩ pull down resistor to create 9 V on the input (Figure 18). The voltage divider across which the square-wave was applied increased the low voltage so that the signal varied between 6 and 12 V. This new square-wave was applied to the inverting input of the comparator. When the Keithley output current was zero, the output of the comparator was zero. When the Keithley output current was 9 mA, the comparator output was a 0 to 12 V square-wave inverted from the original input. Note, the square-wave signal generating circuit operates independent of this circuit. As a result, the square-wave generator was at an arbitrary point on the waveform when the Keithley current source initiated the two-second data collection window.

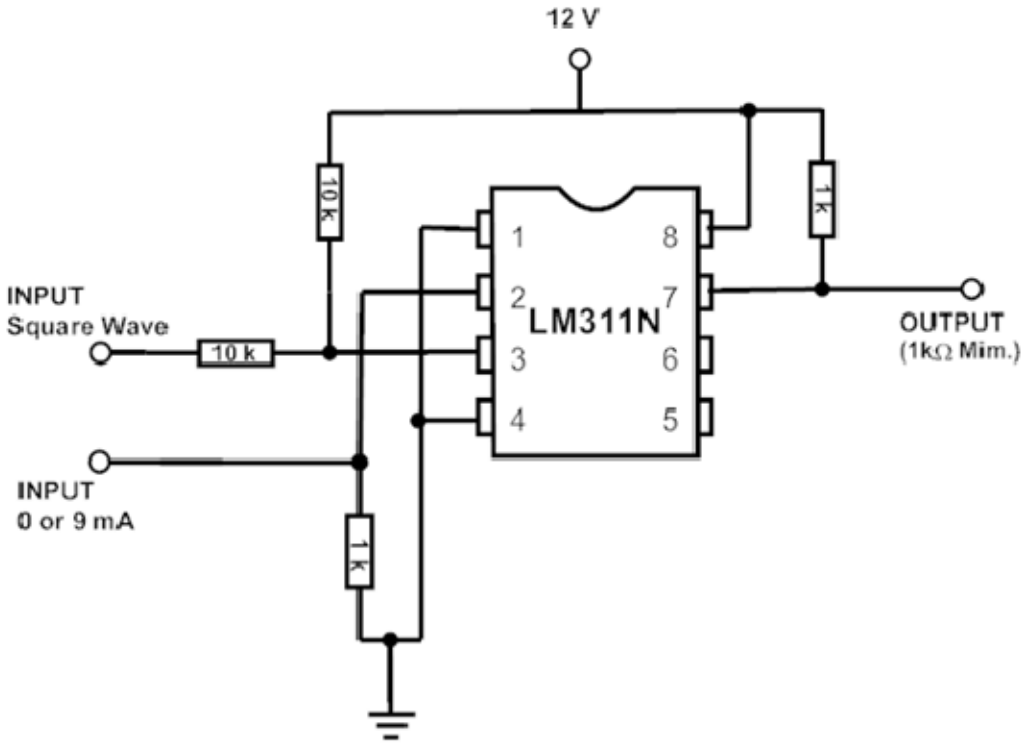

Figure 18. LabVIEW Interface Circuit

LabVIEW was also used to capture and save the detector and emitter voltages. It is important to collect both voltages so that the response curves can later be time shifted to align detector response from the different emitters. Hereafter, data collected by LabVIEW shall refer to the detector voltage unless specified. Once the collected data are zeroed to eliminate voltage due to background radiation, the data are assumed to be a direct measurement of device irradiance in arbitrary units. For the purposes of the laboratory measurements, the relative irradiance between devices is the important figure of merit, not absolute irradiance.

A National Instruments NI USB-6211 digital to analog converter (DAC) was used to digitize the analog voltages. The LabVIEW program took a total of four seconds of data at a 1 ms sample rate each run. In chronological order, a sample run consisted of the following events: First, LabVIEW collected 50 ms of data with the emitter off to establish the background signal baseline. Next,

LabVIEW initiated the two-second pulse to drive the emitters and collected data with the emitter on, either dc or modulated by the square-wave. Finally, LabVIEW continued to collect data for the remainder of the four second window capturing the cool-down behavior of the emitter. Figure 19 shows the experimental bench setup. The emitter panel and detector were mounted on an optical table to ensure proper alignment.

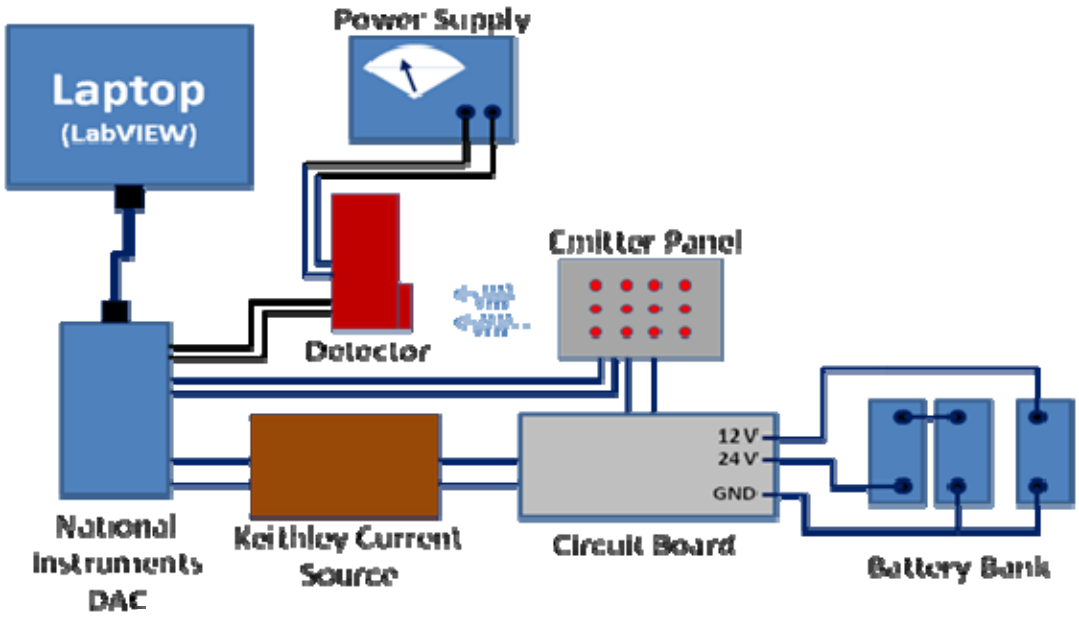

Figure 19. Experimental Bench Set-up

B. 3–5 MICRON EMISSION CHARACTERIZATION

The devices were characterized using the circuit and bench set-up described in Section A. The distance between the emitter and detector was 10 cm for all 3–5 micron measurements. The frequency of the signal applied to the inverting input was varied between DC, 1 to 10 Hz in 1 Hz increments, and 15 Hz. SigmaPlot was used to graph detector voltage data. Each data graph shows the detector response for one modulated frequency. The DC response curve is

also included to show the peak irradiance at that particular frequency versus maximum device capability. Figure 20 and Figure 21 show the Cal Sensors device 1 Hz and 3 Hz data, respectively.

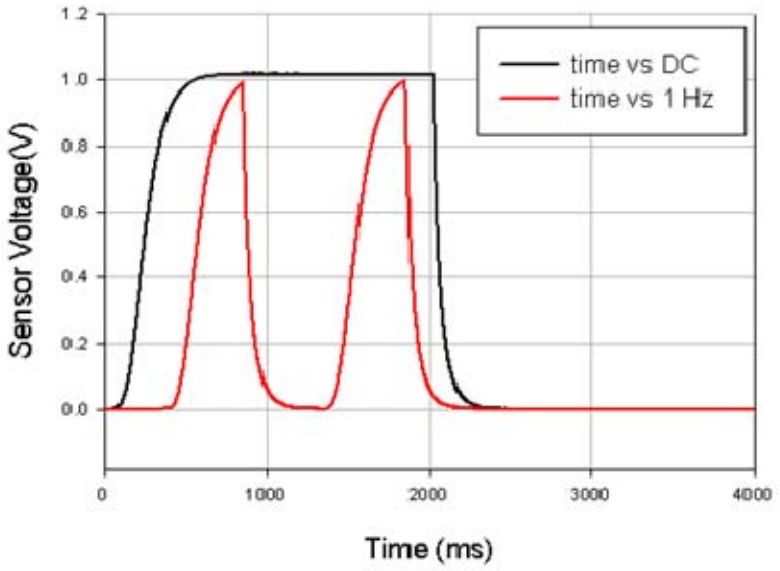

Figure 20. Detector Output Versus Time for Single Cal Sensors Device, On-Axis

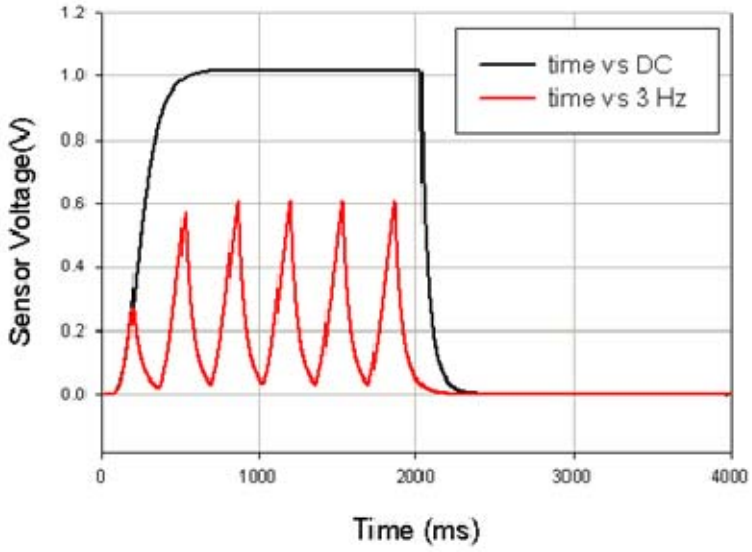

Figure 21. Detector Output Versus Time for Single Cal Sensors Device, On-Axis

On-axis, single-device, 3–5 micron response curves for each device are located in Appendix B. Analysis of the results follows below.

1. Maximum Irradiance at Constant Power

The maximum, on-axis irradiance, with the device driven at the maximum DC power recommended by the manufacturer, was the first property studied. The sensor voltage curves for each device were plotted on the same graph for side-by-side comparison (Figure 22). Figure 22 shows that the two-second driving window was sufficient to allow all devices to reach steady state operation. The maximum on-axis irradiance of the Cal Sensors device was the greatest and registered a sensor voltage of 1.015 V. The maximum on-axis irradiance of the ICX device was second strongest at 0.835 V, 82% of the irradiance of the Cal Sensors device. The IR-50 emits 6% of the radiation of the Cal Sensors device with a maximum sensor voltage of 0.061 V.

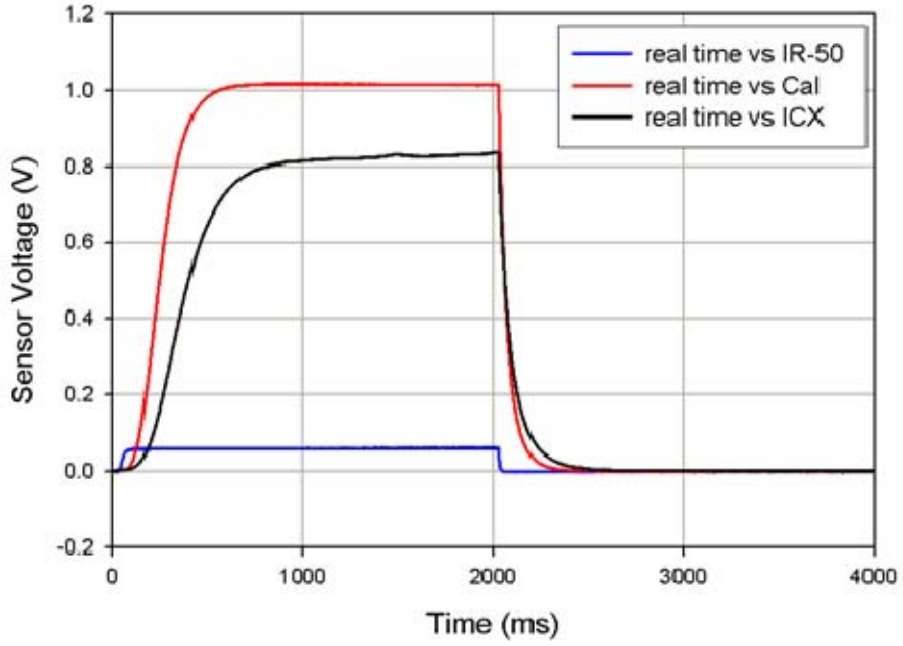

Figure 22. DC Response of IR-50, Cal Sensors, and ICX Devices

2. Device Rise and Fall Time

In order to compare the rise times, the DC data for each device were imported to a SigmaPlot spreadsheet. The data for each device were time shifted so that the device voltage turned on at time t=0. Next, the normalized sensor voltages for each device were obtained by dividing the sensor voltage by the maximum voltage recorded for the data set. The normalized signals for each device were then plotted on the same graph for comparison (Figure 23). The normalized data show that the IR-50 reaches over 90% of its maximum irradiance in approximately 57 ms. By comparison, the Cal Sensors device is second fastest requiring 372 ms to reach 90% of maximum irradiance. Finally, the ICX device requires 606 ms to reach 90% of maximum Irradiance and is the slowest device.

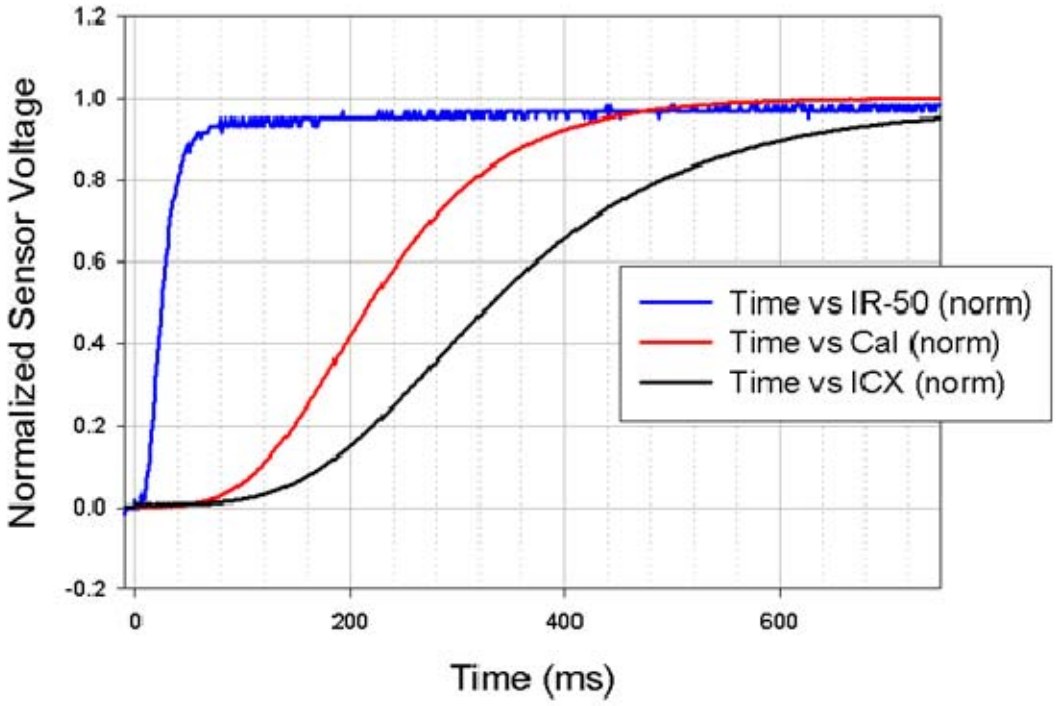

Figure 23. Normalized Transient Rise Response of IR-50, Cal Sensors, and ICX Devices

Next, the short term transient sensor voltages for each device were plotted (Figure 24). Due to the speed of the IR-50, it emits more 3–5 micron wavelength IR radiation than the Cal Sensors device for the first 99 ms if turned on simultaneously. The IR-50 emission is greater than the ICX device for the first 146 ms of operation.

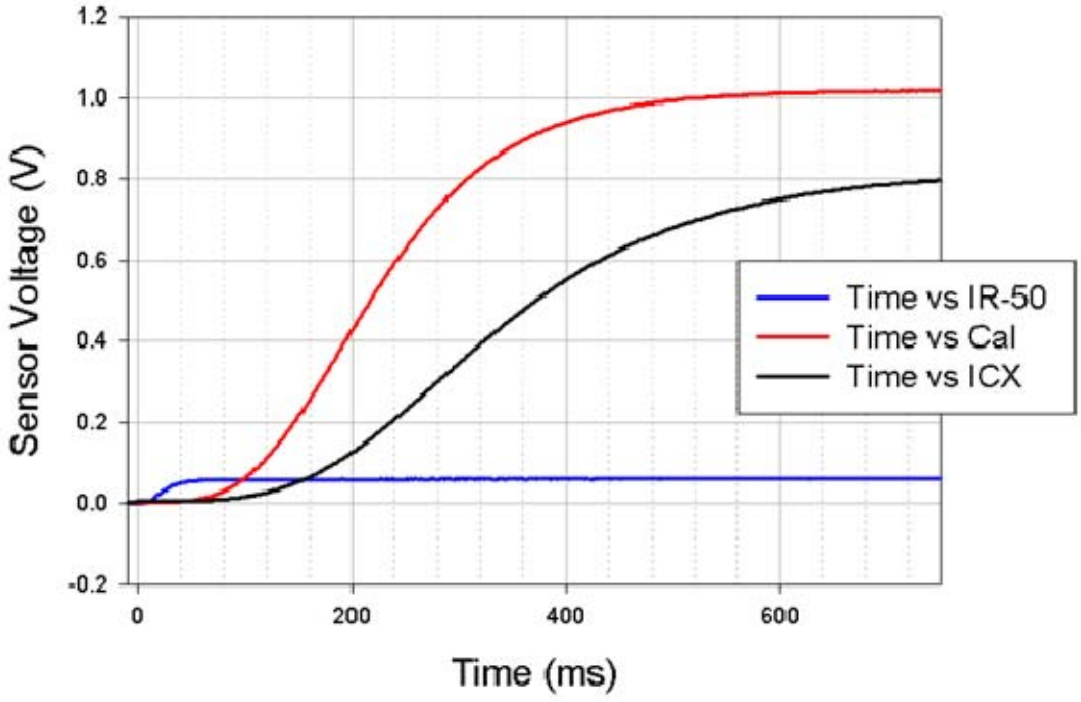

Figure 24. Rise Time Response Comparison of IR-50, Cal Sensors, and ICX Devices

The fall times were studied next. The data are now time shifted so that the device voltage turned off at time t=0. Figure 25 shows the normalized fall time data. The data show that the IR-50 falls to 10% of its maximum irradiance in approximately 12 ms. The Cal Sensors device shows the second fastest fall time requiring 117 ms to fall to 10% of maximum irradiance. Finally, the ICX device requires 178 ms to fall to 10% of maximum Irradiance and is the slowest device.

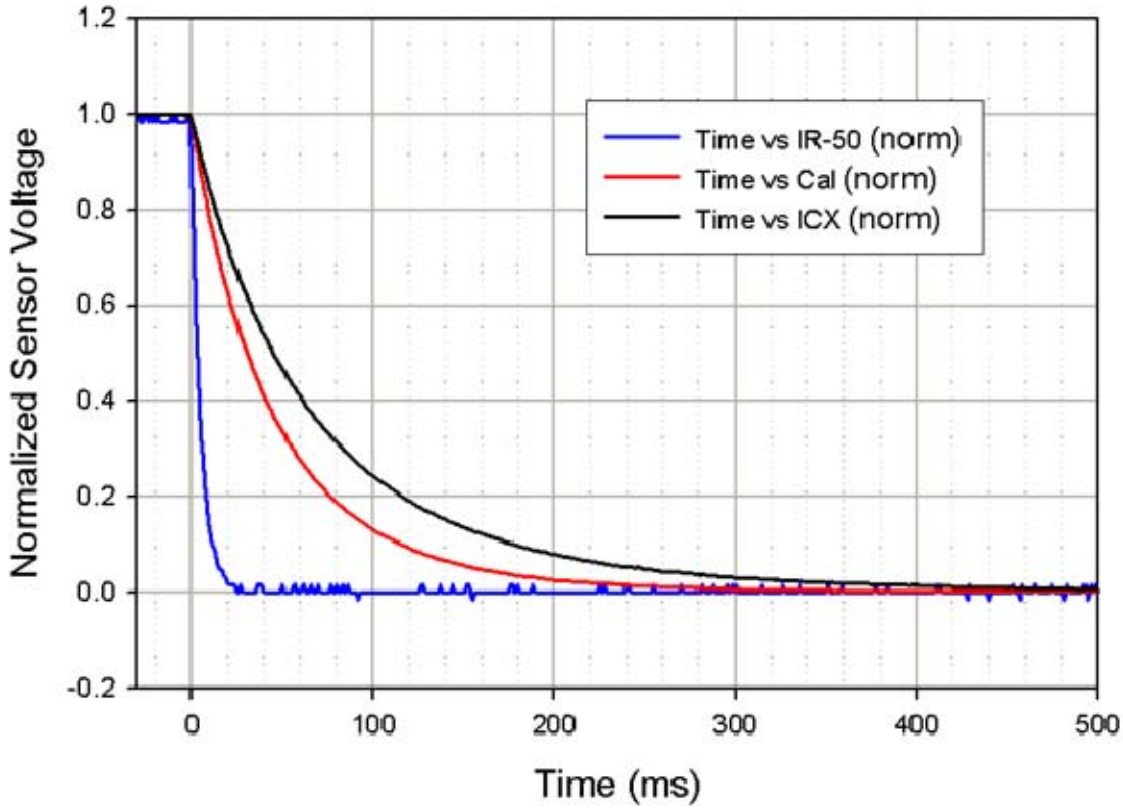

Figure 25. Normalized Transient Fall Response of IR-50, Cal Sensors, and ICX Devices

Figure 26 shows the actual fall time sensor voltages for each device. Again, the speed of the IR-50 is evident. The graph also shows the Cal Sensors device's emission of 3–5 micron radiation is less than that of the ICX device within 29 ms of turn off. The IR-50 has much less active filament area and a much better heat-sink, via the substrate that the filament is grown on, and therefore cools much faster. The Cal Sensors device has less filament volume to heat and cool leading to faster response than the ICX device.

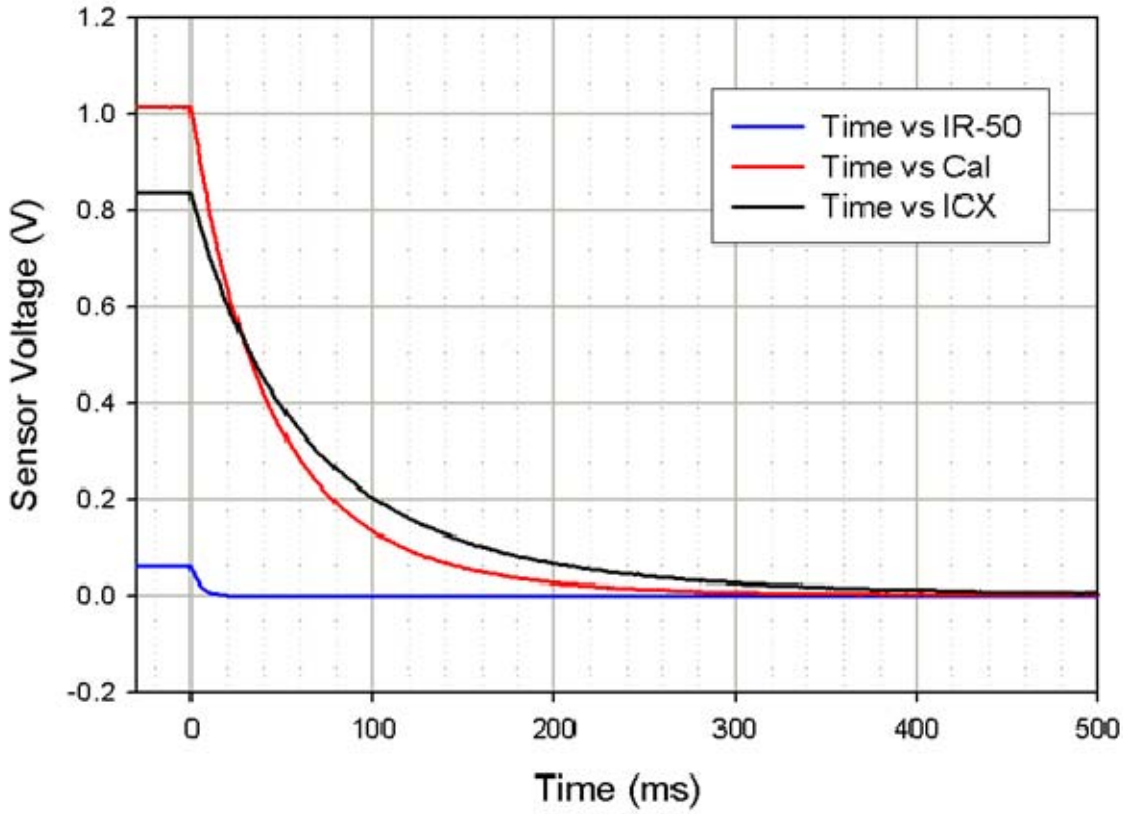

Figure 26. Fall Time Response Comparison of IR-50, Cal Sensors, and ICX Devices

3. Frequency Response

The frequency response of the devices were studied next. Data were taken with the square-wave frequency modulated from zero to ten Hz in one-Hz increments and fifteen Hz. In general, VMIFF Gen III's thermal emitter should have the highest possible irradiance during the "on" portion of the modulating signal for thermal imager observation at long distances. During the off portion of the modulating signal, the thermal emitter should have the lowest possible irradiance so that no signature is visible through the thermal imager. If the emitter has these basic characteristics at the desired modulating frequency, the emission will appear to flash in the thermal imager for easy recognition and discernability from other battlefield emissions.

a. Maximum Irradiance versus Frequency

The maximum sensor voltage recorded during the four-second data capture is taken to be a measure of the device's maximum irradiance. Figure 27 shows the maximum sensor voltage versus frequency for all three devices. The Cal Sensors device has the highest maximum irradiance at all frequencies. The normalized maximum sensor voltage for a given frequency is obtained by dividing the maximum sensor voltage detected by the maximum DC sensor voltage. Figure 28 shows the normalized maximum sensor voltages versus frequency for the three devices. The data show the IR-50 emits over 90% of its maximum DC irradiance at modulation frequencies of 10 Hz and below. The Cal Sensors and ICX devices emit close to the same percentage of their maximum DC irradiance for a given modulating frequency. The most important observation from this data is that the Cal Sensors and ICX devices emit 60% and 58%, respectively, of their maximum DC irradiance at 3 Hz modulation.

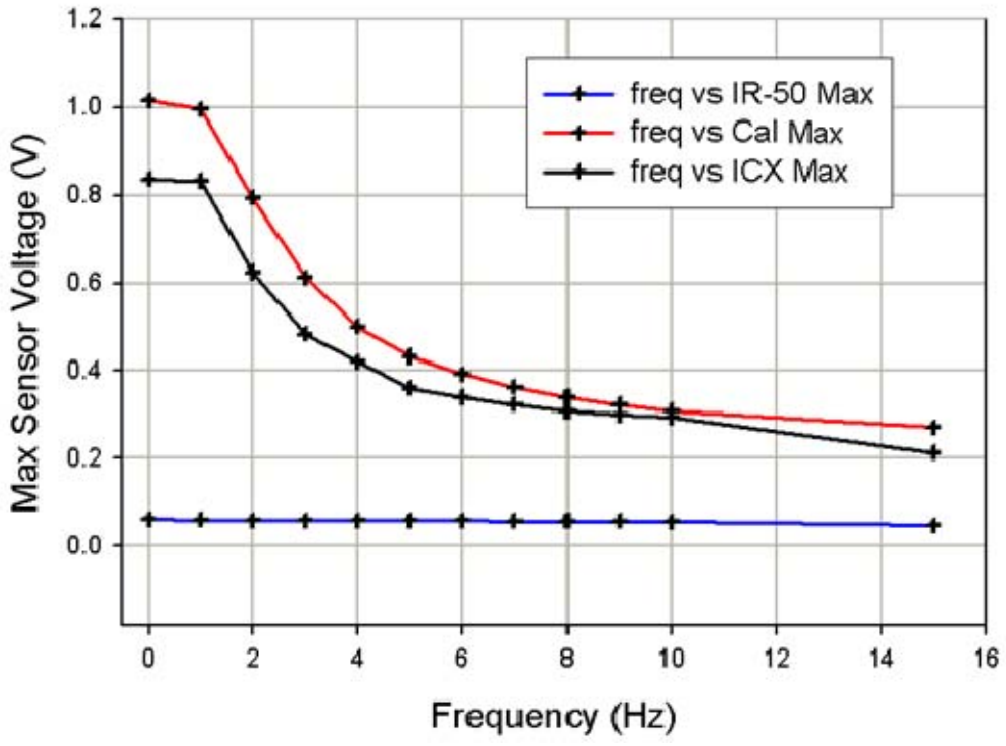

Figure 27. Maximum Irradiance Versus Frequency of IR-50, Cal Sensors, and ICX Devices

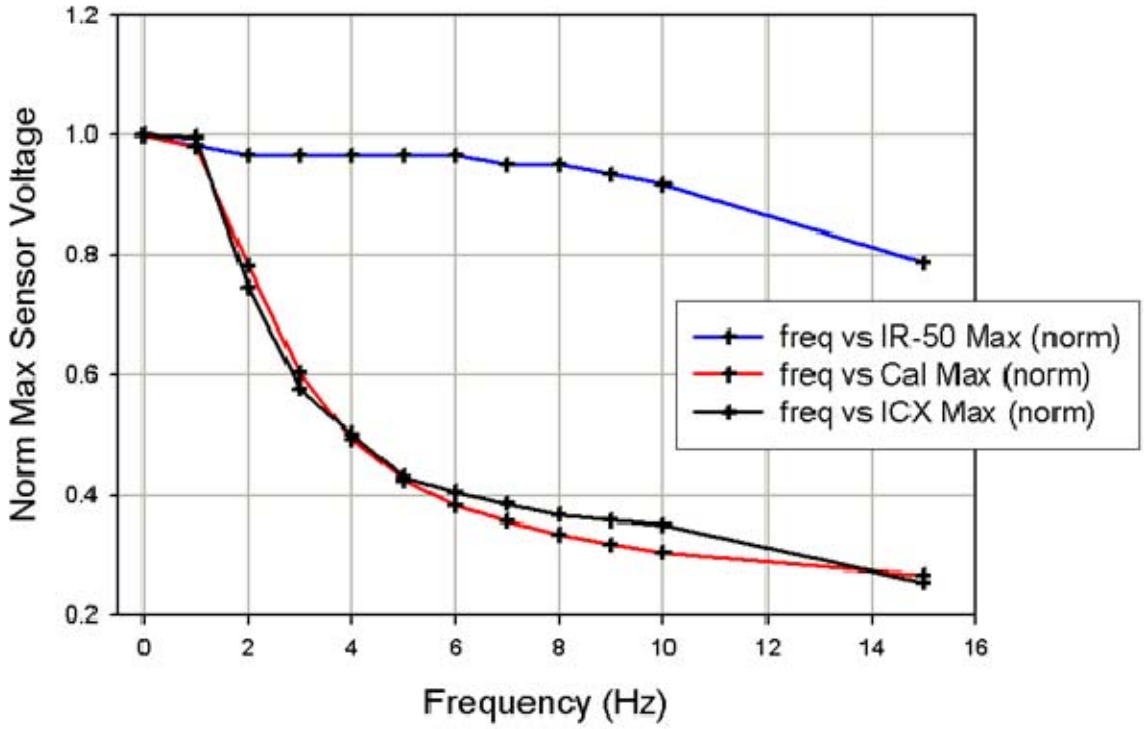

Figure 28. Normalized Maximum Irradiance Versus Frequency of IR-50, Cal Sensors, and ICX Devices

b. Minimum Irradiance versus Frequency

Figure 29 shows the minimum detector voltage versus frequency for the three devices. The IR-50 shows the best response with minimum detector voltage equal to 0 V out to 10 Hz. The minimum detector voltage for the Cal Sensors device is significantly less that the ICX device below 10 Hz. The normalized minimum irradiance data shows the ICX device and Cal Sensors devices fall to only approximately 7.5% and 3%, respectively, of their maximum DC irradiance by 3 Hz. The higher the sensor voltage during the “off” portion of emission, the hotter the device will appear in a thermal imager. The end result is a less dynamic range over which the imager pixel(s) will be excited decreasing recognizability.

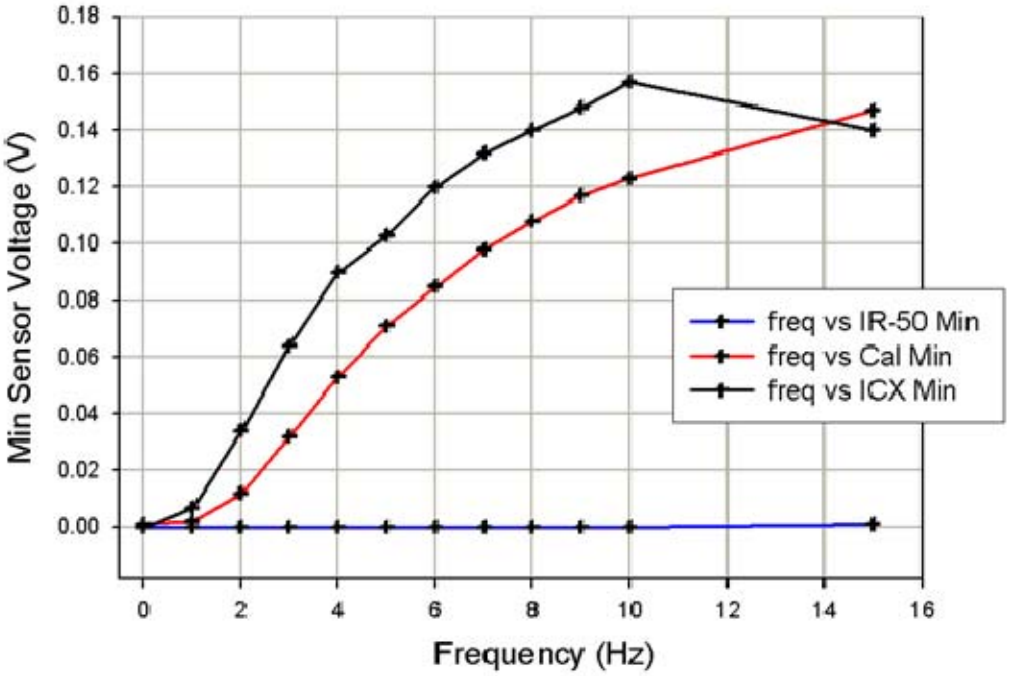

Figure 29. Minimum Irradiance Versus Frequency of IR-50, Cal Sensors, and ICX Devices

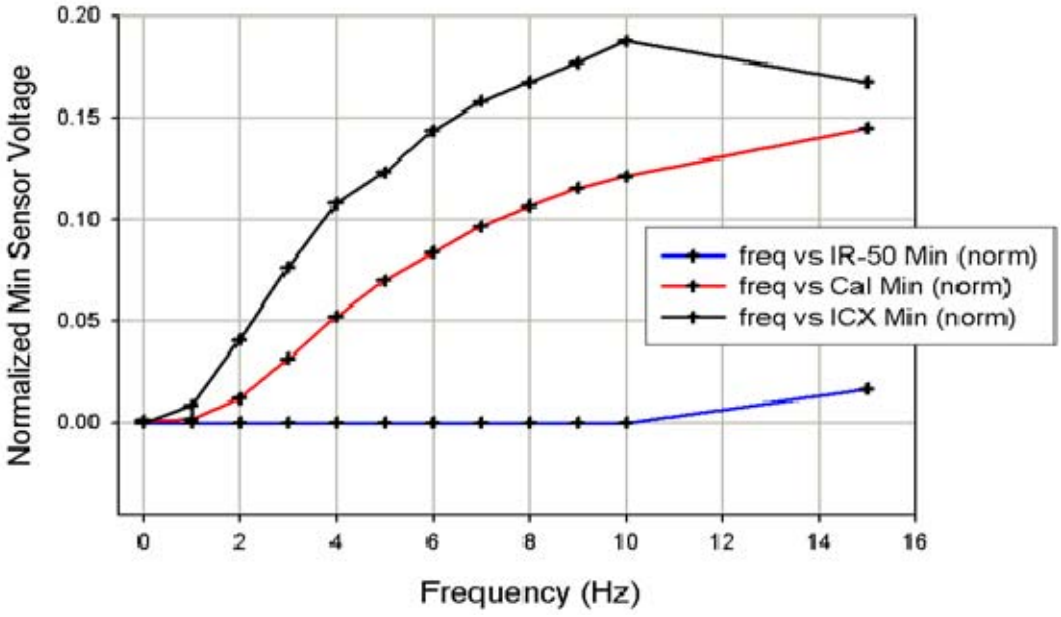

Figure 30. Normalized Minimum Irradiance Versus Frequency of IR-50, Cal Sensors, and ICX Devices

c. Delta Irradiance versus Frequency

The difference between the maximum and minimum irradiance is referred to as delta irradiance. This quantity is a measure of how much irradiance difference will be visible in a thermal imager between the device at its hottest point and its coolest point. Larger delta means the thermal imager pixels excited by the emitter will vary more. The 0 Hz data point is the detector voltage with the emitter driven with a constant current. Figure 31 shows the Cal Sensors device has significantly more delta irradiance at all frequencies. Figure 32 shows the Cal Sensors normalized delta irradiance slightly ahead of the ICX device. Again, due to its faster operating speed, the IR-50 maintained over 90% of its modulation depth for frequencies up to 10 Hz.

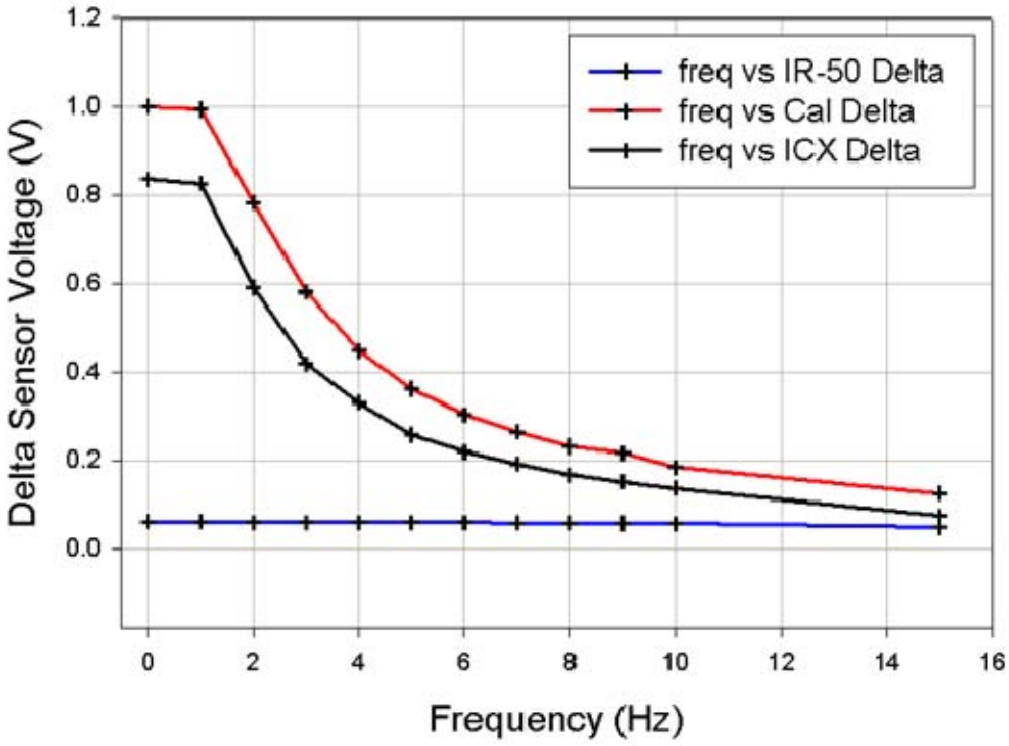

Figure 31. Delta Irradiance Versus Frequency of IR-50, Cal Sensors, and ICX Devices

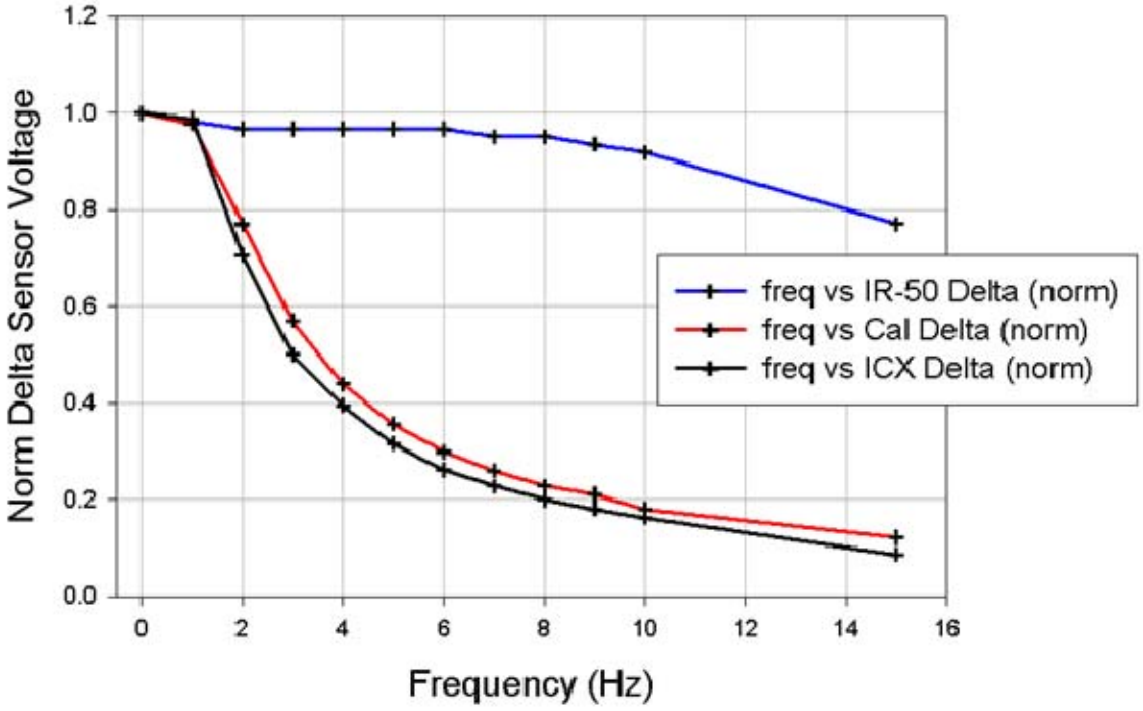

Figure 32. Normalized Delta Irradiance Versus Frequency of IR-50, Cal Sensors, and ICX Devices

4. Off-Axis Irradiance

Finally, off-axis irradiance was studied. The detector was held fixed, while the angle of the panel was changed. The distance between the center of the device window and the detector was held fixed at 5 cm for all measurements. The devices were driven by a two-second DC pulse for all measurements. The figure of merit quoted in the device specification sheets for all three devices is the Full Width Half Maximum (FWHM). FWHM is the angle between which the output irradiance is at least 50% of the maximum on-axis irradiance. Figure 33 shows the sensor voltage versus angle for the three devices. Because the Cal Sensors device is collimated, its irradiance falls off most quickly as the panel angle increases corresponding to a FWHM of about 46°. The ICX and IR-50 data show a FWHM value of approximately 100°. The experimental FWHM values are consistent with the values quoted in the specification sheets.

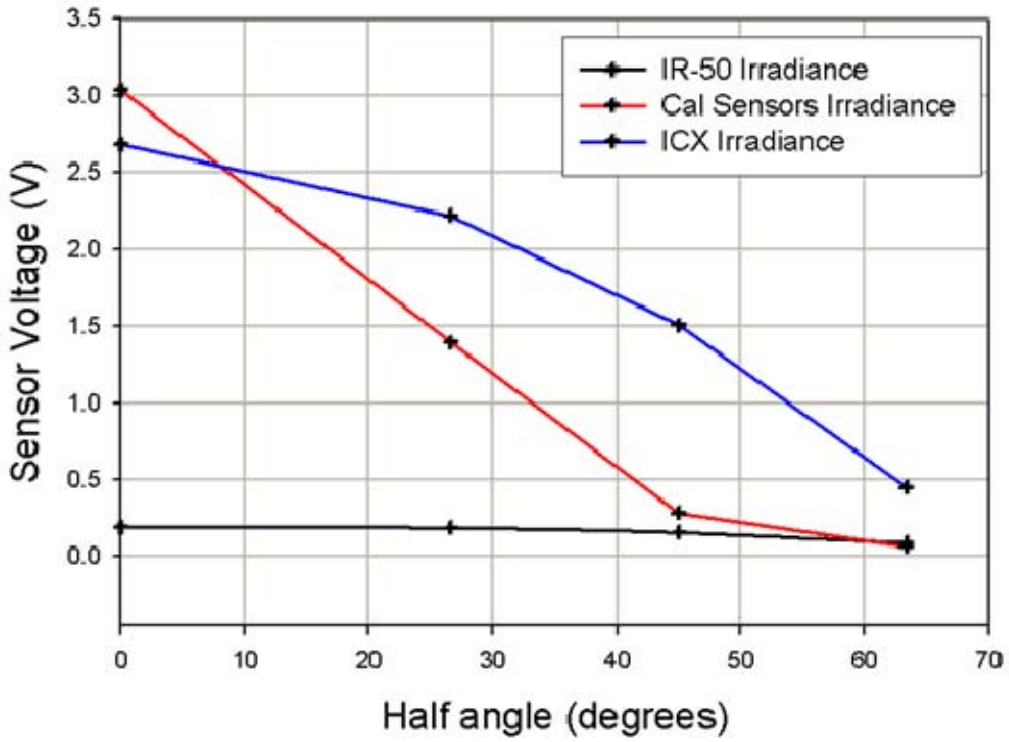

Figure 33. Sensor Voltage Versus Half Angle for IR-50, Cal Sensors, and ICX Devices

C. 8–12 MICRON EMISSION CHARACTERIZATION

The single element MCT detector with band-pass filter was used to collect the devices' 8–12 micron characteristic data. Measurements were carried out exactly as described in section B of this chapter. A DC pre-amplifier was used with the MCT detector. There was a significant amount of drift in the detector output voltage. The detector output voltage was shifted so that the first 50 ms, before the emitters where turned on was equivalent to zero volts. It was assumed that the detector voltage drift was negligible during the four second measurement. In addition, it is important to note that the transmittance of the calcium fluoride windows is very poor in the 8–12 micron wavelength range. The 8–12 micron wavelength emission observed was primarily emission from the calcium fluoride window which was heated by the filament. At the time of this research, devices with window materials transparent to 8–12 wavelength LWIR

were at least 4 times as expensive and devices with calcium fluoride windows. For better response in the 8–12 micron wavelength regime than what is reported here, a window that is more transparent to these wavelength should be used. Nevertheless, with the wide availability of 8–12 micron, room-temperature, micro-bolometer cameras, the data are relevant. The distance between the emitter and detector was 3.5 cm for all 8–12 micron measurements unless otherwise noted.

1. Maximum Irradiance at Constant Power

On-axis irradiance with the device driven at the maximum DC power for the three devices is shown in Figure 34. The Cal Sensors and ICX device reach comparable maximums but the ICX device takes longer to reach the maximum. The graph suggests that the ICX device may have slightly higher emission if driven with a DC current for longer than two seconds. This data point was not obtained because the VMIFF response will be about 2 seconds in duration or shorter. The maximum on-axis irradiance of the Cal Sensors device was the greatest and registered a sensor voltage of 4.30 V. The maximum on-axis irradiance of the ICX device was approximately equal at 4.26 V. The IR-50 emits 10% of the radiation of the Cal Sensors device with a maximum sensor voltage of 0.43 V.

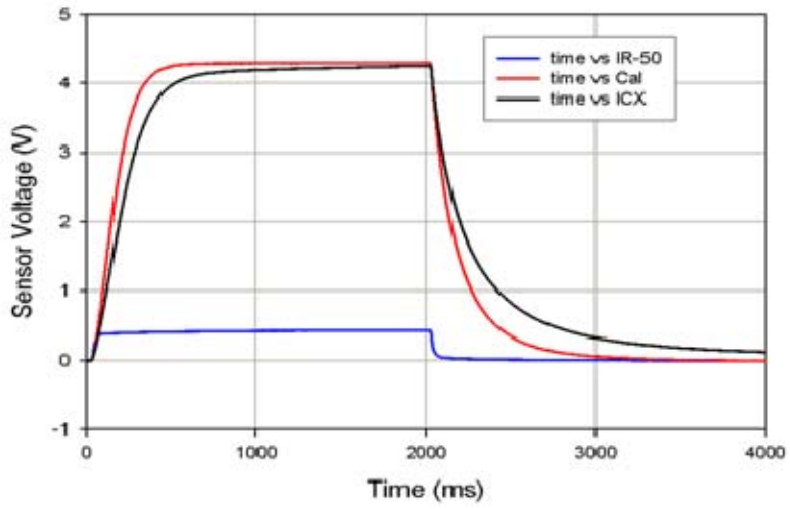

Figure 34. DC Response of IR-50, Cal Sensors, and ICX Devices

2. Device Rise and Fall Time

As in section B of this chapter, the data for each device were time shifted so that the device voltage turned on at time t=0. The normalized signals for each device are plotted in Figure 35. The normalized data shows that the IR-50 reaches over 90% of its maximum irradiance in approximately 127 ms. By comparison, the Cal Sensors device is second fastest requiring 315 ms to reach 90% of maximum irradiance. Finally, the ICX device requires 438 ms to reach 90% of maximum irradiance and is the slowest device.

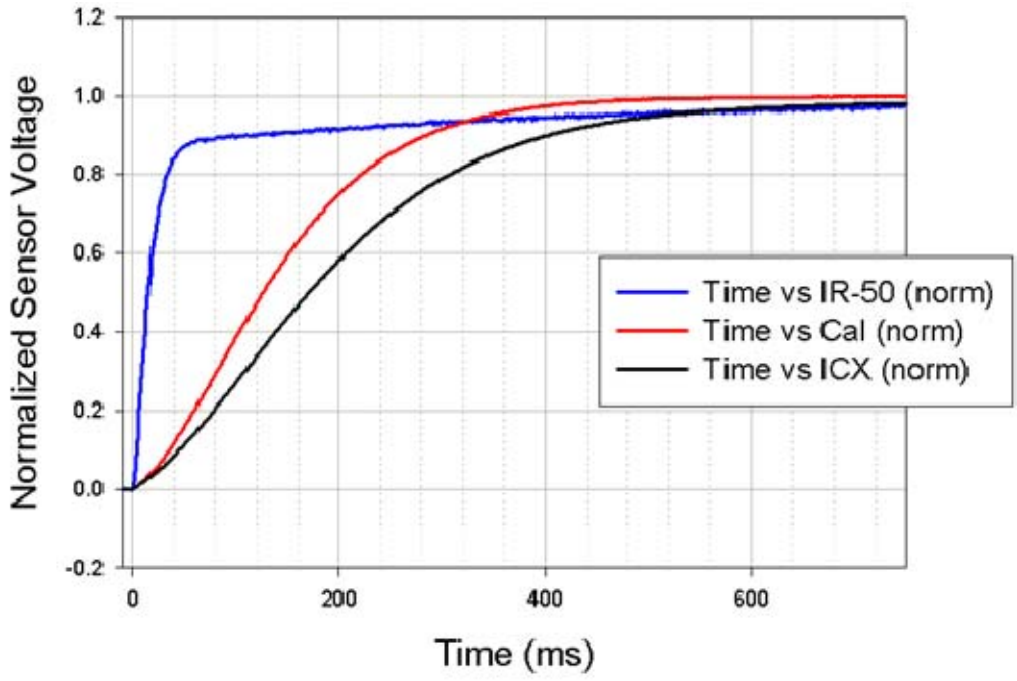

Figure 35. Normalized Transient Rise Response of IR-50, Cal Sensors, and ICX Devices

Figure 36 shows the short-term transient sensor voltage for each device. The time required for the filament to heat the window is the dominant effect controlling the response. It is assumed that the thermal mass of the Calcium Fluoride window is approximately the same for the three devices. The IR-50 filament still heats the fastest, but can only heat the window slightly faster than the Cal Sensors or ICX devices. This is because the Cal Sensors and ICX

devices operate at significantly higher input power therefore heat the window, and the can in general, more quickly. Again, the Cal Sensors device has more emission than the ICX device initially but both emissions are approximately equivalent at the end of the two-second on time.

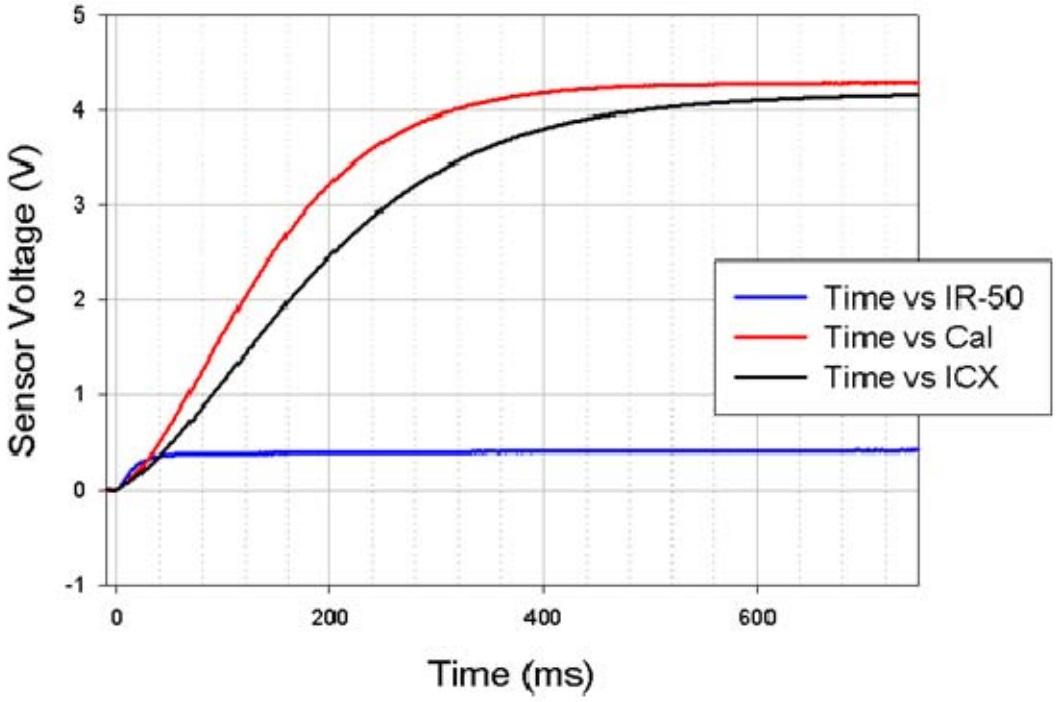

Figure 36. Rise Time Response Comparison of IR-50, Cal Sensors, and ICX Devices

The fall times are discussed next. Figure 37 shows the normalized fall time data. The data show that the IR-50 falls to 10% of its maximum irradiance in approximately 73 ms. The Cal Sensors device requires 421 ms to fall to 10% of maximum irradiance. Finally, the ICX device requires 804 ms to fall to 10% of maximum Irradiance and is the slowest device. The IR-50 has much less active filament area and a much better heat-sink, via the substrate that the filament is grown on, and therefore cools much faster. Additionally, the IR-50 operates at significantly less input power than either the Cal Sensors or ICX devices generating less residual heat in the device. These factors combine to make the IR-50 significantly faster at cooling down.

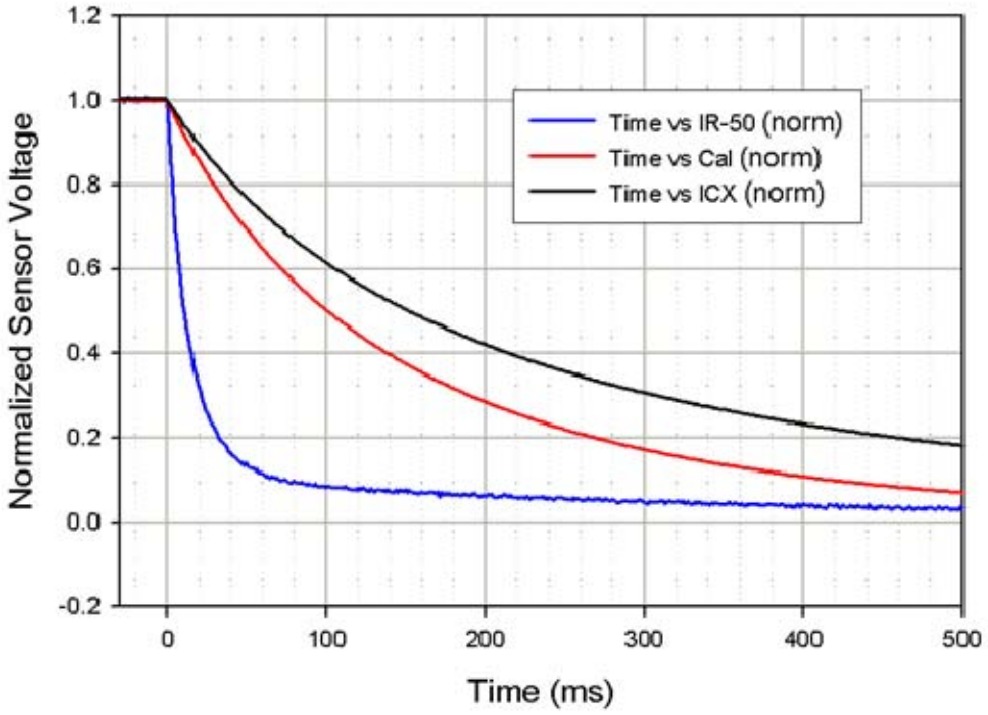

Figure 37. Normalized Transient Fall Response of IR-50, Cal Sensors, and ICX Devices

Figure 38 shows the actual fall time sensor voltages for each device. Again, the speed of the IR-50 is evident. The graph also shows the ICX device has a significantly longer 8–12 micron wavelength emission tail. A long tail with a significant amount of emission could equate to a residual glow when viewed through a thermal imager. Chapter IV contains further discussion of this issue.

3. Frequency Response

a. Maximum Irradiance versus Frequency

Figures 39 and 40 show the maximum sensor voltage and normalized maximum sensor voltage versus frequency, respectively, for all three devices. The Cal Sensors device has the highest maximum irradiance at all frequencies. The data show the IR-50 emits over 90% of its maximum DC irradiance at all modulation frequencies. The Cal Sensors device emits slightly

more 8–12 micron radiation than the ICX device for modulating frequencies less than 7 Hz. The Cal Sensors and ICX devices emit 85% and 78%, respectively, of their maximum DC irradiance at 3 Hz modulation. The increased variability, compared to the 3–5 µm response, is likely due to drift behavior in the DC pre-amplifier used with the MCT detector.

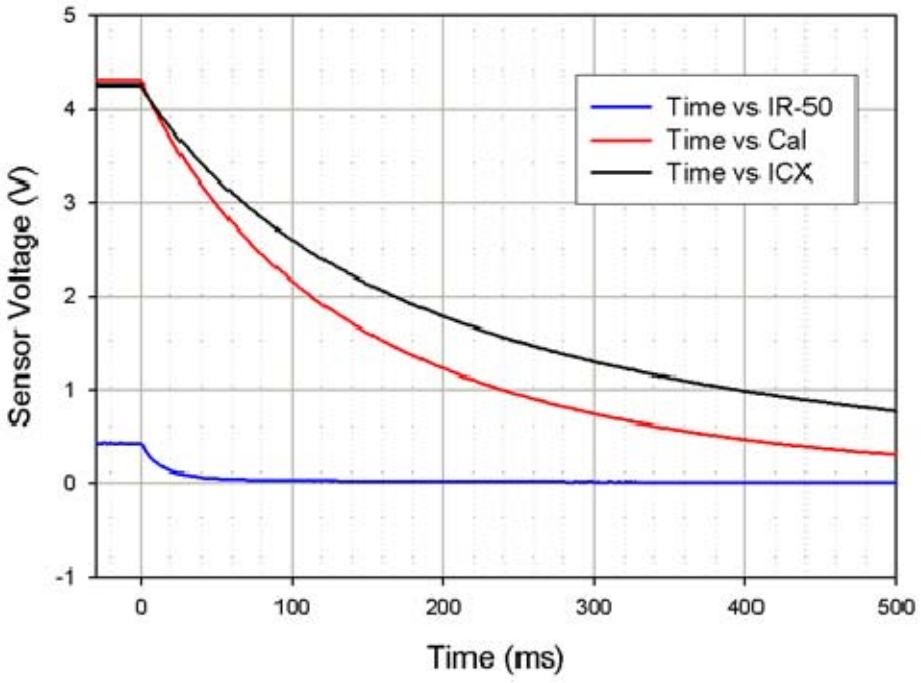

Figure 38. Fall Time Response Comparison of IR-50, Cal Sensors, and ICX Devices

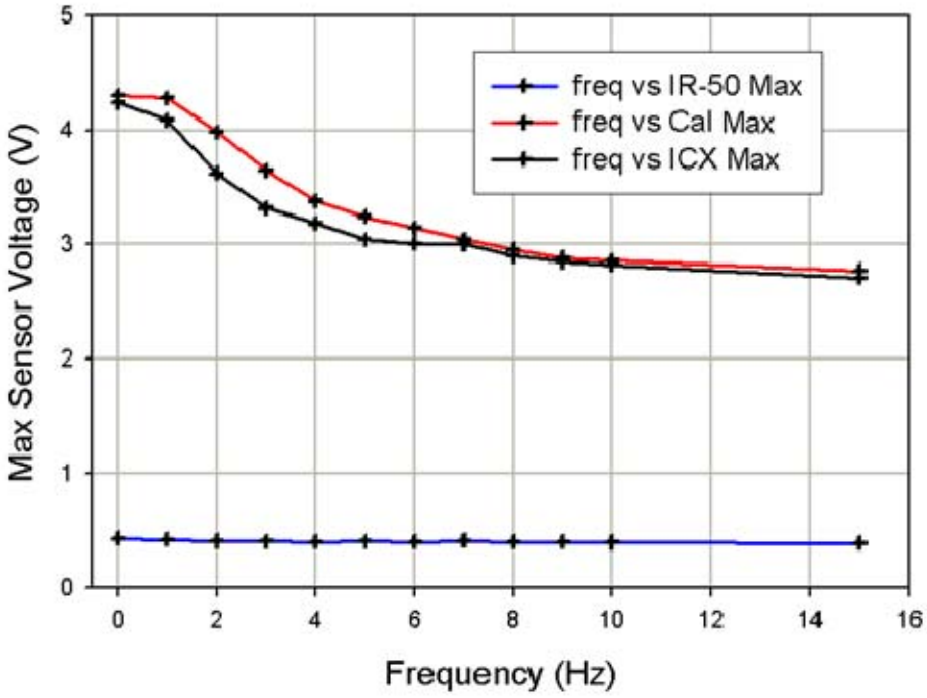

Figure 39. Maximum Irradiance Versus Frequency of IR-50, Cal Sensors, and ICX Devices

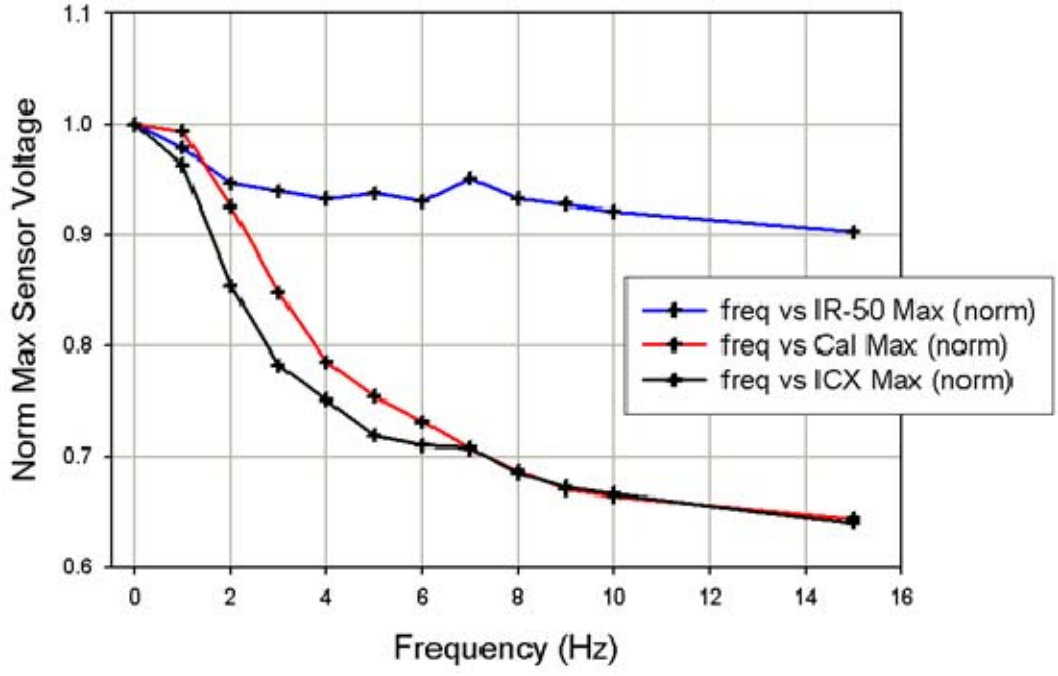

Figure 40. Normalized Maximum Irradiance Versus Frequency of IR-50, Cal Sensors, and ICX Devices

b. Minimum Irradiance versus Frequency

Figures 41 and 42 show the minimum detector voltage versus frequency for the three devices. The IR-50 shows the best response with minimum detector voltage close to 0 V out to 10 Hz. The minimum detector voltage for the Cal Sensors device is less that the ICX device below 10 Hz.

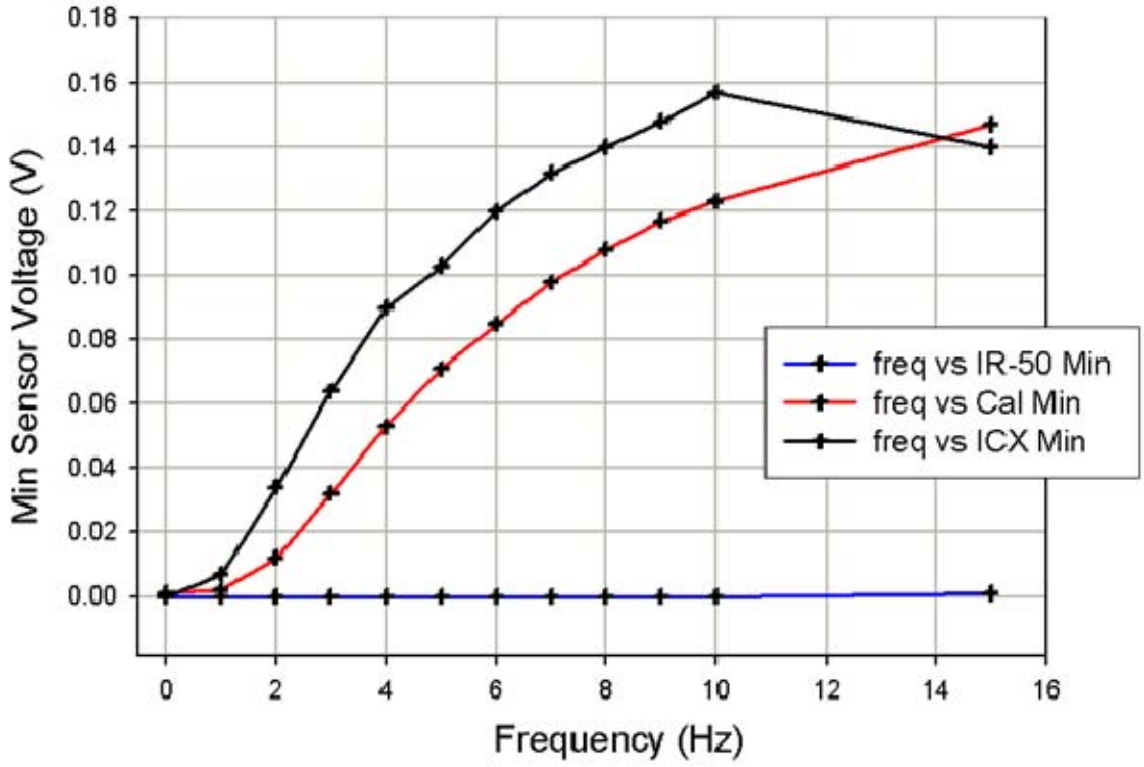

Figure 41. Minimum Irradiance Versus Frequency of IR-50, Cal Sensors, and ICX Devices

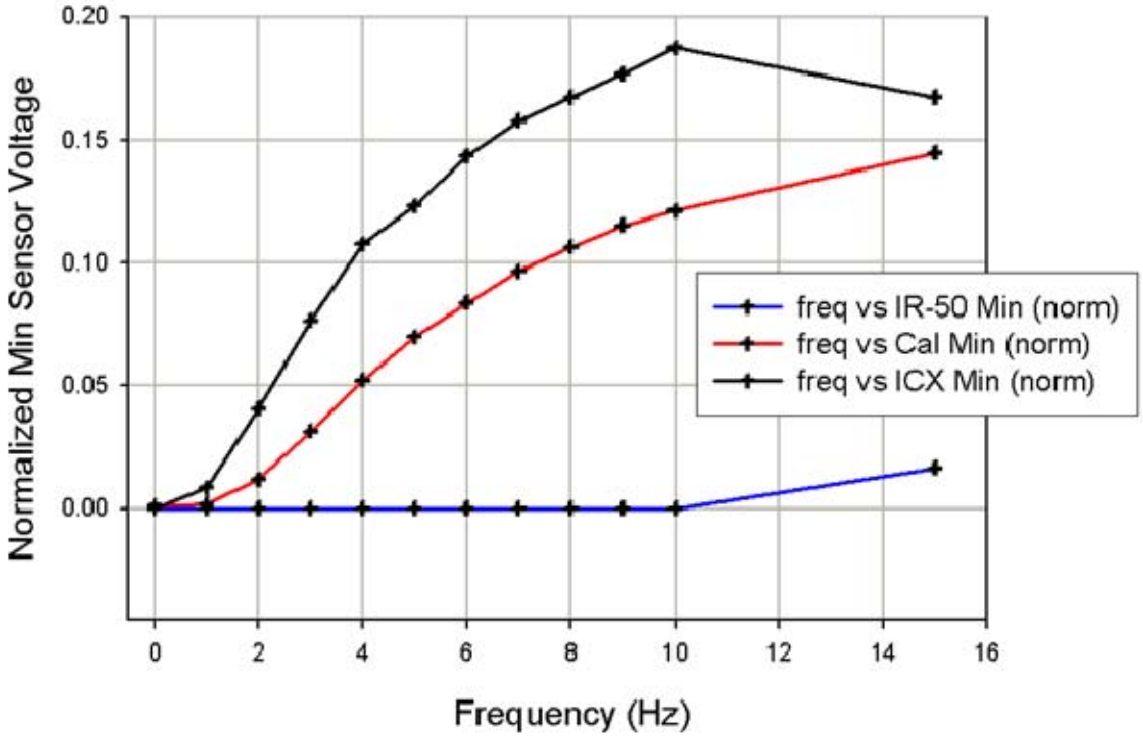

Figure 42. Normalized Minimum Irradiance Versus Frequency of IR-50, Cal Sensors, and ICX Devices

c. Delta Irradiance versus Frequency

Delta Irradiance versus frequency is plotted for all three devices in Figure 43. The data show the Cal Sensors device has significantly more delta irradiance at all frequencies. From Figure 44, the Cal Sensors normalized delta irradiance slightly greater than the ICX device. Again, due to its faster operating speed, the IR-50 maintained over 90% of its modulation depth for frequencies up to 10 Hz. Interestingly, the lower delta irradiance observed with the 8–12 micron detector is due mainly to the minimum irradiance increasing with modulating frequency as opposed to observations with the 3–5 micron detector where lower delta irradiance was primarily due to decreasing maximum irradiance with increasing modulating frequency.

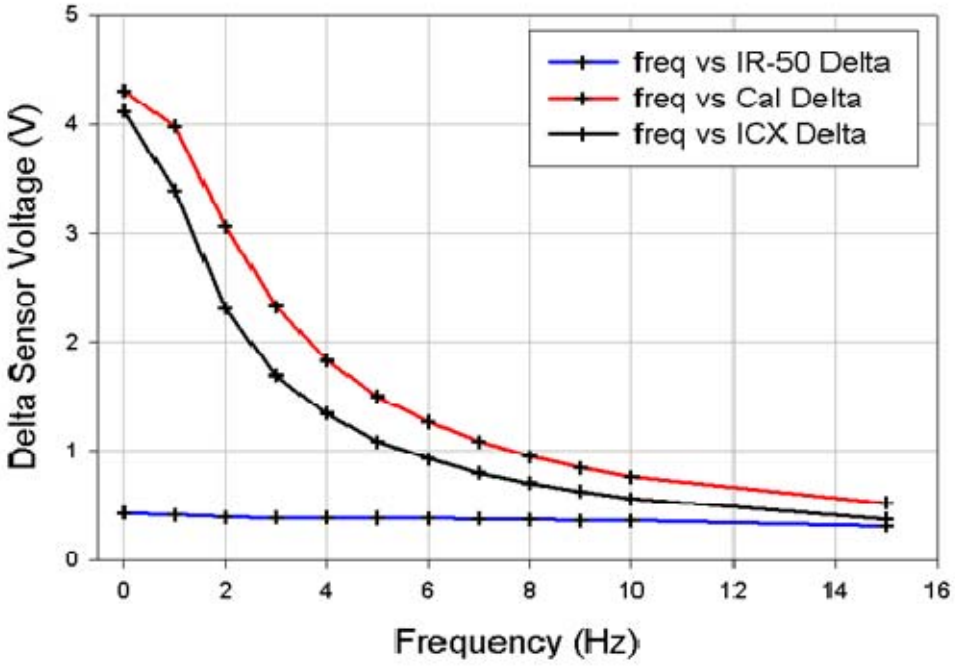

Figure 43. Delta Irradiance Versus Frequency of IR-50, Cal Sensors, and ICX Devices

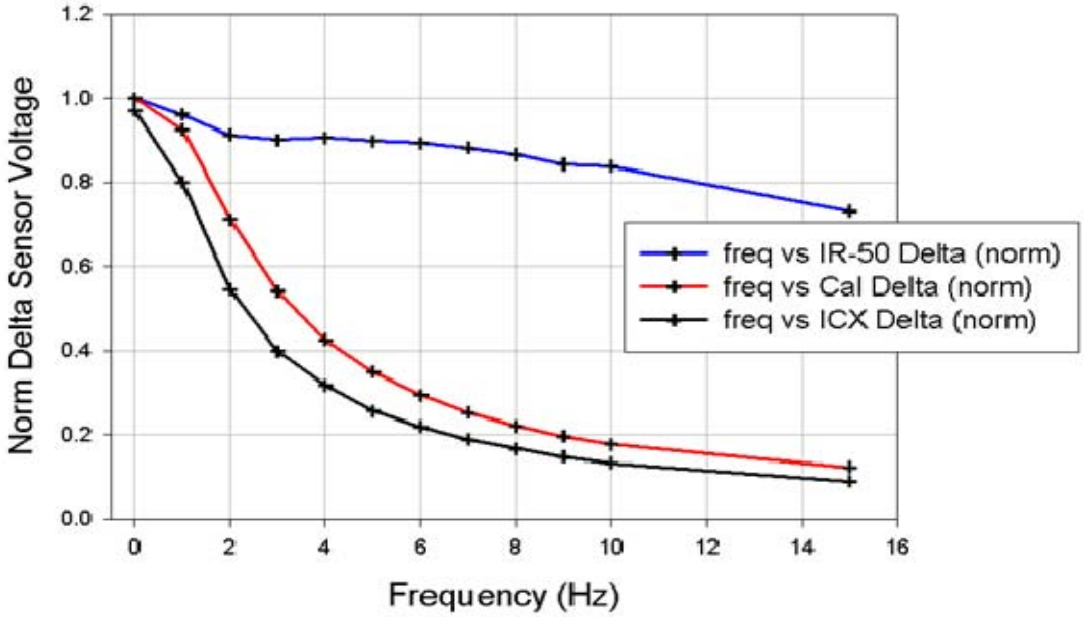

Figure 44. Normalized Delta Irradiance Versus Frequency of IR-50, Cal Sensors, and ICX Devices

D. SUMMARY OF SINGLE DEVICE MEASUREMENTS

The IR-50 is significantly faster than the Cal Sensors and ICX devices, maintaining most of its maximum modulation depth for all frequencies tested. The small active filament area and substrate heat sink are the primary reason for the IR-50's speed. The Cal Sensors device is modestly faster than the ICX device. The Cal Sensors flat, thin filament has a smaller filament cross-sectional area than the ICX filament which means less filament mass to heat and cool. Additionally, the thin flat filament design gives more surface area per volume available to radiate. Due to the collimator, the on-axis irradiance of the Cal Sensors device is significantly more than the ICX device in spite of operating at less than half the input power. The cost per unit for all three devices are comparable. Table 3 summarizes the experimental data.

	Cal Sensors SVF360-8m3	ICX Photonics NL84ACC	HawkEye Technologies IR-50
Max DC Irradiance	1	0.8	0.06
Full Width Half Maximum	46°	100°	100°
Input Power per device	2.5 W	6 W	0.95 W
Input Power (48 devices)	120 W	288 W	45.6 W
Rise Time (90%)	57 ms	372 ms	606 ms
Fall Time (10%)	12 ms	117 ms	178 ms
Modulation Depth (2 Hz)	0.78	0.59	0.07
Cost per Device	$86	$71.25	$62

Table 4. Summary of Single Device Experimental Data

In Table 4, Max DC irradiance is normalized to the Cal Sensors irradiance. Input power (48 devices) is the input power required to drive a four-sided (12 devices per side), solid-state solution. Modulation depth is normalized to the Cal Sensors DC modulation depth.

IV. TWELVE-EMITTER ARRAY MEASUREMENTS

A. LABORATORY MEASUREMENTS

Circuit boards were etched to electrically connect 12-devices and secure them to the heat sink. The 12 ICX and Cal Sensors devices were connected in series and required 14.3 V and 20.1 V across all 12 devices, respectively. Three IR-50 devices were connected in series for one leg. Four legs were connected in parallel to form the 12-device circuit and required 20.1 V across the circuit. The panels were tested for on-axis irradiance versus distance in the lab from 25 cm to 4 m (Figures 45 and 46). The Cal Sensors and ICX devices compared more closely than expected. The IR-50 irradiance was about a decade less than the Cal Sensors and ICX irradiance.

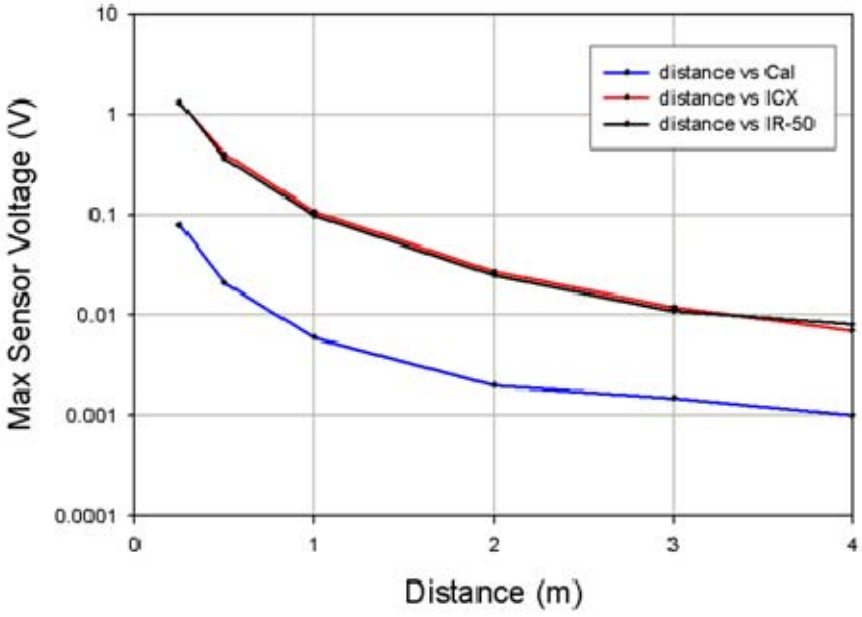

Figure 45. Twelve-Device Array, 3–5 Micron On-Axis Irradiance Versus Distance

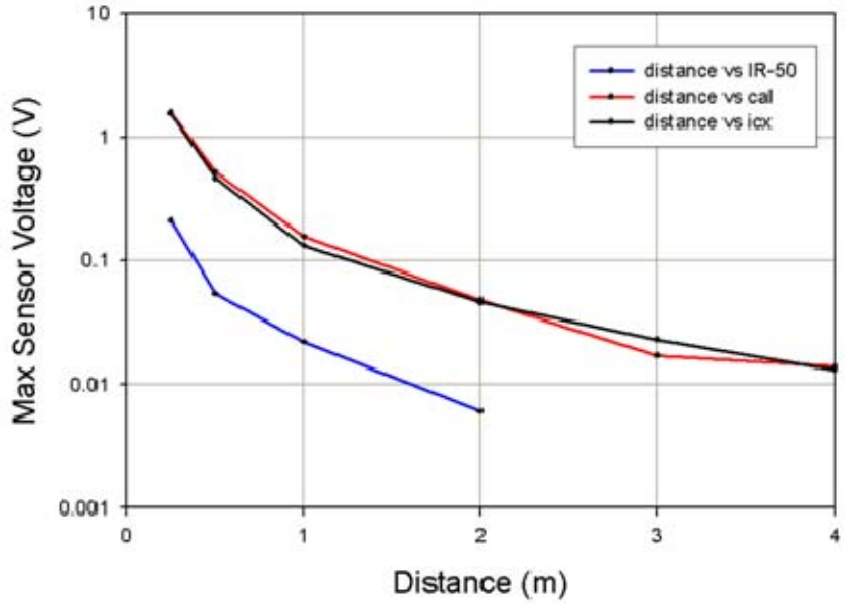

Figure 46. Twelve-Device Array, 8–12 Micron On-Axis Irradiance Versus Distance

B. CAMP PENDLETON FIELD TEST

The arrays were field tested at Camp Pendleton on 15 May 2009. The ICX and Cal Sensors panels where included in the testing. The panels were tested in fixed and rotating configuration. For the fixed configuration, the panels were aimed at the imager and modulated with a 1 Hz, 50% duty cycle square-wave. For the rotating configuration, the panels where driven with a DC current and rotated at 1 revolution/second effectively resulting in 1 Hz modulation.

Several thermal imagers were used to view the panels including: the LAV-25 imager, PAS-13B Thermal Weapon Sight, and an NPS 3–5 micron imager. The panels were not visible in the PAS-13B at any range (Figure 47). It is unknown if the panels were not visible using the PAS-13B due to imager/panel limitation or operator malfunction. The panels were visible in the NPS imager out to a range of 3000 m. The NPS imager has a 20° optical lens with no optical zoom capability. The images taken show one pulsating pixel.

Figure 47. PAS-13B Thermal Weapon Sight [From Raytheon, Retrieved from www.raytheon.com]

The LAV-25 thermal imager was used to view the panels during the day and night. The thermal imager was capable of 10, 20 and 40 X optical zoom. Tables 4 and 5 show the day and night field test results, respectively. The panels were viewed at arbitrary distances driven by the requirement to have line of sight between the imager and the panels and terrain limitations. The panels, lead-acid battery bank, and driver circuit were placed in the back of an SUV and driven to each test distance. The panel was stationary at each test sight, located in the back of the SUV with the back hatch opened.

Both panels were clearly visible in all three magnifications out to 3000 meters during the day. From 3000 m to 4500 m the panels were difficult to see in 10 times magnification but clearly visible in 20 and 40 times magnification. Of note, the Marines observing the panels through the LAV-25 imager commented that the panels were easier to see when rotating.

			LAV		
Range (m)	Emitter	Mode	10X	20X	40X
800/1700	both	both	Y	Y	Y
3000	ICX	Rot	Y	Y	Y
		Fixed	Y	Y	Y
	Cal	Rot	Y	Y	Y
		Fixed	Y	Y	Y
3500	ICX	Rot	Y	Y	Y
		Fixed	Y	Y	Y
	Cal	Rot	Y	Y	Y
		Fixed	Y	Y	Y
4500	ICX	Rot	Y	Y	Y
		Fixed	Y	Y	Y
	Cal	Rot	Y	Y	Y
		Fixed	Y	Y	Y

Table 5. Camp Pendleton Field Test Results- Day

Due to the limited time availability of LAV-25, the night testing conducted at two distances (Table 6). The first test was conducted at the furthest distance achievable on the range while the second test location was approximately the same location as the last day test. At 5640 m range, the neither panel was visible in fixed mode. The ICX panel was not visible using 10 times magnification and barely visible in 20 and 40 times magnification. The Cal Sensors panel was not visible in 10 or 20 times magnification, and barely visible in 40 times magnification. Surprisingly, the panels were less visible at 4500 m during the night than they were during the day. This was probably due in part to the LAV and panel being at slightly different locations. A small variation in the orientation of the panel can have a significant effect on panel visibility. Another surprising data point was that the Cal Sensors panel was more visible in fixed mode than in rotating mode. This data needs to be checked for reproducibility.

			LAV		
Range (m)	Emitter	Mode	10X	20X	40X
4500	ICX	Rot	Y	Y	Y
		Fixed	Y	Y	Y
	Cal	Rot	N	Y	Y
		Fixed	Y	Y	Y
5640	ICX	Rot	N	Y	Y
		Fixed	N	N	N
	Cal	Rot	N	N	Y
		Fixed	N	N	N

Table 6. Camp Pendleton Field Test Results- Night

The main conclusion drawn from the lab panel tests and the Camp Pendleton field test is that a rotating panel with devices driven with a DC current is more visible at longer range than a fixed panel run with a pulsed current when viewed through tactical thermal imagers used by ground troops in the field.

THIS PAGE INTENTIONALLY LEFT BLANK

V. CONCLUSION

A. EXPERIMENTAL RESULTS

The experimental results for the single device and multiple device array measurements are summarized in Table 7 below. These results form the basis for the VMIFF Gen III design recommendation.

	Cal Sensors SVF360-8m3	ICX Photonics NL84ACC	HawkEye Technologies IR-50
Max DC Irradiance	1	0.8	0.06
Full Width Half Maximum	46°	100°	100°
Input Power per device	2.5 W	6 W	0.95 W
Input Power (48 devices)	120 W	288 W	45.6 W
Rise Time (90%)	57 ms	372 ms	606 ms
Fall Time (10%)	12 ms	117 ms	178 ms
Modulation Depth (2 Hz)	0.78	0.59	0.07
Cost per Device	$86.00	$71.25	$62.00
Array visibility range (day)	3500–4500 m	3500–4500 m	N/A
Array visibility range (night)	4500 m	4500 m	N/A

Table 7. Summary of Experimental Data

In the table, max DC irradiance is normalized to the Cal Sensors irradiance. Input power (48 devices) is the input power required to drive a four-sided (12 devices per side), solid-state solution. Modulation depth is normalized to the Cal Sensors DC modulation depth. Array visibility range is the maximum range that the LAV-25 thermal imager viewed the panel in 10-time magnification.

To achieve a solid-state, four-sided VMIFF Gen III design solution, the microradiating device must have a FWHM angle of at least 90° so that at the 45° angle between faces VMIFF emission is sufficient for visibility at the same range as viewed on the optical axis as one of the faces. This eliminates the Cal Sensors device as a possibility for use in a four-sided solid-state solution. Since the IR-50 does not produce the irradiance required to obtain the desired observable range, the ICX device is the most suitable. The ICX device's

modulation depth is significantly reduced when modulated faster than 1 Hz. Based on data collected and field experimentation conducted at Camp Pendleton, a solid-state design solution visible beyond 4.5 km would require in excess of 12 devices per face. Based on experimental findings and anecdotal comments during the Camp Pendleton field test, a rotating design solution appears more feasible at this time.

B. VMIFF GENERATION III DESIGN RECOMMENDATION

A rotating design solution is recommended for VMIFF Gen III thermal signature generation. A rotating solution has several advantages over a non-rotating solution. First, devices can be mounted on one face giving maximum output power in a single direction. Second, the devices evaluated in this thesis are designed for applications that require modulated emission. Rotating the panel accommodates the use of DC emitters which typically have more on axis irradiance than the pulsable emitters. As an example, the specification sheet for Cal Sensors SA10510-8M2 , the DC version of the pulsable Cal Sensors device evaluated in this research, shows 2.5 times the on-axis DC irradiance as the pulsable device for approximately the same input power.

Mounting 48 DC devices on a single face should increase the maximum observable range by a factor $\sqrt{(4 \bullet 2.5)} = \sqrt{10} = 3.16$ achieving a new maximum observable range of 4.5 km * 3.16 = 14 km or 8.8 miles, a significant improvement over legacy JCIMS devices and providing a day and night capability via the imager used in most air-to-ground targeting.

VMIFF Gen III's thermal emission will provide immediate feedback to the shooter, identifying the vehicle as friendly with no requirement for new equipment to be added to aircraft. Compared to legacy JCIMS devices, VMIFF Gen III is less exploitable by the enemy since it is covert unless interrogated by a friendly target laser designator or range finder.

As the Commandant of the Marine Corps, General James Conway has stated, “Shame on us if we continue to kill our young people because we haven’t developed something that either “beeps” or “squawks,” or sends out a transmission or something that tells our troops, “oops, that’s a friendly vehicle”.” The capability the General is referring to is available now in VMIFF Gen II. This thesis work demonstrates that a next generation VMIFF is possible that provides a comparable thermal capability for day as well as nighttime fratricide mitigation.

THIS PAGE INTENTIONALLY LEFT BLANK

APPENDIX A DEVICE SPECIFICATION SHEETS

CAL SENSORS

HANDLING PRECAUTIONS FOR "CAL SOURCE" IR EMITTERS

1. CLEANING: Clean the package window with a 50/50 mixture of isopropyl alcohol and water. Either rinse package gently, or use light strokes with a cotton tipped applicator. Care must be taken to avoid using excessive pressure on the window as you may destroy the window seal. Do not use acetone or halogenated solvents.

   NEVER use an ULTRASONIC CLEANER to clean IR emitter assemblies.

2. INPUT POWER: IR emitters are specified with a maximum input power that MUST NOT BE EXCEEDED. Otherwise, catastrophic failure (burn-out of filament) may occur or the lifetime of the source may be significantly reduced.

   The maximum input power corresponds to an element temperature of 1170° K for the steady state sources and 1000°K for the pulsable sources.

   Typical voltage versus current profiles and maximum recommended input power are indicated on the included model specific power curve.

   Note that the input voltage must be measured at the BASE OF THE HEADER at the point where the pins exit the package.

3. POWER DISSIPATION: A heat sink MUST ALWAYS BE USED to remove the heat generated. Heat sinks using some combination of conduction, convection, and radiation should be used. Under no circumstances should the temperature of the package including the base exceed 100° C.

4. SOLDERING: The same limitations apply as for soldering transistors. When hand soldering observe the following precautions:

   • Use a low wattage microelectronic soldering iron.

   • Use heat sink clips or pliers on lead wires between solder joint and base of package. If heat sinking is not possible then use minimum soldering iron tip temperature and time to form solder joint.

   • DO NOT BEND leads at sharp angles or twist leads near base of package as this may damage the hermetic seals.

   • Clean properly as required after soldering (See Section 1).

5460 Skylane Blvd. • Santa Rosa, CA 95403 • Tel: 707/545-4181 • Fax: 707/545-5113
e.mail: info@calsensors.com • Web Site: www.calsensors.com

CSI: 8024 2/15/2006

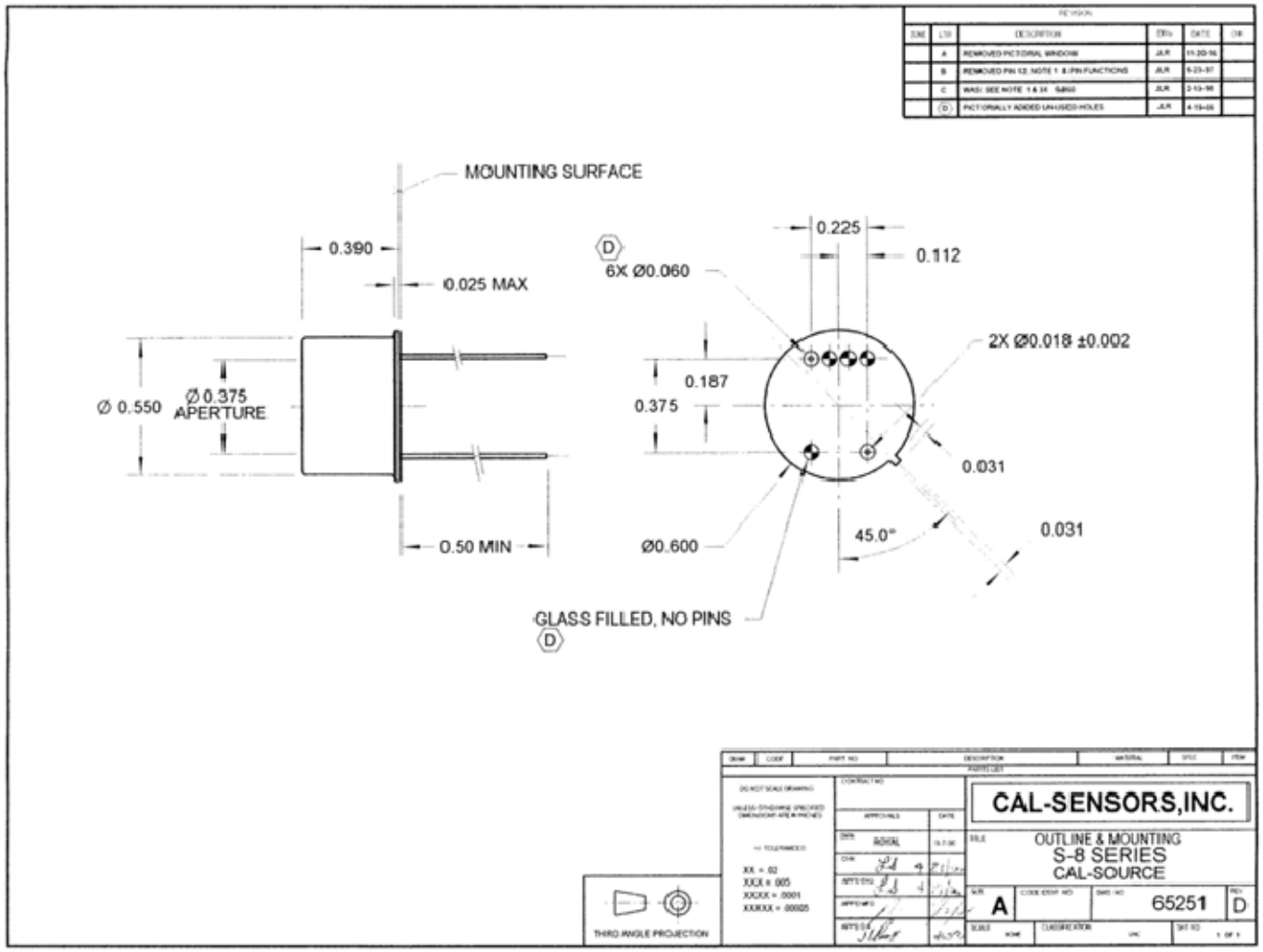
MOUNTING SURFACE
0.390
0.025 MAX
Ø 0.550
Ø 0.375
APERTURE
0.50 MIN
D
6X Ø0.060
0.225
0.112
2X Ø0.018 ±0.002
0.187
0.375
0.031
45.0°
0.031
Ø0.600
GLASS FILLED, NO PINS
D
CAL-SENSORS,INC.
OUTLINE & MOUNTING
S-8 SERIES
CAL-SOURCE
A
65251
D
THIRD ANGLE PROJECTION

Cal-Source™	DC POWER CURVE and MODULATION DEPTH vs. FREQUENCY	PULSABLE INFRARED SOURCE SVF- series TO-8 Patent pending

DC Power Curve[1]

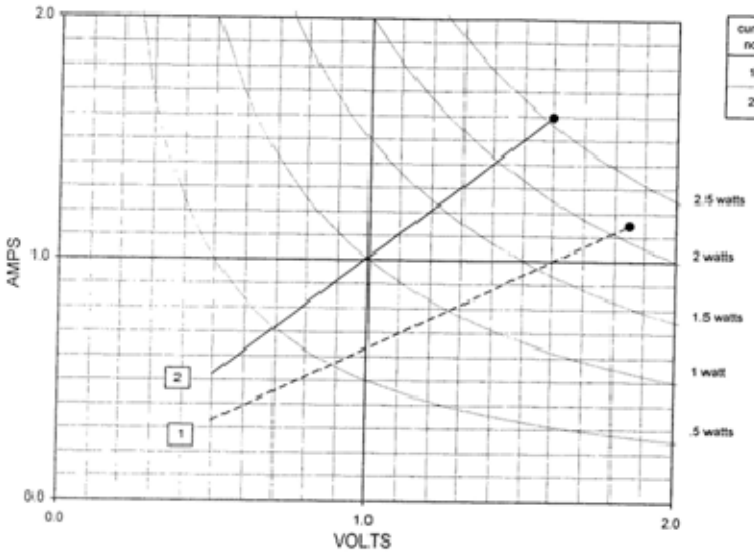

curve no.	source model	Pk DC power (watts)
1	SVF350-8M( )	2.1
2	SVF360-8M( )	2.6

[1] 1000°K at power indicated (•). Exceeding this value will raise element temperature and decrease source lifetime.

Modulation Depth vs. Frequency

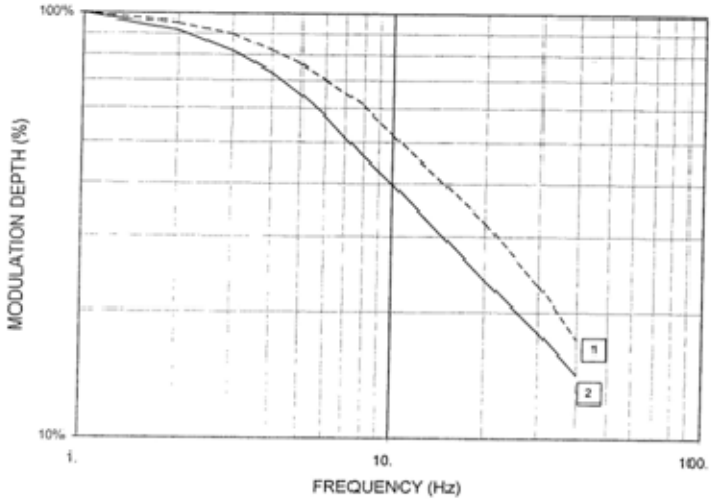

curve no.	source model	Avg. power* (watts)	Freq. @50% modulation
1	SVF350-8M( )	1.05	11 Hz
2	SVF360-8M( )	1.30	7 Hz

* 50 % duty-cycle, square wave

Cal Sensors

E-Mail: info@calsensors.com • www.calsensors.com • Phone: (707) 545-4181 • Fax: (707) 545-5113

CSI 8036 02/99

Distributed by Boston Electronics

ICx photonics

DATA SHEET

Broadband Pulsed Infrared Light Sources

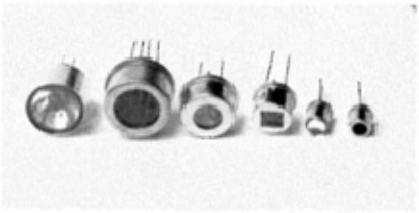

- Broadband IR light sources from 2-20 µm
- Consistent Pulsed Operation
- Large Temperature Modulation
- Many Package and Window options
- Evaluation Kit for Rapid Prototyping
- Highly stable
- Long life

ICx Photonics offers a unique class of electrically pulsed, high intensity infrared radiators for gas analysis, spectroscopy, calibration and tactical identify friend or foe (IFF) applications. These radiators feature a low thermal-mass filament tailored for high emissivity. The filament is fabricated using a patented process such that it supplies bright IR power output while operating much cooler than alternatives. This lower temperature operation reduces the chance of igniting combustible gasses, improves power efficiency, reduces heating of the optics and detectors, and prevents illumination in the SWIR bands. These IR sources are typically pulsed at rates from ½ to 10 Hz with several hundred degrees of temperature modulation.

For demonstration and system design, ICx Photonics provides an Evaluation Kit that includes the light source of your choosing. The Evaluation Kit drive card produces a flat-topped current pulse of adjustable amplitude, length, and frequency that can be run with the pre-programmed settings, or can be connected to a PC for user control via included Windows ™ software.

The table below provides the specifications for each of our broadband IR light sources. If you do not see a product that meets your criteria, please contact us as we may be able to provide a custom solution that meets your needs. Also, we have a line of narrowband IR light sources which use MEMS technology. Because of their spectral tuning, these are extremely efficient devices suitable for battery powered applications. Please see datasheet: TunIR 3-5 and 8-12.

(800)347-5445; (617)566-3821; fax (617)731-0935; isource@bostele.com

SPECIFICATIONS, PART NUMBERS, and WINDOW OPTIONS:

	Parabola	TO-8	Multi-Element		TO-5	TO-46
			2 Element	4 Element		
Windowless	reflectIR-P1N	NL8LNC	NL82LNC	NL84LNC	NL5LNC	NL46LNX
Sapphire 2 to 5.25 µm	reflectIR-P1S	NM8ASC	NM82ASC	NM84ASC	NM5NSC	N/A
Germanium 7 to 12 µm	N/A	N/A	n/a	n/a	NL5NGC	N/A
Calcium Flouride 2 to 9.5 µm	reflectIR-P1C	NL8ACC	NL82ACC	NL84ACC	NL5NCC	N/A
Rated Temperature	750 °C					
Minimum Resistance	1.4 Ohms	2.8 Ω	1.3 Ω per Element		2.5 Ω	0.4 Ω
Maximum Resistance	2.0 Ohms	4.5 Ω	1.7 Ω per Element		3.7 Ω	1.0 Ω
Maximum Input Power	1.7 W	2.2 W	1.6 W per Element		2.0 W	1.1 W
Modulation Speed	Constant - 30HZ; 100% modulation <5hz					
Output Radiation Pattern*	**30 degrees** 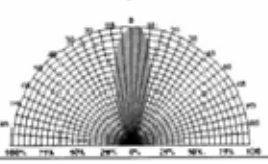		**95 degrees** 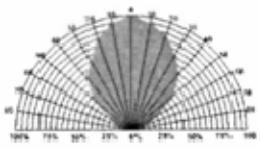			
* Full angle for 50% of peak power						

Custom variations and tighter specification versions are also available.

PULSED OPERATION

Although capable of running at duty cycles of up to 100 % (DC) most users run the filaments with duty cycles of less than 50%. Square-waveform constant current or constant voltage drive schemes are the simplest and most cost effective means of powering the sources. For constant current drives, the power delivered to the source

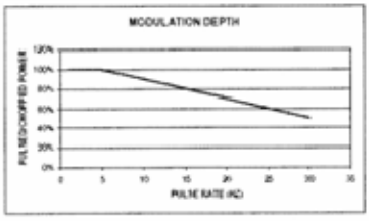

(800)347-5445; (617)566-3821; fax (617)731-0935; insource@bostelec.com

goes as I2 x R. As the source heats up, its resistance increases slightly, causing the power delivered to the source to increase during the "ON" portion of a pulse. For constant voltage drives, delivered power goes as V2/R; therefore the power delivered to the source tends to decrease slightly during the length of a pulse. Other drive schemes can also be employed; constant power or DC for example.

Owing to the extremely low thermal mass of pulsIR emitters, shot-to-shot stability is directly related to drive circuit stability. Variations in drive pulses will translate into variations in output. To determine this we used a liquid nitrogen cooled InSb detector available in our laboratory for detecting energy in the 2-5 µm range. The pulsIR source was driven with a constant-voltage drive circuit that ensures pulse-to-pulse repeatability (standard deviation) of 5.3x10-4. Measurements of the InSb detector reading from 16 seconds of 10 Hz operation was measured to have a comparable standard deviation of 6.8x10-4.

SOURCE LIFETIME

The following graph shows the results (to date) from an ongoing extended life test experiment using an ICx Photonics NM8ASC source. The source is being driven by a constant current drive board at 1 Hz, 30% duty cycle at an approximate temperature of 650° C. Two pyroelectric detectors are monitoring the source output at two distinct wavelengths. In the following chart, the circles show the source output at 4.29 microns (CO_2) while the diamonds show the output at 3.9 microns (reference). The detectors are mounted about four inches from the front face of the source and a dry nitrogen purge is used to prevent water vapor and carbon dioxide in the lab air from affecting the measurement. The temperature in the lab is not very well controlled however, and much of the variation (specifically the bump at ~2000 hours) is due to room temperature swings.

The definition of failure, and thus the definition of lifetime, is very subjective as each system has unique sensitivity to drift (largely related to the A/D bandwidth). We have encountered several applications which define failure as >15% drift from the original power level, so we will adopt this definition for the purposes of this computation. The graph below shows that the median signal level from the 3.9 and 4.29 µm detectors is roughly 4 volts; the linear regression fits to the raw data indicate that both of

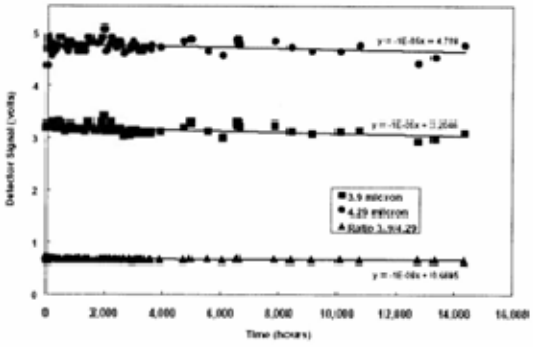

(800)347-5145; (617)566-3821; fax (617)731-0935; irsource@bostonelectronics.com

these signals are decreasing at a rate of 1x10-5 volts/hour. With our assumed signal drift tolerance of 15% and 4 volt signal level, we require a 0.6 volt signal change to signal failure of the light source [0.15 x 4]. With our measured rate of change being 1x10-5 volts/hour it will take approximately **7 years** of continuous operation to obtain a 15% signal change [(0.6v)/(1x10-5v/hr)/(8760hrs/yr)]. Since many systems utilize the ratio of the gas measurement to a reference, they are sensitive not to signal changes, but to change in the ratio of the two signals. With a measured slope of 1x10-6 volts/hour and a 0.75 volt signal the same computation yields a lifetime of **13 years.** Since all of the known filament degradation mechanisms are temperature dependent, the time to 15% failure is strongly dependent upon operating temperature or electrical power applied. Therefore, caution should be used in extrapolating these results to your application.

REFLECTIR PACKAGE DIMENSIONS

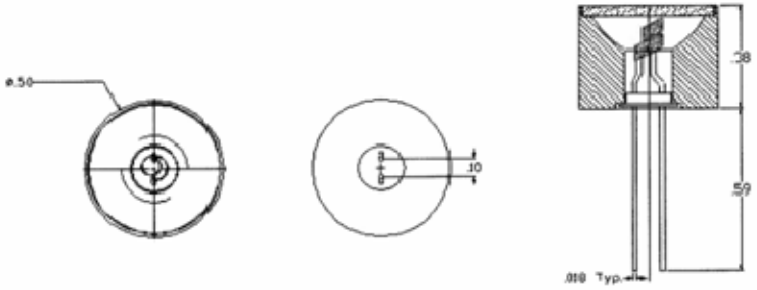

TO-8 PACKAGE DIMENSIONS

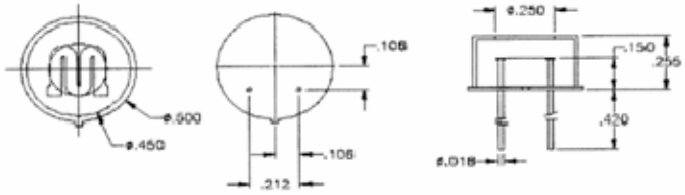

(800)347-5415; (617)566-3821; fax (617)731-0933; irsource@bostelec.com

MULTI-ELEMENT PACKAGE DIMENSIONS

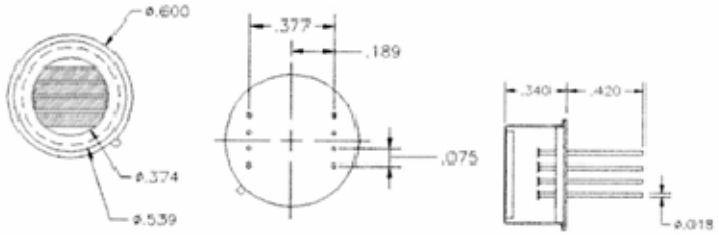

TO-5 PACKAGE DIMENSIONS

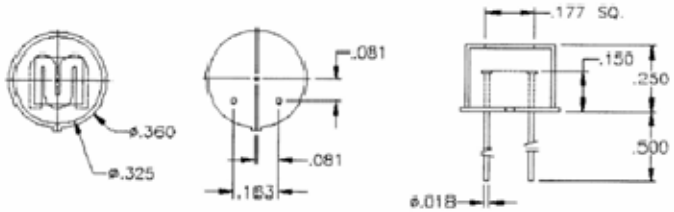

TO-46 PACKAGE DIMENSIONS

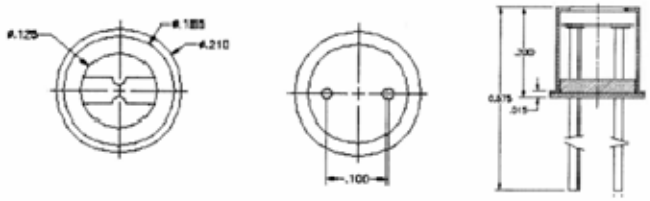

(800)347-5445; (617)566-3821; fax (617)731-0935; insource@bostelec.com

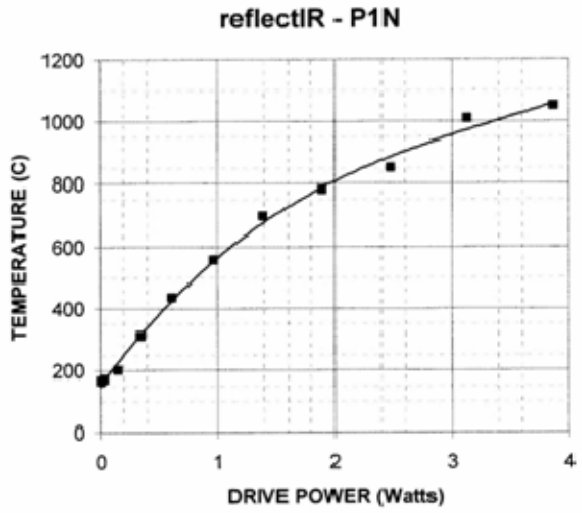

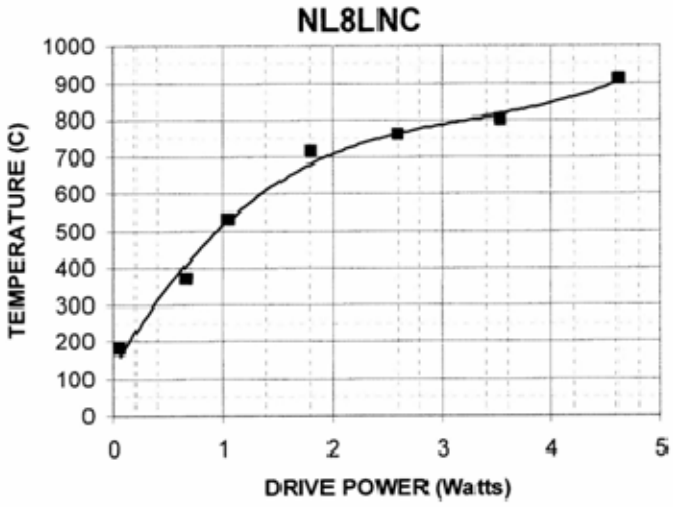

(800)347-5445; (617)566-3821; fax (617)731-0935; irsource@bostelec.com

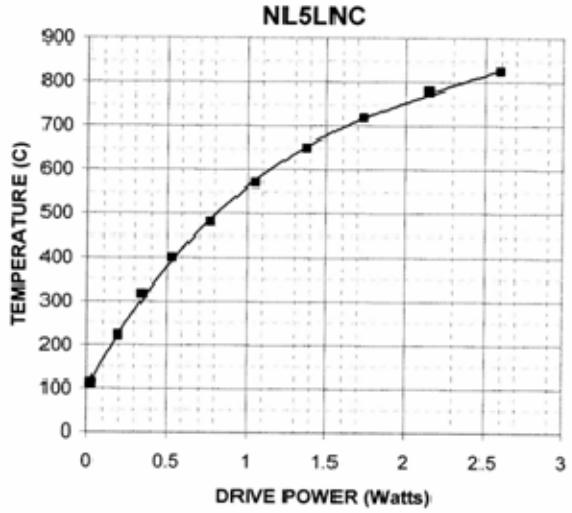

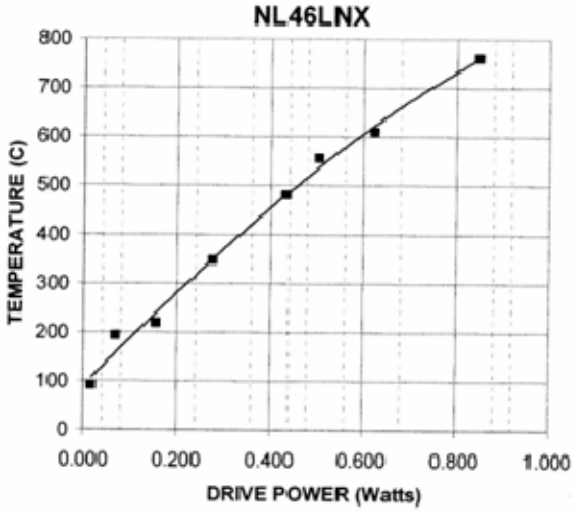

(800)347-5445; (617)566-3821; fax (617)731-0935; irsource@bostelec.com

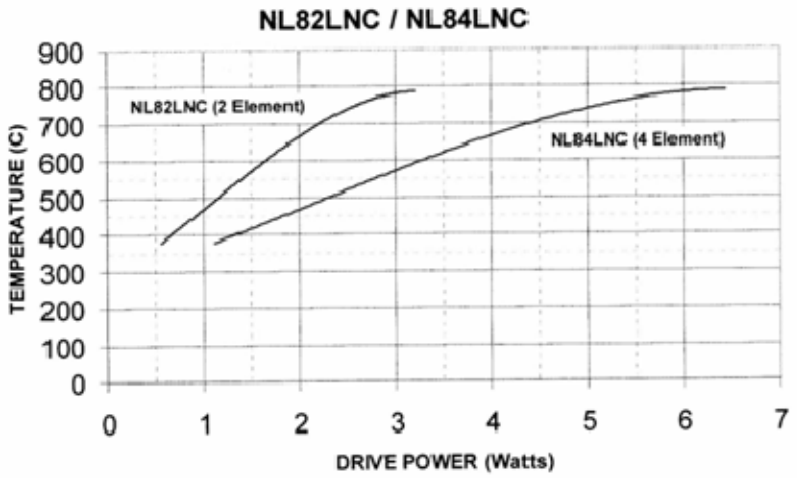
NL82LNC / NL84LNC
900
800
700
600
500
400
300
200
100
0
TEMPERATURE (C)
NL82LNC (2 Element)
NL84LNC (4 Element)
0
1
2
3
4
5
6
7
DRIVE POWER (Watts)

HawkEye Technologies, LLC
We are your Source for Infrared
www.hawkeyetechnologies.com

241 Research Drive #4
Milford, CT. 06460
Phone: 203-878-6892
Fax: 203-878-7462

The HawkEye Technologies IR-50 Series

Operational Guidelines

The HawkEye IR-50 Series utilizes a thin thermoresistive film of conducting amorphous (diamond-like) carbon. Infrared radiation is the result of heating this film by passing an electric current through it.

The maximum temperature of the film should not exceed 750°C in continuous operation. A faint red luminescence of the film is observed during operation at temperatures near 750°C. Short term heating up to 850°C is possible but will reduce the lifetime of the unit.

The specifications shown below assume an infrared source operating without a radiator and at ambient temperature and pressure. A rectangular voltage pulsed at a frequency of 5 hertz and with a duty cycle of 50% is used for heating. Two power leads and a ground are provided per the sketch below. Bi-polar drive voltage may be used.

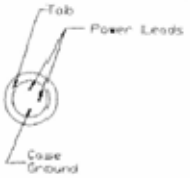

Nominal Parameters (750°C)	Resistance in Hot State (Ohms)	50
	Current (mAmps)	135
	Voltage (volts)	6.4
	Input Power (Watts)	0.9
Maximal Parameters (850°C)	Resistance in Hot State (Ohms)	50
	Current (mAmps)	150
	Voltage (volts)	7.5
	Input Power (Watts)	1.1

The HawkEye IR-50 Series is the perfect solution for an application that requires fast electrical modulation. However, it can also be used in a steady state (dc) mode. In applications where steady state power is used (or if used with electrical modulation but with a duty cycle of greater than 50%), it is recommended that the nominal input power specifications not be exceeded in order to avoid overheating of the membrane.

On the other hand, by reducing the length of the heating pulse or by increasing the frequency of modulation, the membrane will not have sufficient time to reach 750 degrees C. In this case, the pulsed power can be increased to allow 750°C to be maintained. The chart below shows the factor by which the voltage can be increased as frequency is increased. This chart assumes a 50% duty cycle.

Use this Voltage Ratio to maintain constant temperature.

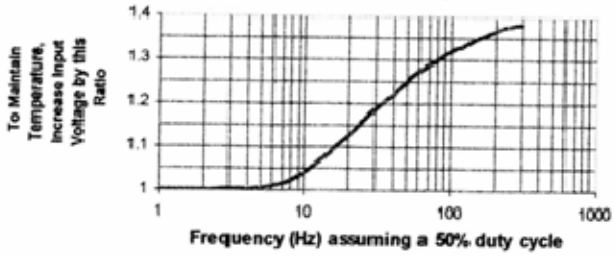

Using a 50% duty cycle and the appropriate power factor as determined above, a 50% modulation depth is achievable at modulation frequencies of more than 60 hertz. This modulation depth can be achieved at even higher frequencies (more than 100 hertz) if a 25% duty cycle were used along with a correspondingly higher power factor (sufficient to maintain the membrane temperature at 750°C). Please contact **HawkEye Technologies LLC** for assistance in determining the proper power factor for the duty cycle to be used in your application.

HawkEye Technologies LLC is a custom fabricator of IR sources. We will customize our existing products to your design specifications. We would be pleased to quote a new custom IR source, including engineering, that will meet your

APPENDIX B 3–5 MICRON FREQUENCY RESPONSE

A. CAL SENSORS SVF360-8M3, SINGLE-DEVICE, ON AXIS FREQUENCY RESPONSE

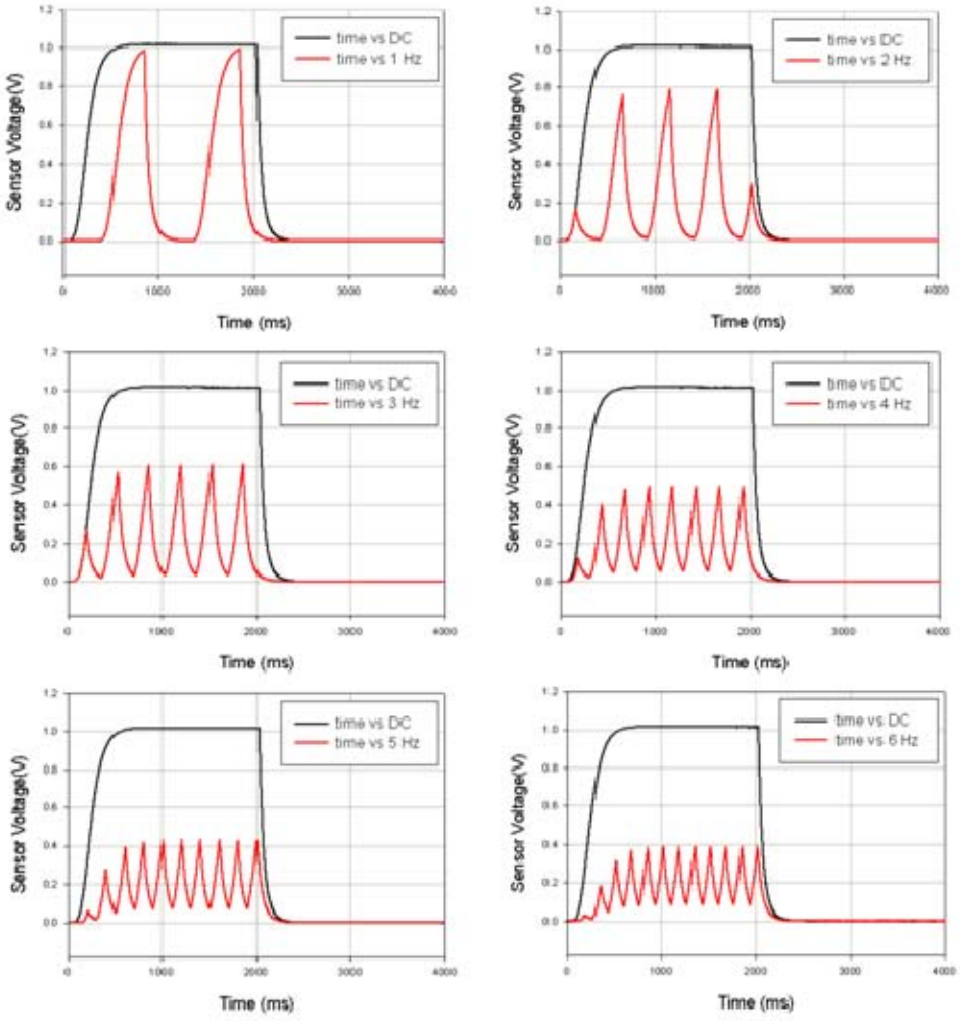

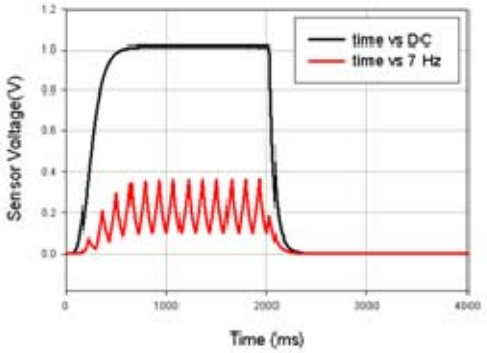
time vs DC
time vs 7 Hz
Sensor Voltage(V)
Time (ms)

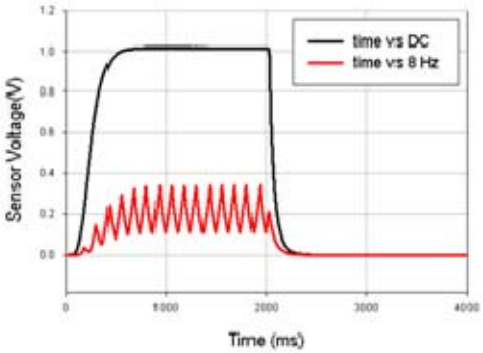
time vs DC
time vs 8 Hz
Sensor Voltage(V)
Time (ms)

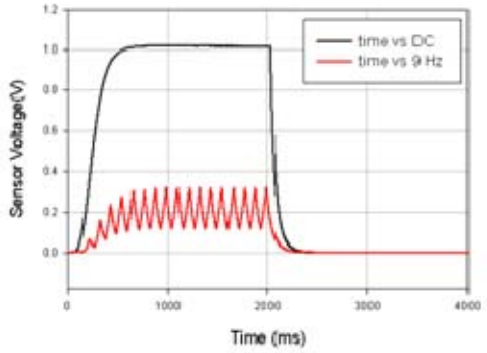
time vs DC
time vs 9 Hz
Sensor Voltage(V)
Time (ms)

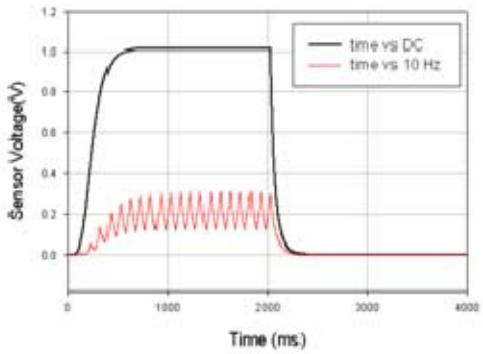
time vs DC
time vs 10 Hz
Sensor Voltage(V)
Time (ms)

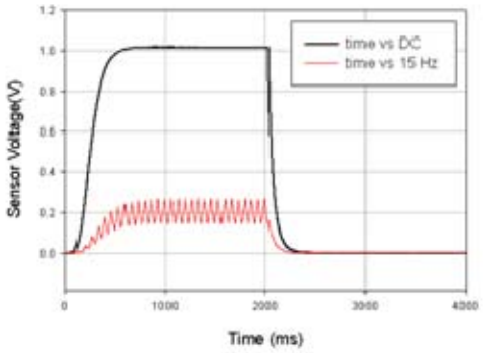
time vs DC
time vs 15 Hz
Sensor Voltage(V)
Time (ms)

B. ICX PHOTONICS NL84ACC, SINGLE-DEVICE, ON AXIS FREQUENCY RESPONSE

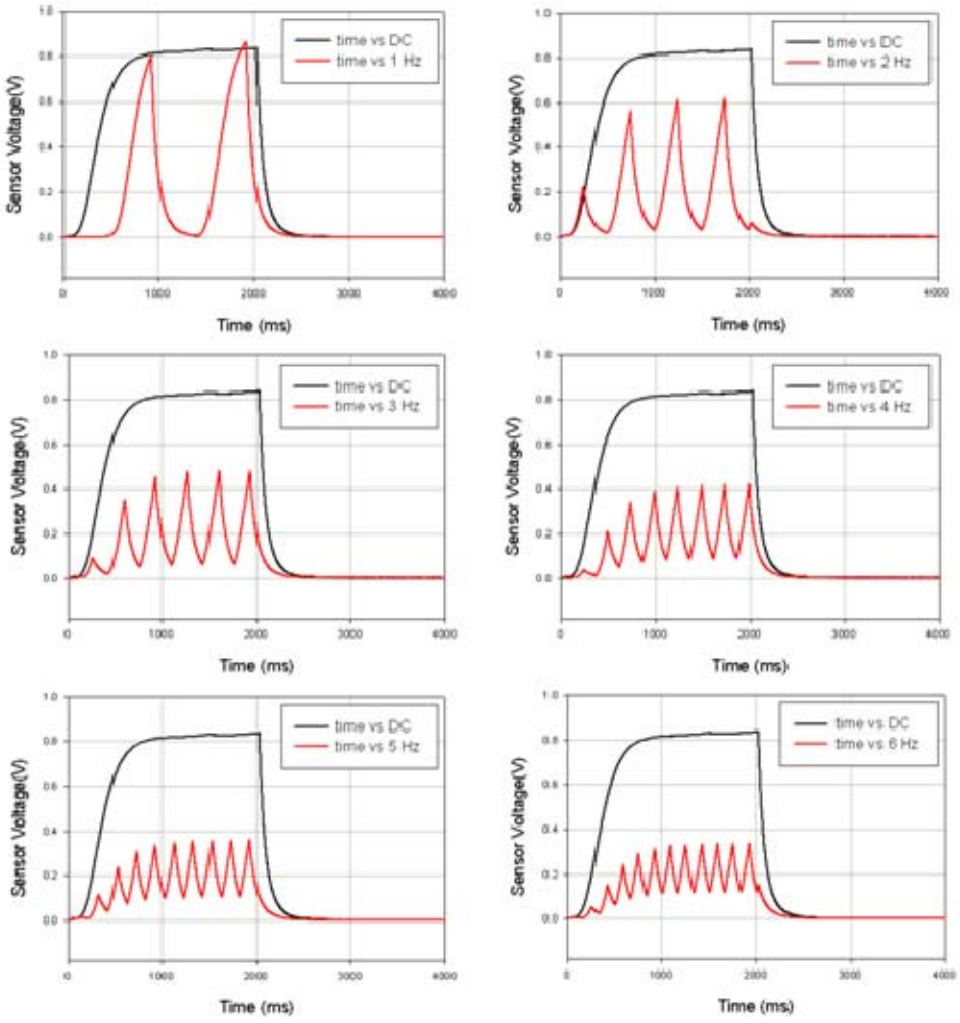

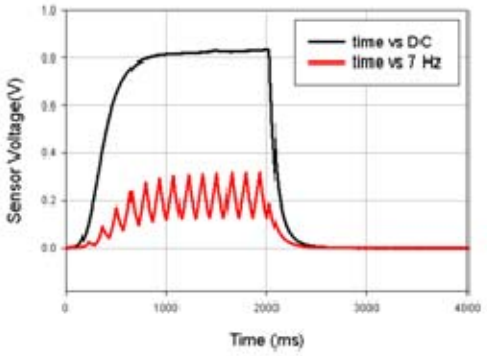
time vs DC
time vs 7 Hz
Sensor Voltage(V)
Time (ms)

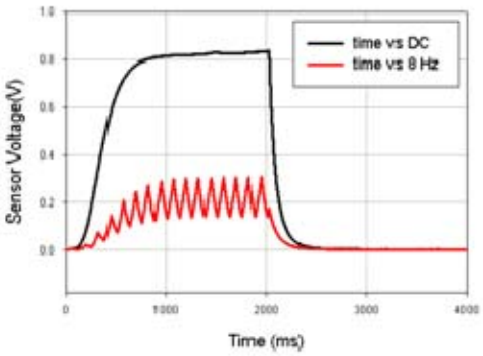
time vs DC
time vs 8 Hz
Sensor Voltage(V)
Time (ms)

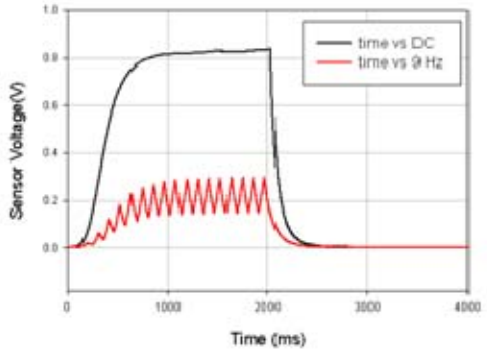
time vs DC
time vs 9 Hz
Sensor Voltage(V)
Time (ms)

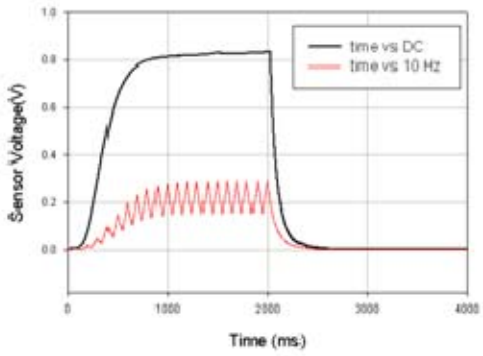
time vs DC
time vs 10 Hz
Sensor Voltage(V)
Time (ms)

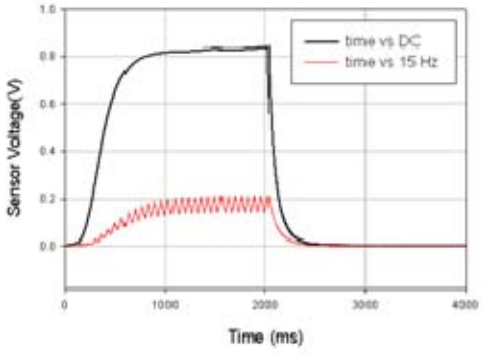
time vs DC
time vs 15 Hz
Sensor Voltage(V)
Time (ms)

C. HAWKEYE TECHNOLOGIES IR-50, SINGLE-DEVICE, ON AXIS FREQUENCY RESPONSE

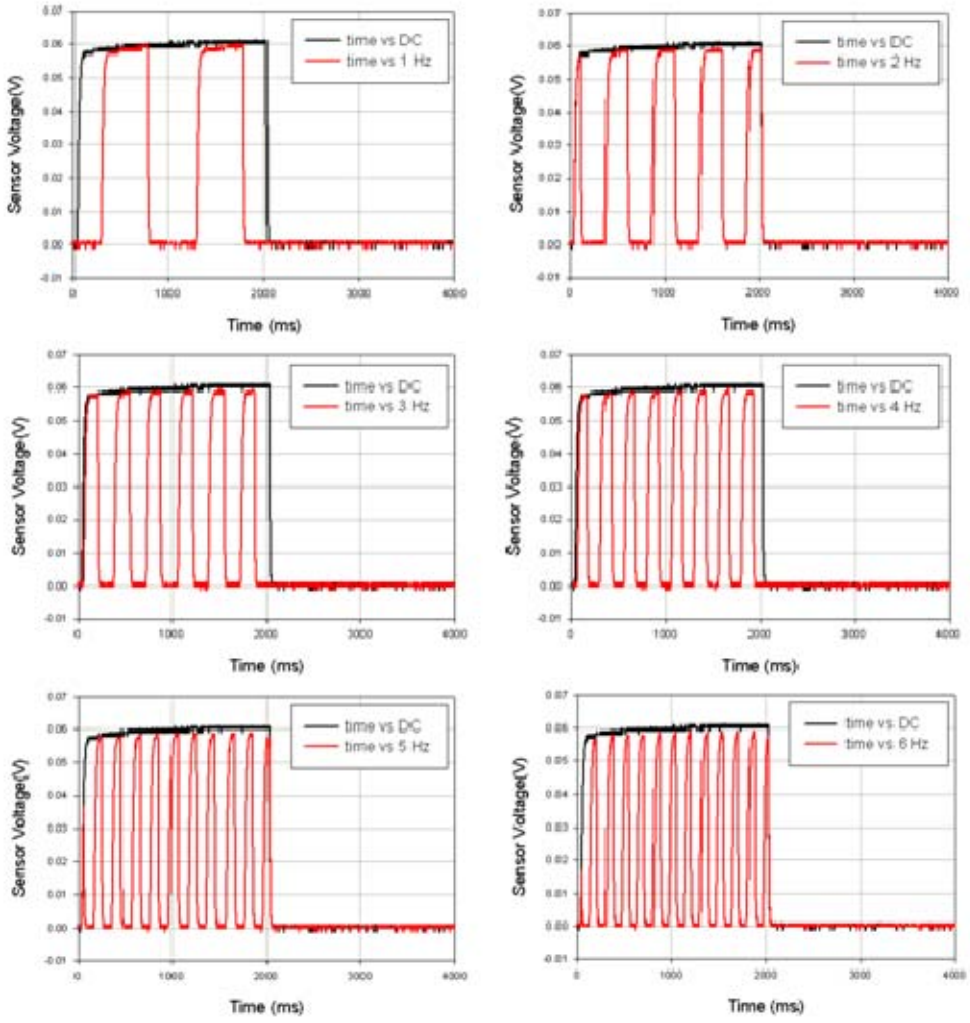

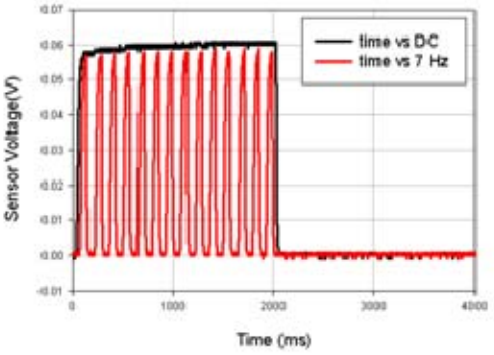
time vs DC
time vs 7 Hz
Sensor Voltage(V)
Time (ms)

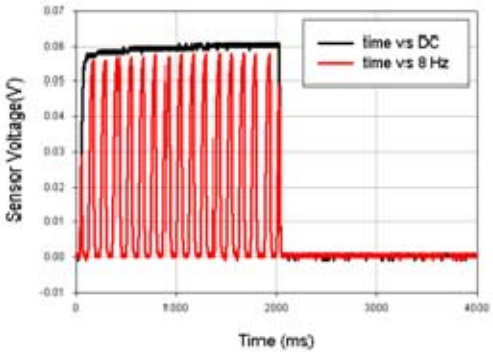
time vs DC
time vs 8 Hz
Sensor Voltage(V)
Time (ms)

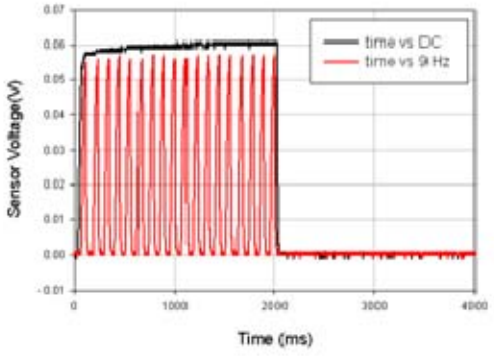
time vs DC
time vs 9 Hz
Sensor Voltage(V)
Time (ms)

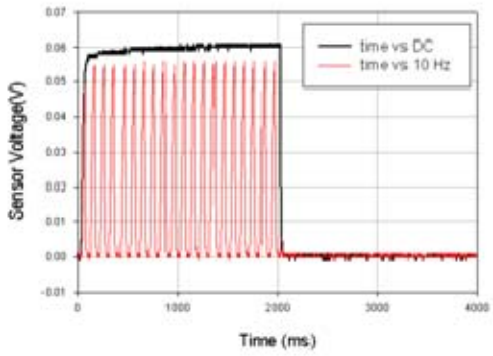
time vs DC
time vs 10 Hz
Sensor Voltage(V)
Time (ms)

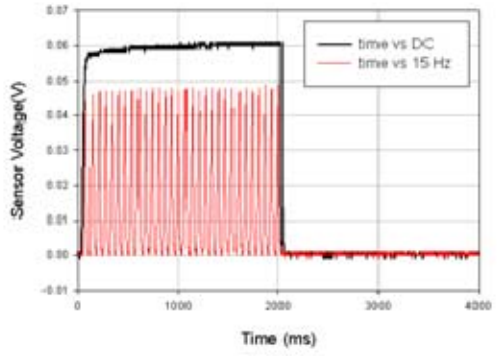
time vs DC
time vs 15 Hz
Sensor Voltage(V)
Time (ms)

APPENDIX C 8–12 MICRON FREQUENCY RESPONSE

A. CAL SENSORS SVF360-8M3, SINGLE-DEVICE, ON AXIS FREQUENCY RESPONSE

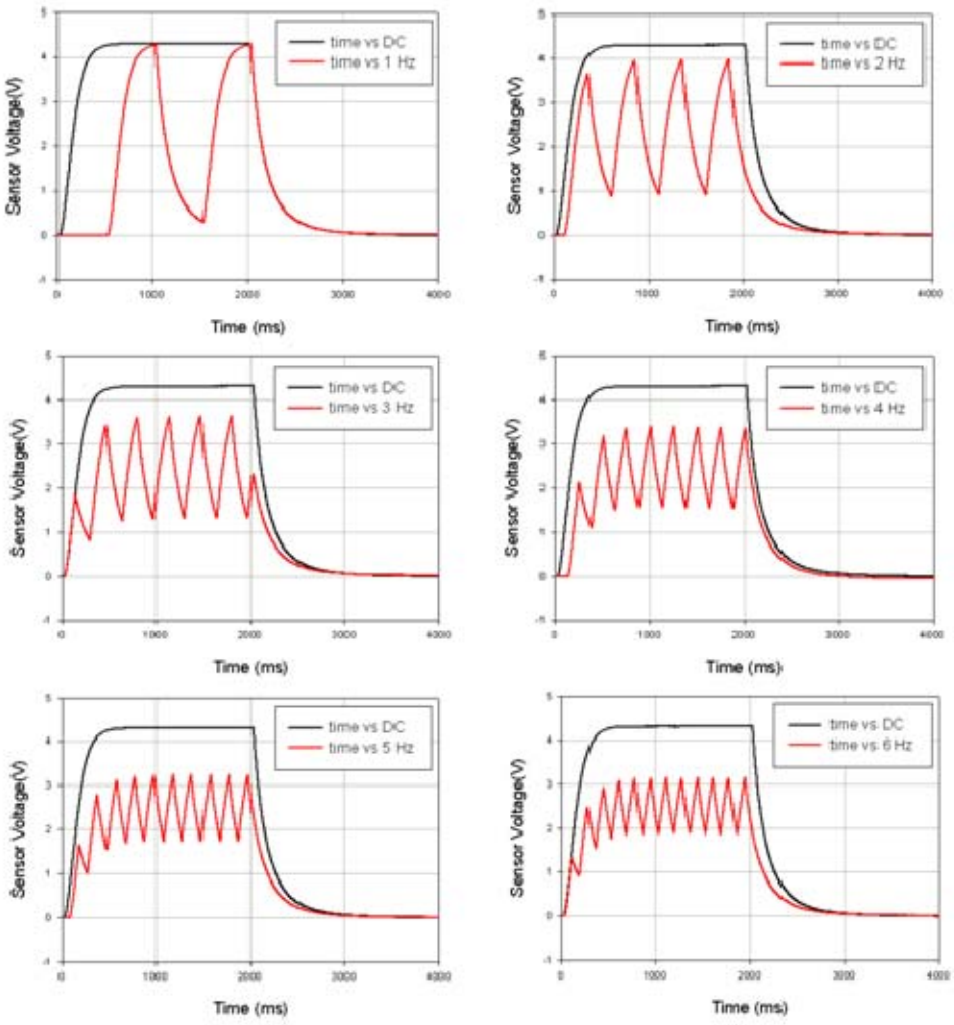

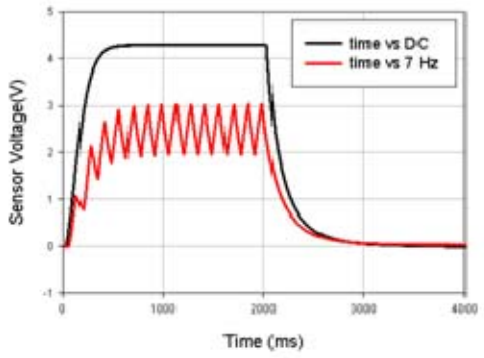
time vs DC
time vs 7 Hz
Sensor Voltage(V)
Time (ms)

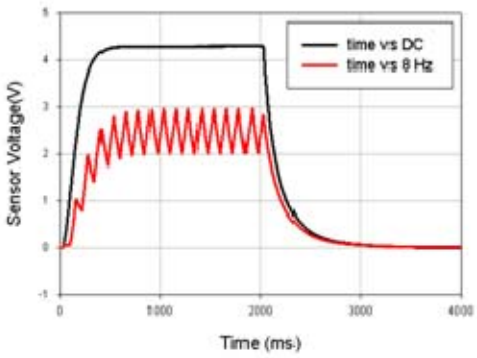
time vs DC
time vs 8 Hz
Sensor Voltage(V)
Time (ms)

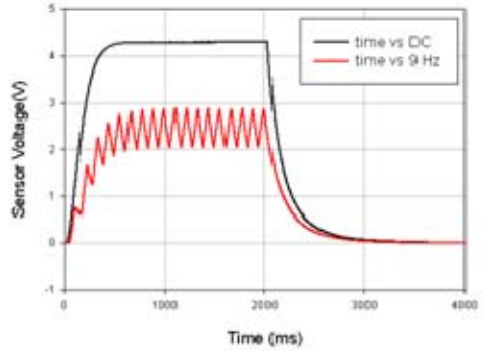
time vs DC
time vs 9 Hz
Sensor Voltage(V)
Time (ms)

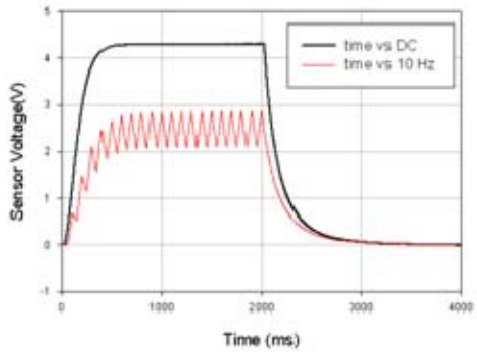
time vs DC
time vs 10 Hz
Sensor Voltage(V)
Time (ms)

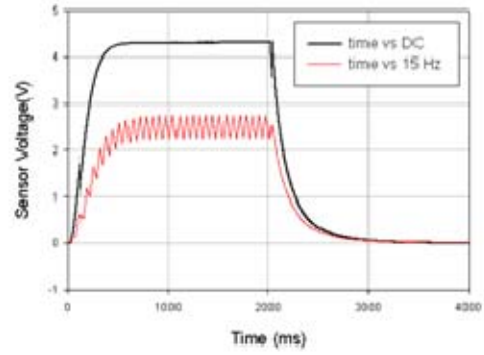
time vs DC
time vs 15 Hz
Sensor Voltage(V)
Time (ms)

B. ICX PHOTONICS NL84ACC, SINGLE-DEVICE, ON AXIS FREQUENCY RESPONSE

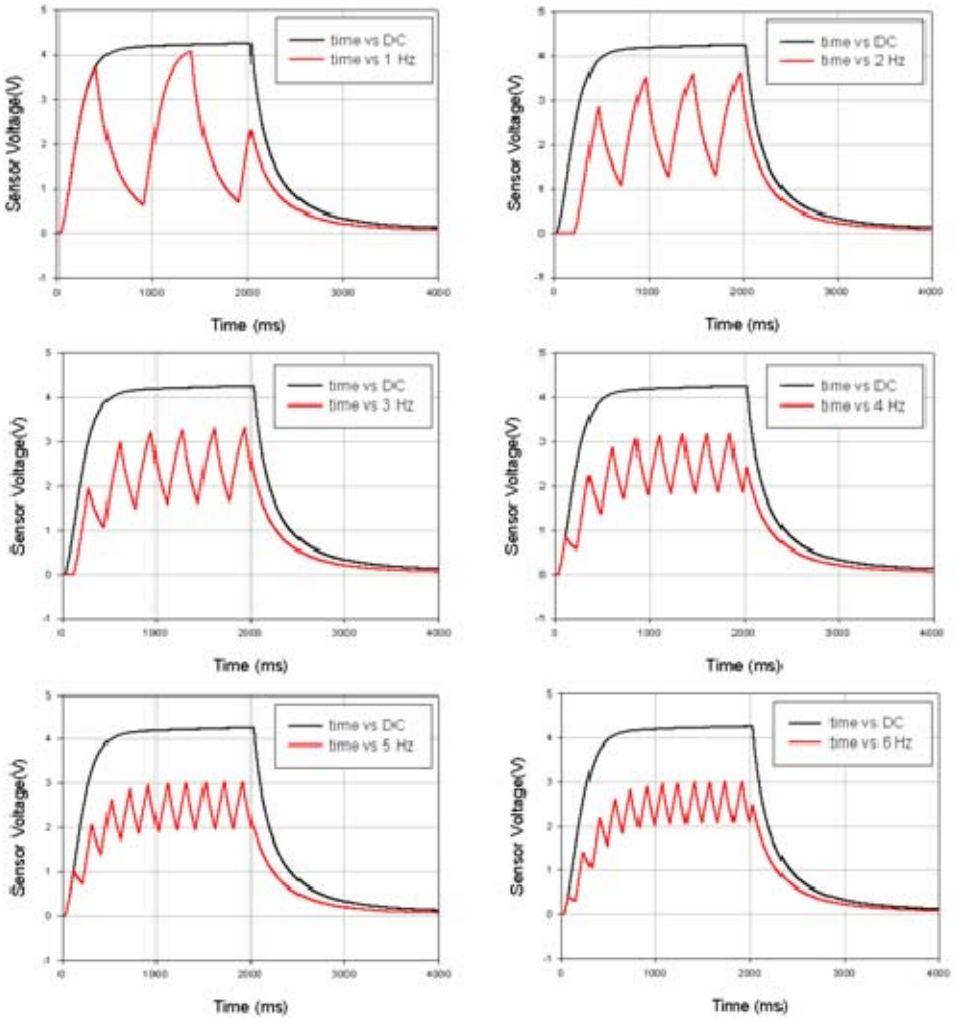

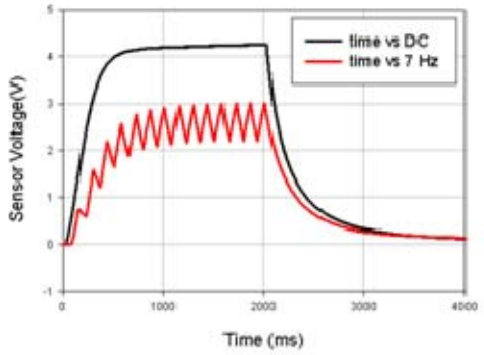
time vs DC
time vs 7 Hz
Sensor Voltage(V)
Time (ms)

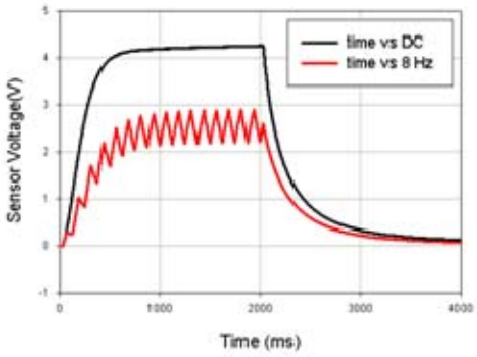
time vs DC
time vs 8 Hz
Sensor Voltage(V)
Time (ms)

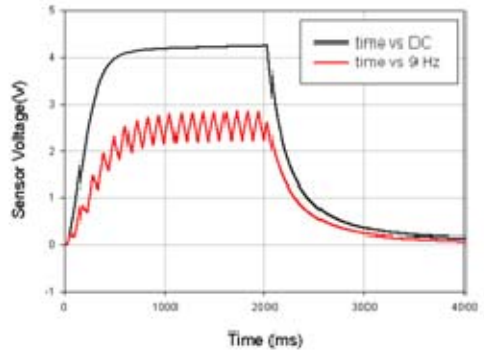
time vs DC
time vs 9 Hz
Sensor Voltage(V)
Time (ms)

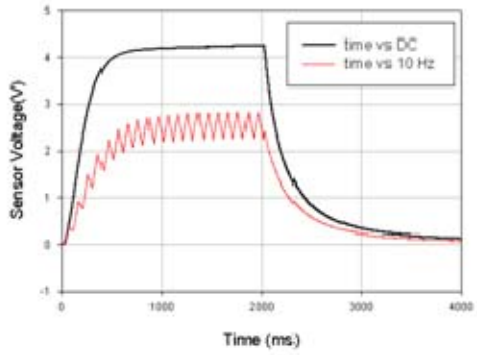
time vs DC
time vs 10 Hz
Sensor Voltage(V)
Time (ms)

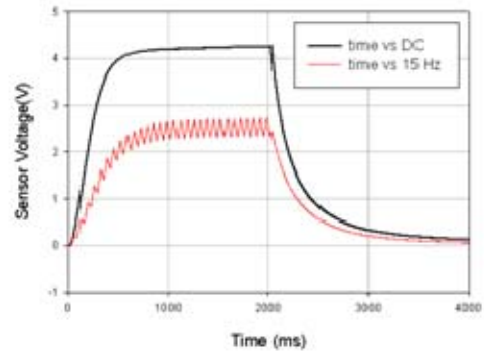
time vs DC
time vs 15 Hz
Sensor Voltage(V)
Time (ms)

C. HAWKEYE TECHNOLOGIES IR-50, SINGLE-DEVICE, ON AXIS FREQUENCY RESPONSE

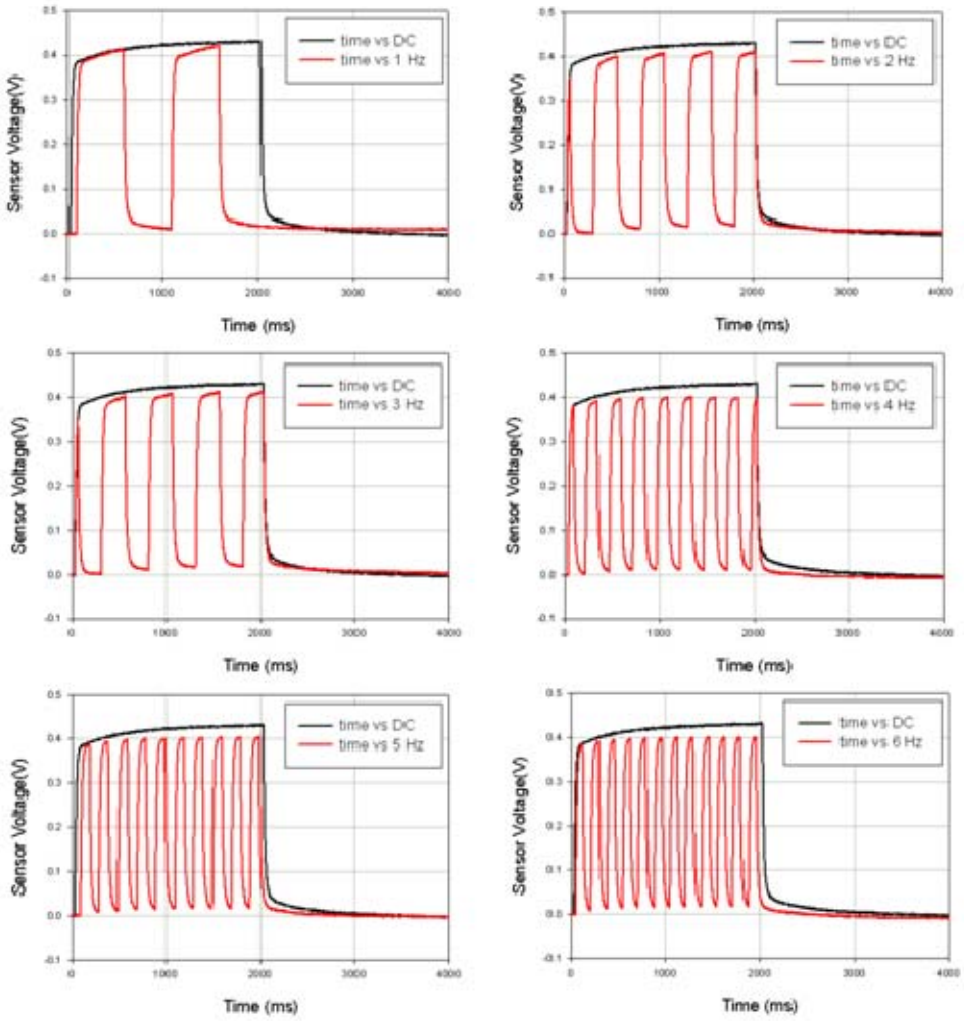

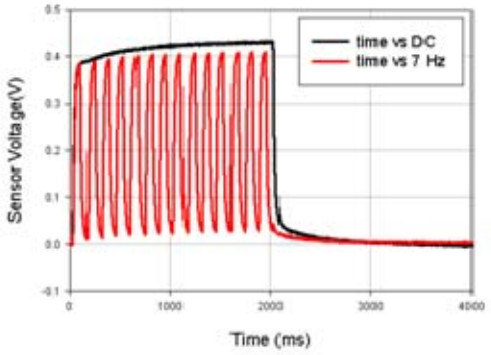
time vs DC
time vs 7 Hz
Sensor Voltage(V)
Time (ms)

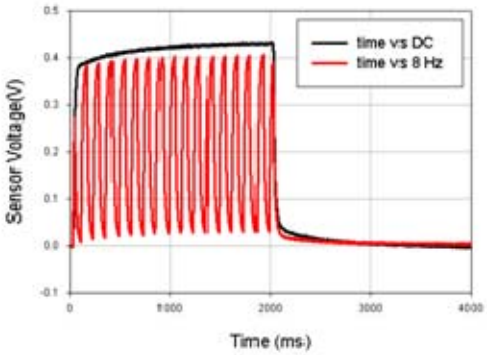
time vs DC
time vs 8 Hz
Sensor Voltage(V)
Time (ms)

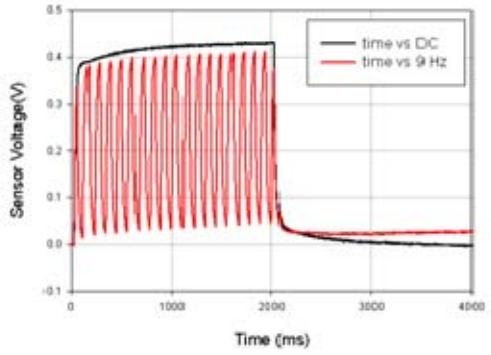
time vs DC
time vs 9 Hz
Sensor Voltage(V)
Time (ms)

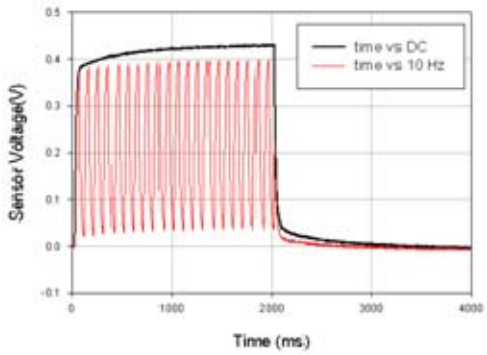
time vs DC
time vs 10 Hz
Sensor Voltage(V)
Time (ms)

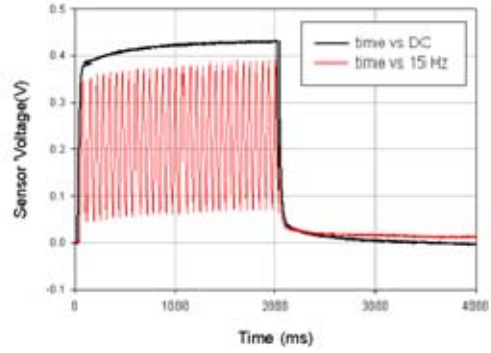
time vs DC
time vs 15 Hz
Sensor Voltage(V)
Time (ms)

APPENDIX D OFF-AXIS SINGLE DEVICE IRRADIANCE

Cal Single Device, 3-5 micron detector, d= 5 cm

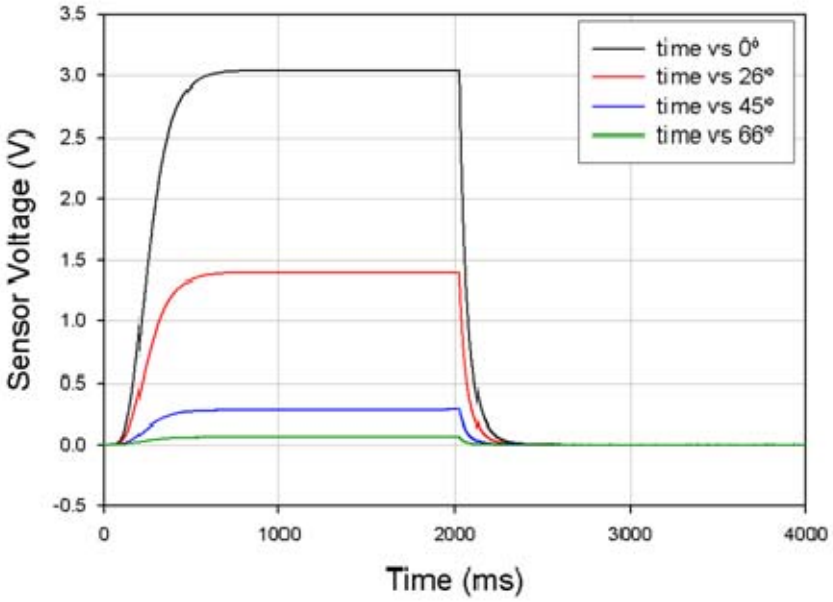

ICX Single Device, 3-5 micron detector, d= 5 cm

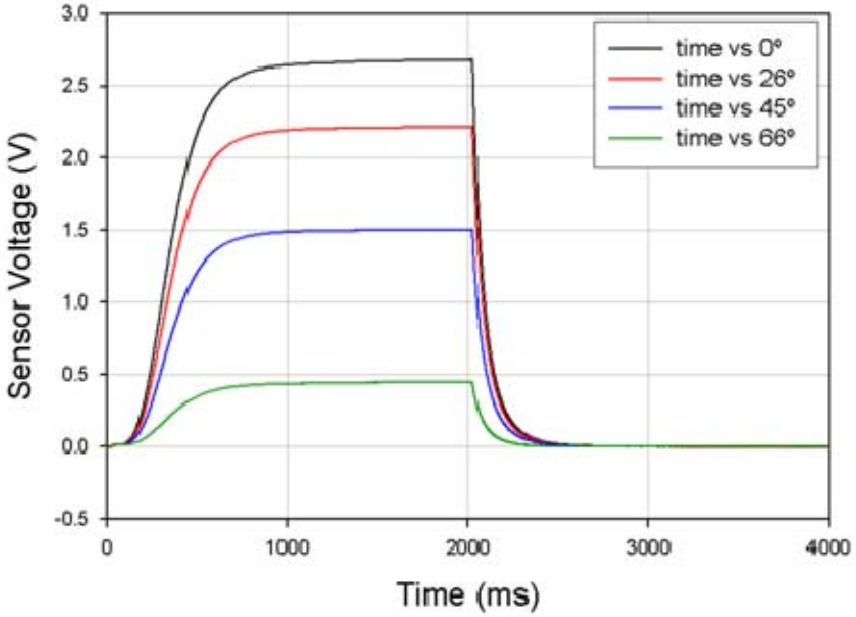

IR-50 Single Device, 3-5 micron detector, d= 5 cm

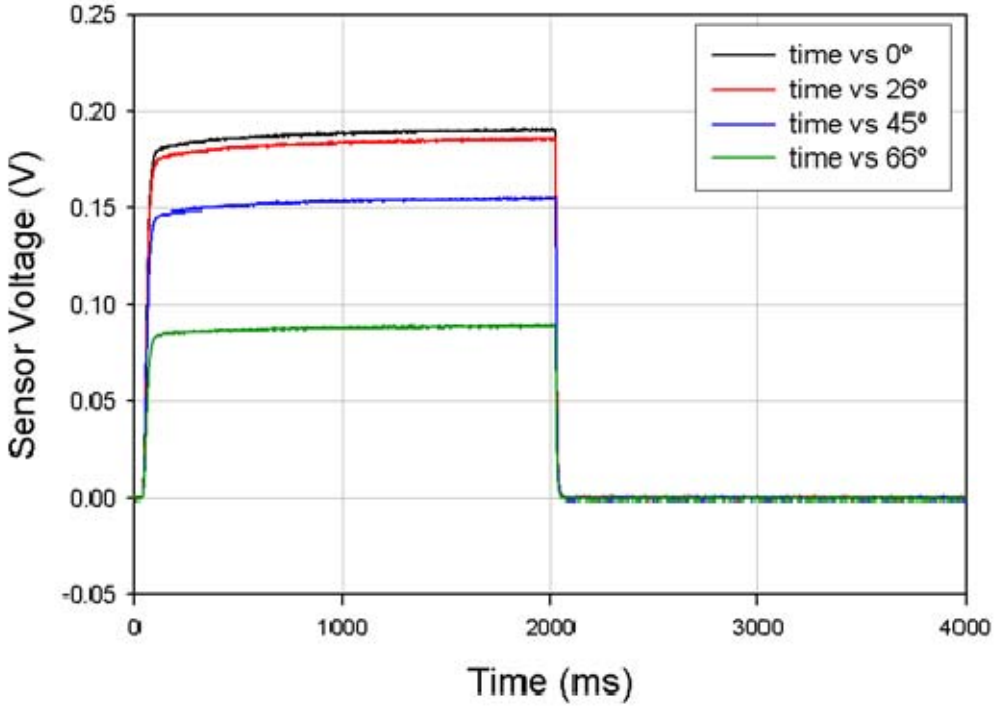

Cal Single Device, 8-12 micron detector, d= 5 cm

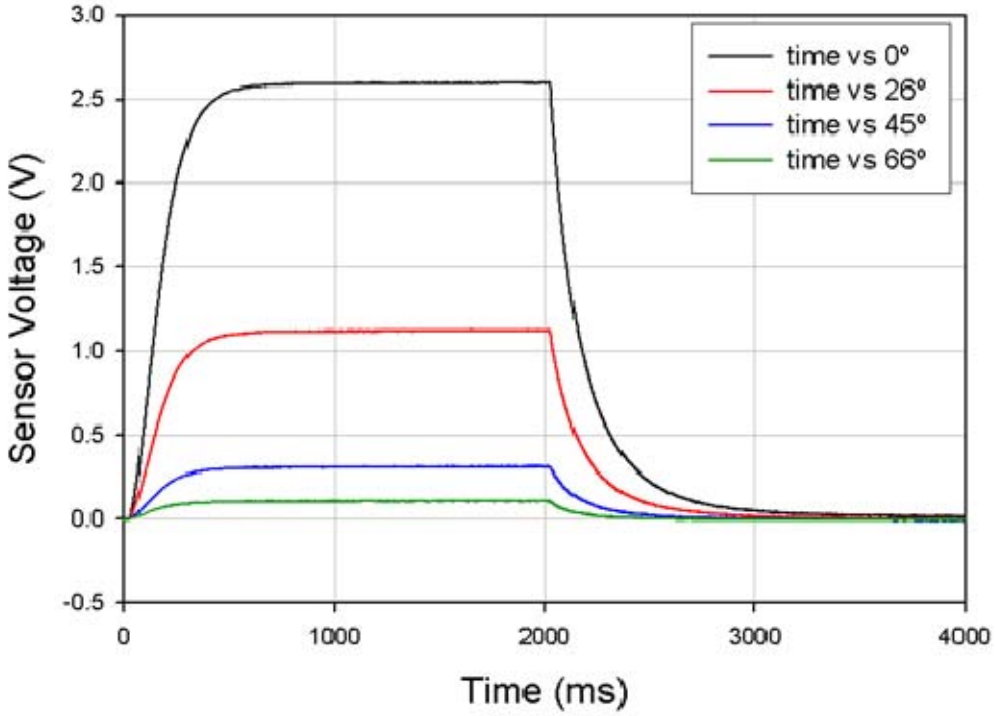

ICX Single Device, 8-12 micron detector, d= 5 cm

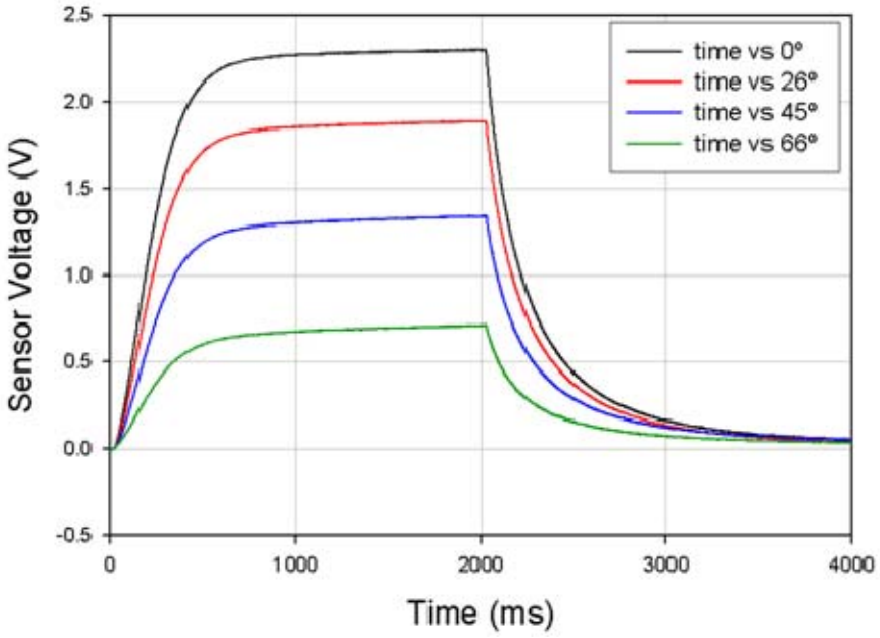

IR-50 Single Device, 8-12 micron detector, d= 5 cm

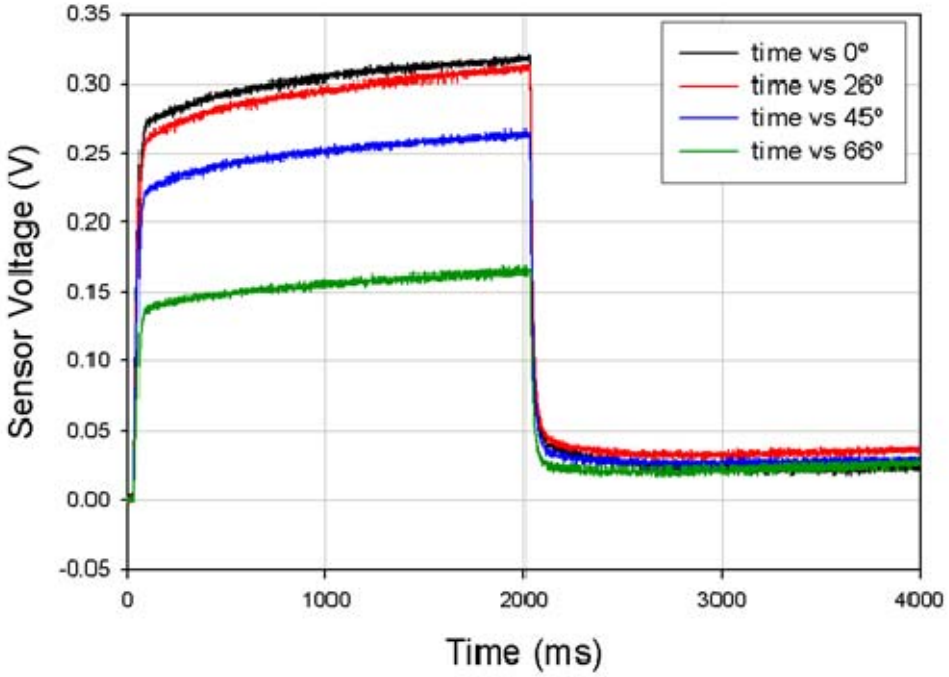

THIS PAGE INTENTIONALLY LEFT BLANK

APPENDIX E PANEL ON-AXIS IRRADIANCE VS DISTANCE

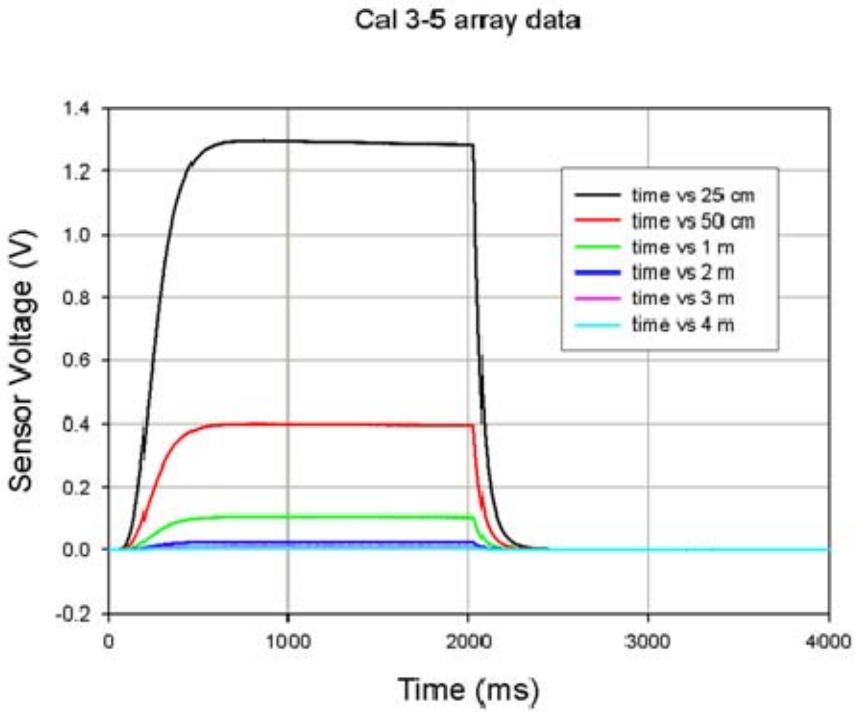

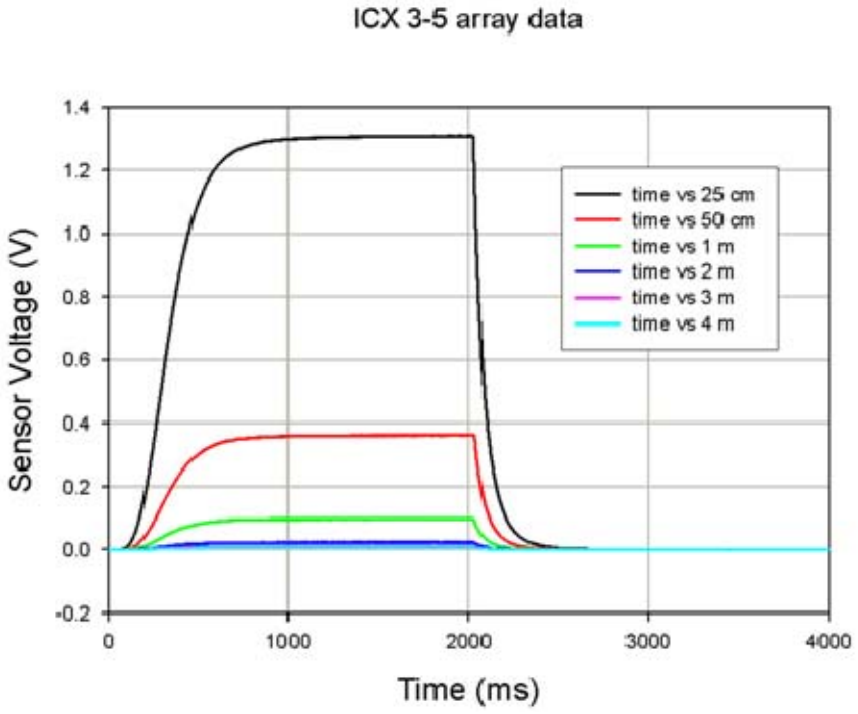

IR-50 3-5 array data

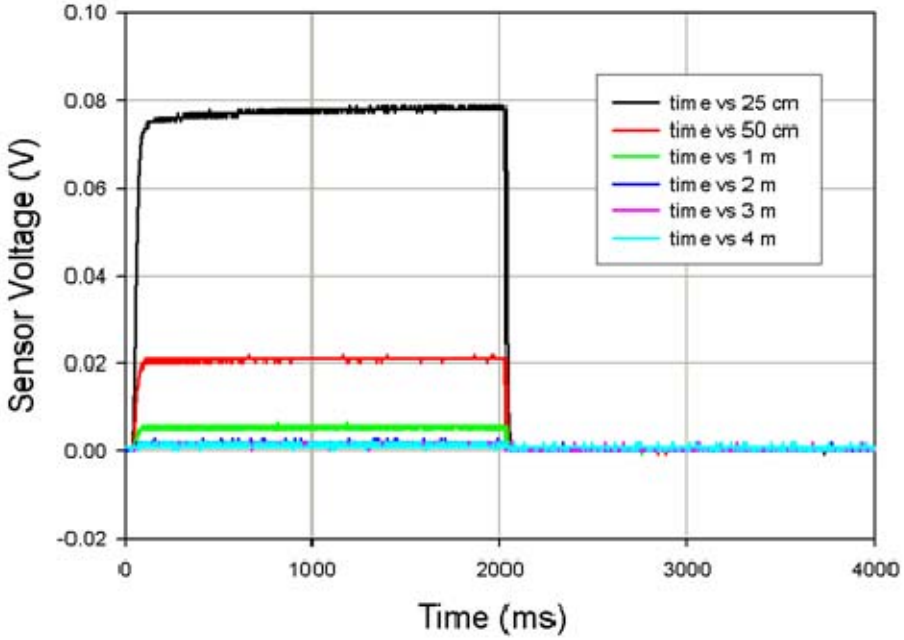

Cal 8-12 array data

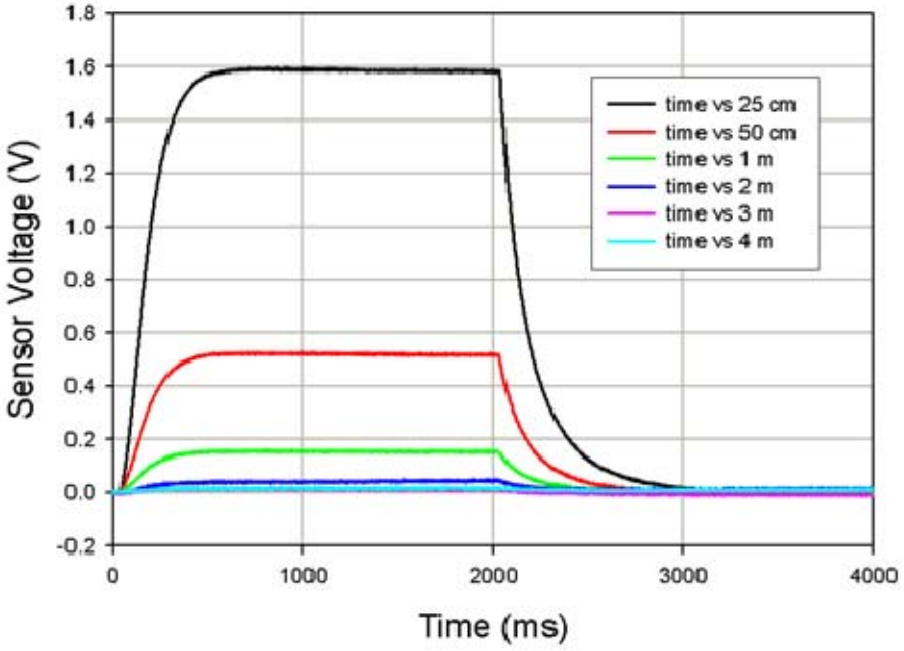

ICX 8-12 array data

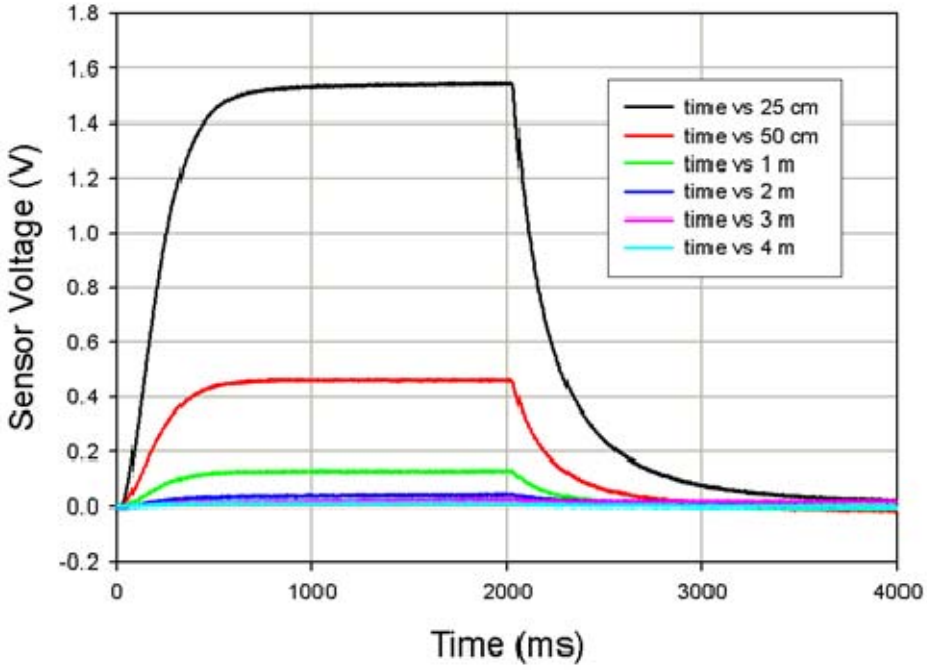

IR-50 8-12 array data

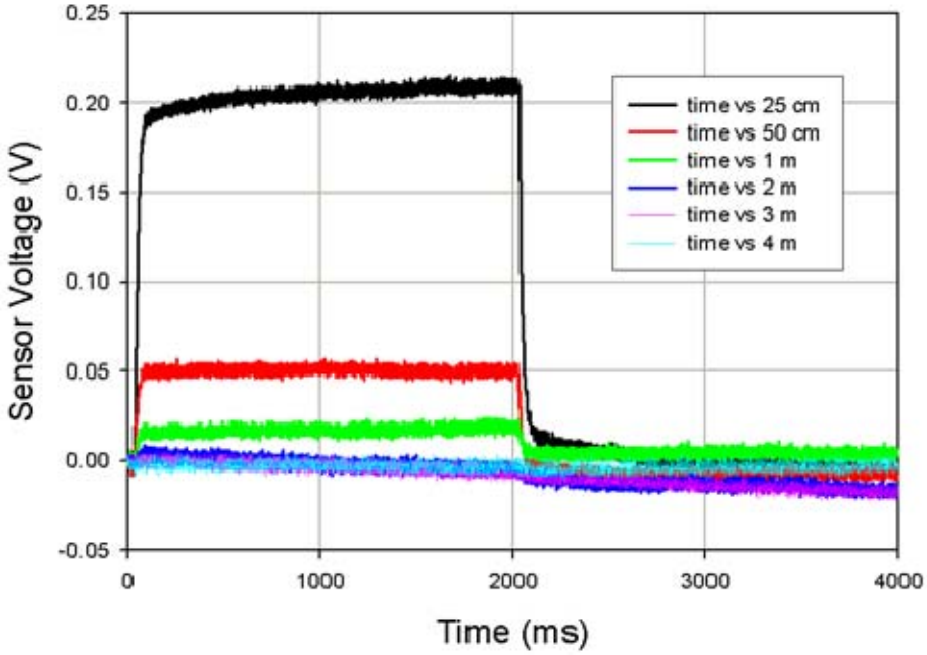

THIS PAGE INTENTIONALLY LEFT BLANK

LIST OF REFERENCES

[1] Marine Corps Doctrinal Publication 1, *Warfighting*: U.S. Marine Corps, 20 June 1997.

[2] Joint Publication 1-02, *Department of Defense Dictionary of Military and Associated Terms*: Joint Chiefs of Staff, Joint Electronic Library, 12 April 2001. As Amended Through 17 October 2008. Retrieved 27 April 2009, from http://www.ditc.mil/doctrine/jel/new_pubs/jp1_02.pdf.

[3] Bobby Cline, JCIMS Military Utility General Threat Assessment PowerPoint Brief: Marine Corps Systems Command, May 2009.

[4] Kenneth K. Steinweg, Parameters, Dealing Realistically with Fratricide: *Journal of the U.S. Army War College*, Volume 22, Number 3, Spring 1995.

[5] David Krause, Anthony Perry, and Richard Dexter, Joint Combat Identification Marking System Analysis Report: 11 March 2008.

[6] Richard Odom, Jon Milner, JCIMS OPFOR Exploitation Assessment Post -Exercise PowerPoint Brief: Army Test and Evaluation Command, 12 December 2005.

[7] Patrick Williams, Triggered Infrared Emitter Displays for Individual Identify Friend-or-Foe (IIFF) and Vehicular Mounted Identify Friend-or-Foe (VMIFF) Devices: Naval Postgraduate School, June 2007.

[8] Ben G. Streetman, Banerjee Sanjay, *Solid State Electronic Devices*: Prentice Hall, 2000.

[9] Richard S. Quimby, *Photonics and Lasers*: John Wiley and Sons, 2006.

THIS PAGE INTENTIONALLY LEFT BLANK

INITIAL DISTRIBUTION LIST

1. Defense Technical Information Center
   Ft. Belvoir, Virginia

2. Dudley Knox Library
   Naval Postgraduate School
   Monterey, California

3. Commanding General, Training and Education Command
   MCCDC, Code C46
   Quantico, Virginia

4. Director, Marine Corps Research Center
   MCCDC, Code C40RC
   Quantico, Virginia

5. Marine Corps Tactical Systems Support Activity (Attn: Operations Officer)
   Camp Pendleton, California

6. Director, Operations Analysis Division
   Code C19, MCCDC
   Quantico, Virginia

7. Marine Corps Representative
   Naval Postgraduate School
   Monterey, California

8. MCCDC OAD Liaison to Operations Research Department
   Naval Postgraduate School
   Monterey, California

9. Professor James H. Luscombe
   Naval Postgraduate School
   Monterey, California

10. Professor Nancy M. Haegel
    Naval Postgraduate School
    Monterey, California

11. Professor Richard M. Harkins
    Naval Postgraduate School
    Monterey, California

12. Captain Eric Q. Rose, USMC
Naval Postgraduate School
Monterey, California

13. Mr. Rick Sams
Marine Corps Experimentation Center
Camp Pendleton, California